Raman spectroscopy for the non destructive characterization of ancient pottery, porcelain and mosaic glass

Paola Ricciardi

Università degli Studi di Firenze

Scuola di Dottorato in Scienze

Dottorato di Ricerca in Scienza per la Conservazione dei Beni Culturali - Ciclo XX

Raman spectroscopy
for the non destructive characterization
of ancient pottery, porcelains and mosaic glasses

Dr. Paola Ricciardi

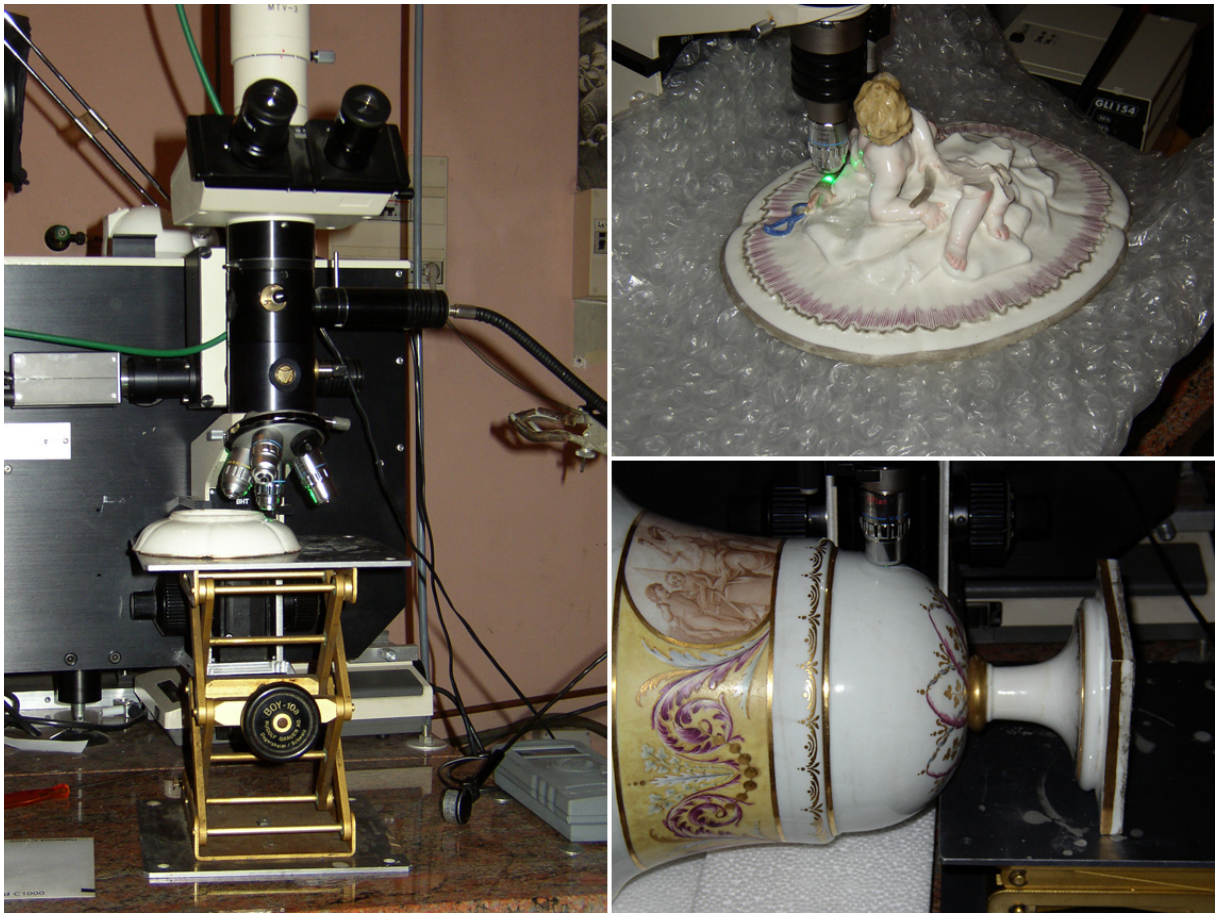

Tutor: Prof. Emilio Mario Castellucci (CHIM/02)
Co-tutor : Dr. Bruno Fabbri, CNR-ISTEC, Faenza

A.A. 2006-2007

Università degli Studi di Firenze

Scuola di Dottorato in Scienze

Dottorato di Ricerca in Scienza per la Conservazione dei Beni Culturali - Ciclo XX

Raman spectroscopy for the non destructive characterization of ancient pottery, porcelains and mosaic glasses

Dr. Paola Ricciardi

Tutor: Prof. Emilio Mario Castellucci (CHIM/02)
Co-tutor : Dr. Bruno Fabbri, CNR-ISTEC, Faenza

A.A. 2006-2007

Science and art belong to the whole world,
and before them vanish the barriers of nationality.

J. W. von Goethe

Ai miei genitori, e alla città di Roma,
che sono "casa" e punto di riferimento.

A Stefano, e alla città di Parigi,
che mi hanno fatto innamorare.

Acknowledgements - Remerciements - Ringraziamenti

This thesis results from three years of life, study, and research, and from the efforts of numerous people who have generously agreed to get involved into my own adventure, shared between Italy and France.

Firstly, I wish to thank prof. Emilio Mario Castellucci, coordinator of the Ph.D., who chose to be my tutor, and gave me the opportunity to carry out my work far from the University of Florence. I may have failed to keep him constantly updated about my work, but he nevertheless always helped out whenever possible, and answered countless questions.

Much of this work has been carried out at the CNR-ISTEC, Institute of Science and Technology for Ceramics, in Faenza, the "city of ceramics" almost by definition, under the tutorship of Dr. Bruno Fabbri, who deserves my deepest acknowledgements. He believed in me from the very first moment, and was always there to push me on, never letting tiredness and seemingly meaningless results be a good reason for stopping.
Besides him, the whole Cultural Heritage group at CNR-ISTEC participated of this work: Dr. Sabrina Gualtieri and Dr. Michele Macchiarola supervised large portions of the research; Idema, Paolo, Fiorella and Andrea were part of the daily horizon and shared thoughts, laughs, and terrible coffees. Special thanks go to Dr. Francesca Amato, colleague and dear friend; words do not suffice to express the gratitude I feel for her.

I am much indebted to Dr. Luca Nodari from the University of Padova, for immersing me into the world of Mössbauer spectroscopy, and to Dr. Francesca Ospitali from the University of Bologna, for introducing me to Raman spectroscopy. My thanks go also to prof. Umberto Russo and prof. Gianfranco Di Lonardo, for allowing me to use their facilities.

Je souhaite remercier M. Philippe Colomban, directeur du LADIR, pour m'avoir accueillie dans son labo, et pour m'avoir fait partager ses precieuses connaissances et sa passion de la spectroscopie Raman et de l'art céramique. Il a eu confiance en moi, et m'a encouragée tout au long de cette dernière année.

Mes remerciements vont aussi à Aurélie Tournié, qui m'a guidée à travers les détails des mesures Raman et ces de la langue française jamais en perdant son sourire et sa disponibilité. Merci à tous ces qui j'ai rencontrés au LADIR, notamment Frédérique, Aneta, Madeleine, Denis, Gwaen, et Chantal.
Je remercie également Mme Véronique Milande, restauratrice du Musée de Sèvres, et Mme Antoinette Fay-Hallé, directrice du Musée. Leur disponibilité et leur collaboration ont permis à la partie centrale de cette thèse de se développer beaucoup plus de ce que j'aurais jamais pu imaginer.
Merci aussi à Mme Françoise Marino de l'Ambassade Française à Rome pour son soutien, et au Ministère Français des Affaires Etrangères pour avoir financé mon stage au LADIR.

Special thanks go to Dr. Simona Varvara, who was a colleague and became a friend, and who even agreed to try out my Italian dishes. Thanks also to Dr. Mihai Gligor, for giving sound archaeological basis to the research on Romanian pottery.
My acknowledgement goes also to prof. Emilio Criado Herrero and his colleagues from the CSIC-Instituto de Ceramica y Vidrio of Madrid, for providing the Spanish porcelain samples and for fruitful discussion on my results. Thanks are also due to Ing. Luca Pinto and to the Museum of Capodimonte in Naples for providing the Italian porcelain samples, and to the researchers of the Istituto G. Caselli also in Naples; it was there that the research on Capodimonte started.

Grazie a tutti coloro che hanno condiviso la mia vita faentina: Francesca C., Veronica, Vincenzo, Margherita, Mathilda, Andrea, Francesco. Grazie a chi è rimasto in contatto con me a distanza per tanto tempo: Antonella, Davide e Stefania, Pepi, Zio Pino, don Andrea, Marga Lluis Alessandro e la piccola Maria, e il resto dell'ADSIS.

E soprattutto grazie a mamma, senza il cui supporto questa tesi non sarebbe giunta a compimento, nè avrebbe mai avuto inizio, e grazie a papà, cui devo la mia passione per la scienza e per l'arte. Grazie a Giulia, e al resto della (grande) famiglia, che ha sopportato con pazienza le mie assenze, e che ha sempre saputo in quale parte del mondo fossi!

Dal profondo del cuore, infine, grazie a Stefano... che mi tiene per mano, e mi dà la forza di camminare sulle mie gambe e di usare le mie ali. *To accomplish great things, we must not only act, but also dream; not only plan, but also believe. (Anatole France)*

Contents

Introduction

Our knowledge of the past has much improved thanks to the introduction of scientific methods in the study of cultural heritage materials; a "new" science has thus been born, under the name of archaeometry. This field of research, which is essentially multidisciplinary, calls for cooperation among historians, museum workers, conservation scientists and archaeologists on the one hand, and spectroscopists, chemists, geologists, biologists and others on the other.

The new "fronteer" of archaeometry is the use of non-destructive techniques, i.e. of scientific methods which do not need sampling the artistic artefact, and can often be applied *in situ*, often with no need to even move the object from its location in a museum, a gallery, or an archaeological site. Among these methods, Raman spectroscopy certainly has a non negligible role, as the past twenty years have seen it gradually assess itself as an established technique for the non-destructive identification and study of cultural heritage materials, with a focus on historic pigments. This role, thanks to instrumental improvements and to versatility among materials, will continue to develop; its expansion will be accompanied by devices that go out of the spectroscopy laboratory to museum conservation labs.

This thesis is in the first place an "adventure" in three domains of application of Raman spectroscopy as a diagnostic tool for the non-destructive study of cultural heritage materials, namely ancient pottery, porcelains and mosaic glasses. The first chapter illustrates the main objectives of the use of scientific techniques for the analysis of these kinds of materials. It also contains a synthetic review of how Raman spectroscopy has so far been applied to archaeometric studies on cultural heritage materials, and specifically on ancient pottery, porcelains and glasses. The research strategy and the organization of the thesis have been based on this review.

The second chapter provides a brief introduction to Raman spectroscopy, with its advantages and limitations, as well as a description of the instrumentations and data processing methodologies which were used during this work.

One of the objectives of this thesis is to make some steps towards the answer of certain questions relative to specific productions, mostly regarding the raw materials used and the objects' manufacturing processes. Chapters 3 to 5 include the main results obtained during experimental work carried out, respectively, on three types of ceramic materials, on 18^{th} century porcelain from the Italian manufacture of Capodimonte as well as from some other coeval productions, and on Roman age mosaic glasses.

Chapter 3 includes three different experiences regarding the application of Raman spectroscopy to ceramic materials, both in the form of ancient artefacts and of modern test samples. In all cases this technique has been combined with other analytical methods, in order to provide information on the raw materials and/or on the production processes of ancient pottery.

Chapter 4 constitutes the most voluminous part of this thesis. It deals in general with the Raman analysis of porcelain, and more specifically with the characterization of the 18^{th} century productions of the Bourbon manufactures of Capodimonte and Buen Retiro. They have had a very peculiar history; this makes it interesting *per se* to characterize their production, which can however also be of use as a "case study" for a methodological objective. Some results of this work, focused on the analysis of a single porcelain typology, could in fact be extended to the whole variety of artefacts made with such an aesthetically perfect and technologically advanced material.

Chapter 5 details the results of a preliminary Raman study which has been carried out on Roman age mosaic glass *tesserae*, in order to gain some information on this production, and also to test the potential of the technique for the analysis of an homogeneous set of glass samples.

These are then the reasons of interest for the three chosen domains of application of Raman spectroscopy; it seems important to point out how, while dealing with different

materials, they are far from being "stranger" to each other. In fact, we will be dealing with colouring agents used as pigments in the decoration layers of ancient pottery and porcelain, as well as in bulk glasses. Also, pottery and porcelain glazes have the same material structure as mosaic glasses, and therefore the treatment of their Raman spectra will be undertaken in exactly the same way, and similar kinds of information will be extracted for glazes and glasses. Needless to say, lastly, that these three types of materials are often found together in historical and archaeological contexts, or even in the same work of art (such as ancient mosaics, often realized using both ceramic and glass *tesserae*), and may therefore suffer similar pollution and degradation conditions, or need to be jointly analyzed and restored.

I would like to underline how the focus on the use of Raman spectroscopy as the chief analytical technique for the analysis of these materials has come as a result of a variegated path which has taken me through the use of several other analytical methods for the study of pottery. The subject of this thesis has been very much driven by the results which were step by step obtained, and it has thus shifted from the generic topic of the investigation of the technology of ancient pottery by means of physical and chemical techniques to a narrow focus on the potential of using Raman spectroscopy on these materials.

Much of this work has been carried out at the CNR-ISTEC, Institute of Science and Technology for Ceramics, in Faenza, the "city of ceramics" almost by definition, under the tutorship of Dr. Bruno Fabbri, and with the supervision of Dr. Sabrina Gualtieri for ceramics, and of Dr. Michele Macchiarola for glass materials. The acquisition of Raman spectra has at first taken place at the Physical and Inorganic Chemistry Dept. of the Industrial Chemistry Faculty, University of Bologna, thanks to the courtesy of Prof. Gianfranco Di Lonardo, and with the help of Dr. Francesca Ospitali. During the second and third year of research, Raman analyses have been carried out at the LADIR, Laboratoire Dynamique Interactions et Réactivité of Thiais (France), a unit of both the French CNRS and the University Pierre et Marie Curie (Paris VI). The French government has funded a seven months internship supervised by the director of the LADIR, Dr. Philippe Colomban, and one further month of scientific work in this lab has been possible thanks to a research contract awarded by the CNRS. Other types of analyses have been carried out in different labs, for which credits will be given during the course of this work.

Chapter 1

The scientific analysis of ancient pottery, porcelain and glass

Ancient man-made artefacts, such as both decorative and useful ceramics and glasses, have always been the object of a scientific interest because of their artistic quality, and also, in the case of pottery, because it might serve as a chronological indicator within archaeological contexts. More recently, recognition has been given of an added value, due to the fact that such objects carry numerous pieces of information regarding their provenance, production process, use and the conservation conditions through which they have survived until nowadays. Such information can be precious to researchers in terms of knowledge of the material culture of a people, the evolution of its technical skills over time, and the reconstruction of relationships and commercial trades among populations.

Ceramics and synthetic glasses have much evolved in style and technology over their long history, and such evolution has been the object of many studies. Such established knowledge on these subjects lies at the foundation of this thesis and will not be dealt with in detail; reference can be made at some of the numerous sourcebooks existing on these topics (e.g. Fabbri and Gianti 2003; Farneti 1993; Fiori 1995; Rice 1987; Savage and Newman 1992).

Each kind of material questions the researcher on different issues, mainly regarding its provenance and technology, each of them requiring the combination of a number of analytical techniques in order to be clarified. The first part of this chapter briefly illustrates the scientific methods most commonly used for

the analysis of ancient ceramics and glasses, depending on the archaeological and technological questions to be answered. The second part of the chapter aims at reviewing, without pretending to be comprehensive, what have so far been the main applications in particular of Raman spectroscopy in the field of archaeometric research on ancient pottery, porcelain and glasses.

1.1 Provenance studies

Provenance studies aim at identifying the production site of an artefact; the role of scientific techniques is particularly relevant when macroscopic or typological criteria do not suffice, or when there do not exist sure provenance markers (kiln wastes, factory marks, ...). This does not mean that archaeometric analyses give a direct indication of the production area; they rather describe some qualitative and quantitative features of the studied material which, if correctly interpreted, yield some information on the possible provenance of raw materials, and thus indirectly on the place of production. Provenance studies mostly consist of two main phases:

- characterization of ceramic and glass products;

- study of local raw materials.

The objects for which it is easier to ascertain the provenance are those having a close connection between raw materials and the finished product. Typically, such studies are undertaken on common pottery, because the production process in that case has been simple, meaning that it has not included excessive and arbitrary modifications of the raw materials. Archaometric studies for the identification of provenance usually focus on bulk materials (bulk glasses and ceramic pastes); they are seldom concerned with ceramic coatings, which with few exceptions are more rarely produced with local raw materials. It is nonetheless true that the study of glassy coatings can also provide interesting information for distinguishing different productions in a more indirect way (cfr. section 1.2).

Provenance studies require the combined use of mineralogical methods, such as optical microscopy in thin section, XRD and FT-IR, and of chemical analyses, by means of e.g. XRF and ICP. The first help identifying the minerals which form the ceramic paste or might have been added as opacifiers in the glass, and therefore give indications on the raw materials. In addition to this, granulometric analyses are undertaken to characterize

clay sediments. The measure of the major chemical elements instead reflects the general character of a sample, and their variations might indicate distinctive technological features. Minor and trace elements are more apt to help identifying a supplying source of raw materials or discriminating among different productions.

1.2 Identification of production technologies

Studies on manufacturing technologies aim at reconstructing the production processes and are based on the assumption that such processes remain imprinted onto historic artefacts. Questions to be answered regard, in this case, how the objects have been manufactured, in terms of the raw materials used, their preparation (purification, mixing, ...), the firing/melting conditions, and further treatment (such as the application of coatings and/or decorations on ceramics). As already mentioned, technological studies can indirectly produce information regarding provenance and/or dating, because they might identify production processes which have belonged specifically to a certain region and/or age. If provenance studies are most appropriate for those objects in which there exists a strong relationship between raw materials and finished product, studies on manufacturing technologies become perhaps more interesting when the analyzed object underwent a more complex production process.

Studies on prodution technologies require the combined use of petrographic, chemical and physical methods. A good research procedure should most generally begin with analyses which deepen the visual observation of the sample (radiography, optical microscopy in reflected light and in thin section, SEM). Afterwards, depending of the kind of information one is most interested into, one can proceed to apply other techniques.

In the case of pottery, depending on the typology of the material there are different technological information which one might be interested in knowing:

- for archaeological ceramics: refinement of the raw material, shaping, surface treatment, coatings, kiln type, firing atmosphere and maximum temperature reached during firing;

- for medieval and modern pottery: processing of the raw materials, coatings, decorations, firing temperature, number of successive firing;

- for contemporary materials: use of synthetic products and of peculiar manufacturing techniques.

A distinction must be made in this case between analyses to be carried out respectively on pastes and on coatings (slips and/or glazes). Paste analysis is undertaken by means of chemical (XRF), mineralogical (XRD, FT-IR, Mössbauer spectroscopy), and/or physical methods (measure of the density and porosity, thermal and colorimetric analysis). The nature of coatings and decorations can be investigated with specific techniques, such as SEM-EDS, PIXE, and ICP to determine the chemical composition; imaging methods for the stratigraphic observation of coating layers, and Raman spectroscopy e.g. for the identification of pigments or the structural characterization of glazes.

In the case of glasses, probably the most interesting information regard the technologies used to opacify them, and to obtain particular chromatic effects. SEM-EDS analyses are very often the main source of information on glass technology, as they allow not only to determine the overall chemical composition of the material, but also to examine details and inclusions, and to identify the presence of dishomogeneities, fractures and bubbles. They can be used to distinguish "primary" opacifiers from secondary ones, i.e. those which crystallized by separation from the melt during cooling. Mineralogical analyses by means of XRD aims at determining the nature of crystalline opacifying and colouring agents within the glass matrix. Raman spectroscopy can again help identify pigments and characterize the structure of the glass. Finally, physico-chemical analyses of degradation products may also help shedding light on production processes and identifying the "recipes" used by the ancient glassmaker.

1.3 Review of Raman studies on ancient pottery, porcelain and glass

The abundance and variety of cultural heritage materials to which Raman spectroscopy can be profitably applied precludes a comprehensive treatment of the subject here, which would also be beyond the scope of this work. The reviews published by Smith and Clark (2001, 2004) have already well fulfilled this objective. It is rather more interesting for our purposes to try to describe briefly what kind of studies have so far been undertaken using Raman spectroscopy as the chief technique for the characterization of pottery, porcelain

and ancient glass, as already partially done by Colomban (2005a,b), Smith (2006), and Clark (2007).

The distinction between pottery and porcelain in the following paragraphs has been made because studies on pottery usually deal with paste and pigment characterization, while porcelain analysis often focuses on the characterization of glazes, which have a glassy structure and for which the data processing treatments are the same as for ancient glasses *sensu stricto* (stained-glass windows, glass mosaic *tesserae*, ...). This is also the reason why all the published works dealing exclusively with the characterization of ceramic glazes have been included in the review of Raman studies on glasses.

Ancient pottery

The use of Raman spectroscopy for the characterization of ancient pottery started about ten years ago, and it has since been focused mostly on the identification of the pigments used on ceramic shards of different periods and provenances. Pigments have been examined, among others, on prehistoric and protohistoric shards from Egypt (Clark and Gibbs 1997), Serbia (Miŏc *et al.* 2004), China (Zuo *et al.* 1999, 2003), Colorado (van der Weerd *et al.* 2004), and the Anasazi nation (Striova *et al.* 2006), on Greek pottery from an Iberian necropolis (Pérez and Esteve-Tébar 2004), on Italian prehistoric to medieval pottery (Barilaro *et al.* 2005; Clark and Curri 1998; Clark *et al.* 1997) and 15^{th}-16^{th} century majolicas (Sakellariou *et al.* 2004; Sandalinas *et al.* 2006), on 13^{th} century glazed ceramics from Iran (Colomban 2003a), on Della Robbia glazes (Sendova *et al.* 2007), and on 18^{th}-19^{th} century French faiences (Marco de Lucas *et al.* 2006). The mineralogical composition of the ceramic body has also been investigated, given that some mineralogical phases and the transitions between them can act as "mineralogical thermometers" or give indications about the firing atmosphere, in the attempt to identify raw materials and/or manufacturing processes of prehistoric pottery from Syria (Zoppi *et al.* 2005), Turkey (Akyuz *et al.* 2007), and Africa (Lofrumento *et al.* 2005), and on shards from Bronze Age Cyprus (Sendova *et al.* 2005), Hellenistic Greece (Wopenka *et al.* 2002), and medieval to modern Italy (Bersani *et al.* 2007; Marengo *et al.* 2005) and South Africa (Legodi and de Waal 2007). A deeper understanding of the firing process applied for the production of 2^{nd} century Roman black-gloss coated pottery has also been achieved by Raman spectroscopy (Di Lonardo *et al.* 2004). This same technique has also effectively been applied to the well-studied production of *sigillata*, both for the characterization of

its body and red slip (Lofrumento *et al.* 2004), and for a systematic study of the effect of *Al*-for-*Fe* substitution on the Raman spectrum of hematite in *sigillata* slips (Zoppi *et al.* 2006, 2007). Finally, a number of works have been published regarding the spectroscopic characterization of Vietnamese and Chinese celadons and (proto)porcelains; the analyses have allowed identifying the composition and microstructure of the pastes and glazes (Colomban *et al.* 2004d; Liem *et al.* 2000, 2002), and re-dating some artefacts on a technological basis (Prinsloo *et al.* 2005).

Porcelain

Raman studies on porcelain artefacts were first published in 2001 thanks to the collaboration between the LADIR and the National Ceramics Museum and Manufacture of Sèvres, which allowed characterizing a large number of porcelain pigments on standard colour "palettes", as well as some 18^{th} to 20^{th} century French porcelain types, based on the spectroscopic analysis of both body and glaze (Colomban and Treppoz 2001; Colomban *et al.* 2001, 2004a). Some more studies followed, published by other groups, on the possibility to distinguish English porcelains issued from different manufactures (Edwards *et al.* 2004; Leslie 2003), and on some Chinese shards from the Ming period (de Waal 2004; Kock and De Waal 2007). A few essays have also been made of the use of a portable spectrometer for the *in situ* characterization of extremely precious artefacts, such as two 16^{th} century dishes from the Medicis' production (Colomban *et al.* 2004c) and several porcelain and stoneware objects dating to the early years of the Meissen manufacture (Colomban and Milande 2006).
These studies have well demonstrated how the Raman spectra of a porcelain fragment or whole object can be obtained in a completely non-destructive way to determine characteristic body and glaze signatures, making it possible to determine the type of porcelain (hard-paste, soft-paste, bone ash, ...). Being such a technologically advanced material, porcelain has had since its beginning very specific recipes, whose secrets were also carefully guarded and therefore represent a real "factory mark" from the point of view of manufacturing technology. In this sense, a technique such as Raman spectroscopy, which shows its efficacity in distinguishing technological parameters in a completely non-destructive way, is of unquestionable importance. There have in fact been cases in which a comparison between an (unmarked) porcelain artefact and a marked piece have been made, providing analytical support for an attribution to the same factory (e.g. Edwards *et al.* 2004).

Historic glasses

Early works dealing with the Raman characterization of historic glasses were published at the end of the 1990s and were once again devoted to the analysis of pigments, in stained-glass windows (Edwards and Tait 1998) as well as in 19^{th} century British glazed roof tiles (Brooke *et al.* 1999). The identification of colouring and opaquening agents in ancient glasses, often accompanied by the identification of glass type, has been the object of a certain number of studies on 13^{th}-20^{th} century stained-glass windows (Bouchard-Abouchacra 2001), on Roman mosaic *tesserae* (Galli *et al.* 2004), on glass beads from South Africa (Prinsloo and Colomban 2007) and the Far East (Welter *et al.* 2007), and on a wide range of beads, rings and mosaic tiles from Tunisia (Colomban *et al.* 2003). Also in this case, on-site studies have been undertaken, both on precious Kütahya and Iznik ceramic glazes (Colomban *et al.* 2004b, 2005), and more recently on an exquisite and totally unmovable work of art such as the stained-glass windows of the Sainte Chapelle, in Paris (Colomban and Tournié 2007).

Colomban and co-workers have further treated Raman data from some of these works by extracting a number of parameters which have been related to the structure, melting temperature and composition of glass (e.g. Colomban 2003b; Colomban and Paulsen 2005; Colomban *et al.* 2003), as detailed in section 2.3. Six years of experience have allowed them to gather over 700 Raman spectra of glassy materials, among which 30 representative ones have been chosen and used to tentatively distinguish seven glass "families" (Colomban *et al.* 2006). This work is completed by a multivariate data analysis (by means of PCA and cluster analysis), which had long been used to classify stones, ceramics and glasses from their elemental compositions, and has more recently been extended to spectroscopic (IR and Raman) parameters extracted from the spectra (Brody *et al.* 2001; De Benedetto *et al.* 2005). The same procedure has been applied by Ricci *et al.* (2007) in a work on Renaissance majolica glazes which focused largely on the temperature factor, rather than on the composition of the glass.

An ongoing work of slightly different nature is that of Laurianne Robinet and co-workers (2004, 2006a, 2006b, 2007), who have combined Raman spectroscopy with several other analytical techniques to investigate in detail the weathering mechanisms of glass in a humid and/or acidic atmosphere, based on the real problematic situation of the collection of historic glasses of the National Museum of Scotland. Corrosion products in the form of

crystalline deposits have been identified, and the effect of organic pollutants on the glass structure and on its Raman spectrum has been studied, also by means of ageing experiments. They have established a "standard" model for the decomposition of the Raman spectra of alkali-silicate glasses, and their most recent challenge is the extension of such a model for other types of silicate glasses.

Additional remarks

In most of the cited works on pottery, porcelain and glass, (micro)Raman spectroscopy has been effectively used together with other techniques, mainly XRD, XRF, SEM-EDS, FT-IR and thermal expansion, and more rarely UV-visible reflectance spectroscopy, ion chromatography and electron microprobe analysis. Interesting results have also been obtained, as mentioned, by applying multivariate data analysis methods to parameters extracted from the Raman spectra of glazes and glasses, even though it does not seem that a "standard" or unified procedure for the statistical treatment of Raman data has been established so far.

About two thirds of the cited articles have been published by the Journal of Raman Spectroscopy, while the remaining ones have appeared on a number of international journals both dedicated to "hard" sciences (Applied Spectroscopy, Journal of Non Crystalline Solids, Journal of Molecular Structure, ...) and to archaeometry and conservation science (Archaeometry, Journal of Cultural Heritage, ...). A few works can also be found in conference proceedings, or as chapters of specialized books.

One last remark can be made, regarding the geographic provenance of these works; as it is evident from the schematic representation of figure 1.1, the main sources of the existing Raman data on pottery, porcelain and ancient glasses can be identified in a limited number of labs in the United Kingdom (London, Edinburgh), France (Thiais) and Italy (Florence). In the past few years, this knowledge has gradually spread to labs in other European and extra-European countries, which have also started producing interesting although numerically still limited researches in this field, often thanks to collaborations with the above mentioned "pioneer" institutions.

Figure 1.1: Schematic representation of the geographic provenance of published works dealing with the application of Raman spectroscopy to ancient pottery, porcelain and glasses (larger dots indicate a higher number of articles)

1.4 References

Akyuz S., Akyuz T., Basaran S., Bolcal C., Gulec A. (2007). FT-IR and micro-Raman spectroscopic study of decorated potteries from VI and VII century BC, excavated in ancient Ainos - Turkey. *Journal of Molecular Structure*, **834-836**, 150–153.

Barilaro D., Barone G., Crupi V., Donato M. G., Majolino D., Messina G., Ponterio R. (2005). Spectroscopic techniques applied to the characterization of decorated potteries from Caltagirone (Sicily, Italy). *Journal of Molecular Structure*, **744-747**, 827–831.

Bersani D., Lottici P. P., Virgenti S., Mora A., Ospitali F., Salvioli-Mariani E., Catarsi M., Pedrelli C. Micro-Raman and SEM-EDS investigation of medieval pottery. IV Raman in art and archaeology Conference, Modena, Book of abstracts p.45.

Bouchard-Abouchacra M. (2001). *Evaluation des capacités de la microscopie Raman dan la caractérisation minéralogique et physico-chimique de matériaux archéologiques: métaux, vitraux et pigments*. Ph.D. Thesis, Museum National d'Histoire Naturelle, Laboratoire de Minéralogie.

Brody R. H., Edwards H. G. M., Pollard A. M. (2001). Chemometric methods applied to the differentiation of Fourier-transform Raman spectra of ivories. *Analytica Chimica Acta*, **427**(2), 223–232.

Brooke C. J., Edwards H. G. M., Tait J. K. F. (1999). The Bottesford blue mistery: a Raman spectroscopic study of post-mediaeval glazed tiles. *Journal of Raman Spectroscopy*, **30**, 429–434.

Clark R. J. H. (2007). Raman microscopy as a structural and analytical tool in the fields of art and archaeology. *Journal of Molecular Structure*, **834-836**, 74–80.

Clark R. J. H., Curri L. (1998). The identification by Raman microscopy and X-ray diffraction of iron-oxide pigments and of the red pigments found on Italian pottery fragments. *Journal of Molecular Structure*, **440**, 105–111.

Clark R. J. H., Gibbs P. G. (1997). Non-destructive *in situ* study of ancient Egyptian faience by Raman microscopy. *Journal of Raman Spectroscopy*, **28**, 99–103.

Clark R. J. H., Curri L., Henshaw G. S., Laganara C. (1997). Characterization of brown-black and blue pigments in glazed pottery fragments from Castel Fiorentino (Foggia,

Italy) by Raman microscopy, X-ray powder diffractometry and X-ray photoelectron spectroscopy. *Journal of Raman Spectroscopy*, **28**, 105–109.

Colomban P. (2003a). Lapis lazuli as unexpected blue pigment in Iranian Lâjvardina ceramics. *Journal of Raman Spectroscopy*, **34**, 420–423.

Colomban P. (2003b). Polymerization degree and Raman identification of ancient glasses used for jewelry, ceramic enamels and mosaics. *Journal of Non-Crystalline Solids*, **323**, 180–187.

Colomban P. (2005a). Case study: glasses, glazes and ceramics - recognition of ancient technology from the Raman spectra. In *Raman spectroscopy in archaeology and art history*. Edwards H. G. M., Chalmers J. M. (eds.), pp. 192–206. Royal Society of Chemistry, Cambridge, UK.

Colomban P. (2005b). Raman μ-spectrometry, a unique tool for on-site analysis and identification of ancient ceramics and glasses. In *Mater. Res. Soc. Symp. Proc.*, vol. 852. OO8.3.

Colomban P., Milande V. (2006). On-site Raman analysis of the earliest known Meissen porcelain and stoneware. *Journal of Raman Spectroscopy*, **37**, 606–613.

Colomban P., Paulsen O. (2005). Non-destructive determination of the structure and composition of glazes by Raman spectroscopy. *Journal of the American Ceramic Society*, **88**(2), 390–395.

Colomban P., Tournié A. (2007). On-site Raman identification and dating of ancient/modern stained glasses at the Sainte-Chapelle, Paris. *Journal of Cultural Heritage*, **8**, 242–256.

Colomban P., Treppoz F. (2001). Identification and differentiation of ancient and modern European porcelains by Raman macro- and micro-spectroscopy. *Journal of Raman Spectroscopy*, **32**, 93–102.

Colomban P., Sagon G., Faurel X. (2001). Differentiation of antique ceramics from the Raman spectra of their coloured glazes and paintings. *Journal of Raman Spectroscopy*, **32**, 351–360.

Colomban P., March G., Mazerolles L., Karmous T., Ayed N., Ennabli A., Slim H. (2003). Raman identification of materials used for jewellery and mosaics in Ifriqiya. *Journal of Raman Spectroscopy*, **34**, 205–213.

Colomban P., Robert I., Roche C., Sagon G., Milande V. (2004a). Identification des porcelaines "tendres" du 18^{eme} siècle par spectroscopie Raman: Saint-Cloud, Chantilly, Mennecy et Vincennes/Sèvres. *Revue d'Archéométrie*, **28**, 153–167.

Colomban P., Milande V., Le Bihan L. (2004b). On-site Raman analysis of Iznik pottery glazes and pigments. *Journal of Raman Spectroscopy*, **35**, 527–535.

Colomban P., Milande V., Lucas H. (2004c). On-site Raman analysis of Medici porcelain. *Journal of Raman Spectroscopy*, **35**, 68–72.

Colomban P., Khoi D. N., Liem N. Q., Roche C., Sagon G. (2004d). Sa Huynh and Cham potteries: microstructure and likely processing. *Journal of Cultural Heritage*, **5**, 149–155.

Colomban P., de Laveaucoupet R., Milande V. (2005). On-site Raman spectroscopic analysis of Kütahya fritwares. *Journal of Raman Spectroscopy*, **36**, 857–863.

Colomban P., Tournié A., Bellot-Gurlet L. (2006). Raman identification of glassy silicates used in ceramics, glass and jewellery: a tentative differentiation guide. *Journal of Raman Spectroscopy*, **37**, 841–852.

De Benedetto G. E., Fabbri B., Gualtieri S., Sabbatini L., Zambonin P. G. (2005). FTIR-chemometric tools as aids for data reduction and classification of pre-Roman ceramics. *Journal of Cultural Heritage*, **6**, 205–211.

de Waal D. (2004). Raman investigation of ceramics from 16^{th} and 17^{th} century Portuguese shipwrecks. *Journal of Raman Spectroscopy*, **35**, 646–649.

Di Lonardo G., Ospitali F., Tullini F., Morandi N., Nannetti M. C., Sabetta T. (2004). Impiego della spettroscopia Raman nello studio di rivestimenti di ceramiche romane a vernice nera. In *Metodologia di ricerca e obiettivi degli studi: lo stato dell'arte*. Berti F., Fabbri B., Gualtieri S., Guarnieri C. (eds.), Atti della 6^a Giornata di Archeometria della Ceramica, Ferrara 9 Aprile 2002, pp. 59–64. University Press Bologna, Imola.

Edwards H. G. M., Tait J. K. F. (1998). FT-Raman spectroscopic study of decorated stained glass. *Applied Spectroscopy*, **52**(5), 679–682.

Edwards H. G. M., Colomban P., Bowden B. (2004). Raman spectroscopic analysis of an English soft-paste porcelain plaque-mounted table. *Journal of Raman Spectroscopy*, **35**, 656–661.

Fabbri B., Gianti A. (2003). *L'avventura della ceramica*. Consiglio Nazionale delle Ricerche, Roma.

Farneti M. (1993). *Technical-historical glossary of mosaic art - with an historical survey of mosaic art*. Longo Editore, Ravenna.

Fiori C. (ed.) (1995). *Mosaico - analisi dei materiali e problematiche di restauro. Parte Prima*, vol. 4 of *Mosaico e restauro musivo*. CNR-IRTEC.

Galli S., Mastelloni M., Ponterio R., Sabatino G., Triscari M. (2004). Raman and scanning electron microscopy and energy-dispersive x-ray techniques for the characterization of colouring and opaquening agents in Roman mosaic glass tesserae. *Journal of Raman Spectroscopy*, **35**, 622–627.

Kock L. D., De Waal D. (2007). Raman studies of the underglaze blue pigment on ceramic artefacts of the Ming dynasty and of unknown origins. *Journal of Raman Spectroscopy*, **38**, 1480–1487.

Legodi M. A., de Waal D. (2007). Raman spectroscopic study of ancient South African domestic clay pottery. *Spectrochimica Acta Part A*, **66**, 135–142.

Leslie K. A. (2003). Identification of porcelain type using Raman spectroscopy. In *Ceramic in the Society - Proceedings of the 6th EMAC, Fribourg, Switzerland, 3-6 October 2001*. Di Pierro S., Serneels V., Maggetti M. (eds.), pp. 189–196. Earth Science Dept., University of Fribourg, Switzerland.

Liem N. Q., Sagon G., Quang V. X., Tan H. V., Colomban P. (2000). Raman study of the microstructure, composition and processing of ancient Vietnamese (proto)porcelains and celadons (13-16th centuries). *Journal of Raman Spectroscopy*, **31**, 933–942.

Liem N. Q., Thanh N. T., Colomban P. (2002). Reliability of Raman micro-spectroscopy in analysing ancient ceramics: the case of ancient Vietnamese porcelain and celadon glazes. *Journal of Raman Spectroscopy*, **33**, 287–294.

Lofrumento C., Zoppi A., Castellucci E. M. (2004). Micro-Raman spectroscopy of ancient ceramics: a study of French *sigillata* wares. *Journal of Raman Spectroscopy*, **35**, 650–655.

Lofrumento C., Zoppi A., Castellucci E. M. (2005). La spettroscopia micro-Raman: un "termometro mineralogico" nello studio delle ceramiche archeologiche. In *Tecnologia di lavorazione e impieghi dei manufatti*. Fabbri B., Gualtieri S., Volpe G. (eds.), Atti della 7^a Giornata di Archeometria della Ceramica, Lucera 10-11 Aprile 2003, pp. 21–28. EDIPUGLIA, Bari.

Marco de Lucas M. C., Moncada F., Rosen J. (2006). Micro-Raman study of red decorations in French faiences of the 18^{th} and 19^{th} centuries. *Journal of Raman Spectroscopy*, **37**, 1154–1159.

Marengo E., Aceto M., Robotti E., Liparota M. C., Bobba M., Pantò G. (2005). Archaeometric characterization of ancient pottery belonging to the archaeological site of Novalesa Abbey (Piedmont, Italy) by ICP-MS and spectroscopic techniques coupled to multivariate statistical tools. *Analytica Chimica Acta*, **537**, 359–375.

Miŏc U. B., Colomban P., Sagon G., Stojanović M., Rosić A. (2004). Ochre decor and cinnabar residues in Neolithic pottery from Vinča, Serbia. *Journal of Raman Spectroscopy*, **35**, 843–846.

Pérez J. M., Esteve-Tébar R. (2004). Pigment identification in greek pottery by Raman microspectroscopy. *Archaeometry*, **46**, 607–614.

Prinsloo L. C., Colomban P. (2007). A Raman spectroscopic study of the Mapungubwe oblates; glass trade beads excavated at an Iron Age archaeological site in South Africa. *Journal of Raman Spectroscopy*. In press (DOI: 10.1002/JRS.1816).

Prinsloo L. C., Wood N., Loubser M., Verryn S. M. C., Tiley S. (2005). Re-dating of Chinese celadon shards excavated on Mapungubwe Hill, a 13^{th} century Iron Age site in South Africa, using Raman spectroscopy, XRF and XRD. *Journal of Raman Spectroscopy*, **36**, 806–816.

Ricci C., Miliani C., Rosi F., Brunetti B. G., Sgamellotti A. (2007). Structural characterization of the glassy phase in majolica glazes by Raman spectroscopy: a comparison between Renaissance samples and replica processed at different temperatures. *Journal of Non-Crystalline Solids*, **353**, 1054–1059.

Rice P. M. (1987). *Pottery analysis - a sourcebook*. The University of Chicago Press, Chicago and London.

Sakellariou K., Miliani C., Morresi A., Ombelli M. (2004). Spectroscopic investigation of yellow majolica glazes. *Journal of Raman Spectroscopy*, **35**, 61–67.

Sandalinas C., Ruiz-Moreno S., López-Gil A., Miralles J. (2006). Experimental confirmation by Raman spectroscopy of a *Pb-Sn-Sb* triple oxide yellow pigment in sixteenth century Italian pottery. *Journal of Raman Spectroscopy*, **37**, 1146–1153.

Savage G., Newman H. (1992). *An illustrated dictionary of ceramics*. Thames and Hudson Ltd, London.

Sendova M., Zhelyaskov V., Scalera M., Ramsey M. (2005). Micro-Raman spectroscopic study of pottery fragments from the Lapatsa Tomb, Cyprus, ca 2500 BC. *Journal of Raman Spectroscopy*, **36**, 829–833.

Sendova M., Zhelyaskov V., Scalera M., Gulliford C. (2007). Micro-Raman spectroscopy characterization of Della Robbia glazes. *Archaeometry*, **49**, 655–664.

Smith D. C. (2006). A review of the non-destructive identification of diverse geomaterials in the cultural heritage using different configurations of Raman spectroscopy. *Special Publications*, **257**, 9–32.

Smith G. D., Clark R. J. H. (2001). Raman microscopy in art history and conservation science. *Reviews in Conservation*, **2**, 96–110.

Smith G. D., Clark R. J. H. (2004). Raman microscopy in archaeological science. *Journal of Archaeological Science*, **31**, 1137–1160.

Striova J., Lofrumento C., Zoppi A., Castellucci E. M. (2006). Prehistoric Anasazi ceramics studied by micro-Raman spectroscopy. *Journal of Raman Spectroscopy*, **37**, 1139–1145.

van der Weerd J., Smith G. D., Firth S., Clark R. J. H. (2004). Identification of black pigments on prehistoric Southwest American potsherds by infrared and Raman microscopy. *Journal of Archaeological Science*, **31**, 1429–1437.

Welter N., Schüssler U., Kiefer W. (2007). Characterisation of inorganic pigments in ancient glass beads by means of Raman microspectroscopy, microprobe analysis and X-ray diffractometry. *Journal of Raman Spectroscopy*, **38**, 113–121.

Wopenka B., Popelka R., Pasteris J. D., Rotroff S. (2002). Understanding the mineralogical composition of ancient Greek pottery through Raman microprobe spectroscopy. *Applied Spectroscopy*, **56**(10), 1320–1328.

Zoppi A., Castellucci E. M., Lofrumento C. (2005). Phase analysis of third millennium Syrian ceramics by micro-Raman spectroscopy. In *Raman spectroscopy in archaeology and art history*. Edwards H. G. M., Chalmers J. M. (eds.), pp. 217–227. Royal Society of Chemistry, Cambridge, UK.

Zoppi A., Lofrumento C., Castellucci E. M., Dejoie C., Sciau P. (2006). Micro-Raman study of aluminium-bearing hematite from the slip of Gaul *sigillata* wares. *Journal of Raman Spectroscopy*, **37**, 1131–1138.

Zoppi A., Lofrumento C., Castellucci E. M., Sciau P. (2007). Al-for-Fe substitution in hematite: the effect of low al concentrations in the Raman spectrum of Fe_2O_3. *Journal of Raman Spectroscopy*. In press (D.O.I. 10.1002/JRS.1811).

Zuo J., Xu C., Wang C., Yushi Z. (1999). Identification of the pigment in painted pottery from the Xishan site by Raman microscopy. *Journal of Raman Spectroscopy*, **30**, 1053–1055.

Zuo J., Zhao X., Wu R., Du G., Xu C., Wang C. (2003). Analysis of the pigments on painted pottery figurines from the Han Dynasty's Yangling tombs by Raman microscopy. *Journal of Raman Spectroscopy*, **34**, 121–125.

Chapter 2

Raman spectroscopy: theory and practice

Raman spectroscopy owes its name to the discoverer of the homonymic effect, the Indian scientist Chandrasekhara Venkata Raman (1888-1970), among the founders of scientific research in India, and Asia's first Nobel Prize winner in science. Early in 1928, after years of accurate experiments on the scattering of light, came his discovery of a "new radiation" as he simply called it, which was soon to be recognized as an entirely new phenomenon and named after him. C. V. Raman was then awarded the Nobel Prize in physics in 1930, remarkably soon after his discovery (Miller and Kauffman 1989).

Raman spectroscopy probes molecular and crystal lattice vibrations and therefore is sensitive to the composition, bonding, chemical environment, phase, and crystalline structure of the sample material. These characteristics make it an exceptional method for unambiguously identifying materials in any physical form: gases, liquids, solutions, and crystalline or amorphous solids. Raman spectroscopy has thus become an established technique for the study of cultural heritage materials over the past 20 years.

The first section of this chapter includes a brief theoretical description of the Raman effect; there follow details about the structure and Raman spectra of silicate glasses, and some specifications of the instrumentation, experimental methodologies and data processing procedures used during this work. The main advantages and limitations of Raman spectroscopy, especially regarding its applications to cultural heritage materials, are summarized at the end of the chapter.

2.1 The Raman effect

The basic theory of the Raman effect was developed long before its discovery; anomalies in the fluorescence emissions had in fact been described as early as 1878. Later on the effect itself had been repeatedly predicted by applying quantum mechanics to molecules (Schrader 1995, p. 3). When light quanta of energy $h\nu_0$ hit matter, a small fraction of the incident radiation is scattered, either elastically (Rayleigh scattering, fig. 2.1a) or inelastically, giving rise to emitted photons of energies either higher or lower than that of the incoming radiation: this is what is called the Raman effect. The photons emitted at the lower energy, $h\nu_0 - h\nu_1$, are called Stokes Raman photons (fig. 2.1b). The energy difference $h\nu_1$ arises from the energy lost from the incoming photon to promote the molecule into an excited vibrational level of the ground electronic state. Anti-Stokes Raman photons (fig. 2.1c) appear at the same energy difference in relation to the excitation line, but on the high-energy side of the Rayleigh photons. The intensities of anti-Stokes Raman bands are very weak, and temperature dependent (following the Boltzmann law). Consequently, Raman spectra reported in the literature commonly include only the Stokes portion.

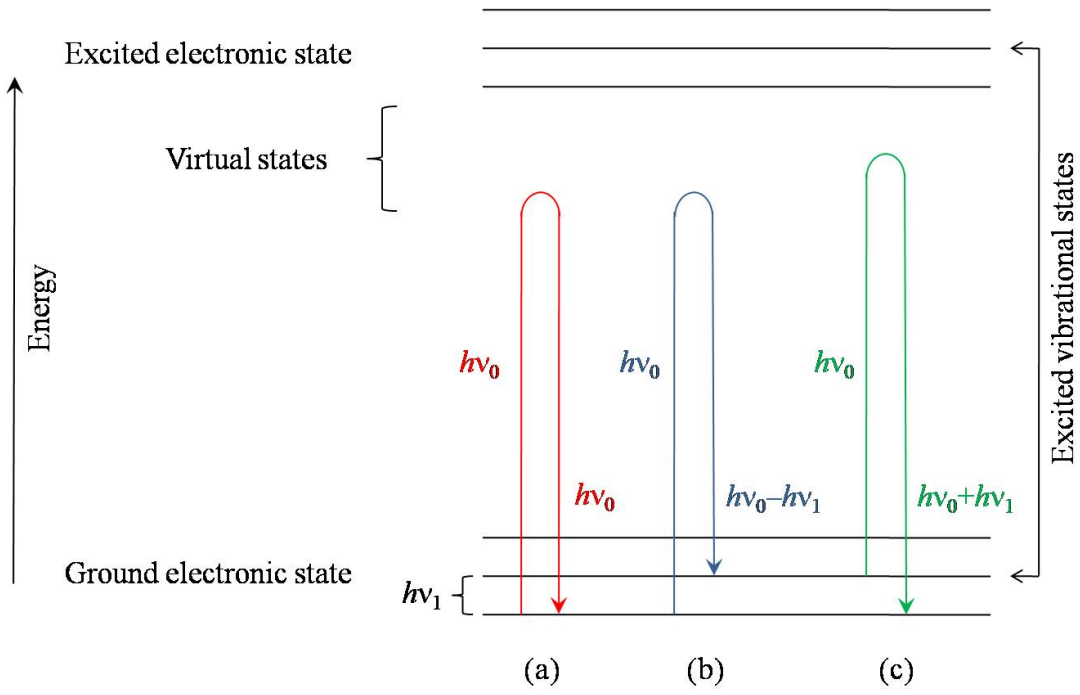

Figure 2.1: Schematic representation of the (a) Rayleigh, (b) Stokes Raman and (c) anti-Stokes Raman scattering effect

Figure 2.1 describes a single vibrational mode of a diatomic molecule. Other photons of potentially different energies, $h\nu_i$, will be generated by a polyatomic molecule for each of its i normal vibrational modes meeting the selection rules for Raman scattering. By spectrally sorting the Raman scattered photons generated from these Raman-active modes, a highly characteristic vibrational spectrum can be obtained for the molecule under study. In order to make Raman spectra easier to evaluate, frequency or even better wavenumber[1] shifts are usually recorded; the exciting radiation defining the zero of this recorded variable. The wavenumber shift for a Raman band is in fact constant, regardless of the excitation line used (which might affect only the relative intensity of lines), and it directly relates to the energy of the vibrational level being probed, $h\nu_i$. It is therefore analogous to the vibrational information provided by IR absorption spectroscopy, but complementary to it rather than identical, owing to the different selection rules governing Raman scattering (mandatory change in polarizability) and IR absorption (mandatory change in dipole moment). Further explanations of the physical laws governing Raman scattering, and exact calculations of the wavenumber positions and relative intensities of Raman bands can be found in a variety of reference books (e.g. Schrader 1995), and will therefore not be detailed here.

> *In crystalline solids, chemical units have fixed orientations which yield Raman spectra characterized by sharp bands, whose intensities may vary with orientation when dealing with single crystals. In the case of non-crystalline solids, however, the Raman effect is associated with the short-range vibration of molecular species, but the distribution of bonding forces and bond angles within the tetrahedral network causes the broadening and overlapping of the Raman bands. It is still possible to gain structural information on amorphous solids from the knowledge of the characteristic vibration frequencies of the short-range molecular species (such as silicate tetrahedra in silicate glasses). A brief description of the basic structure of glasses and of the interpretation of their Raman spectra is presented in the following section.*

[1] wavenumbers are commonly used to tabulate spectroscopic data, and can be defined in terms of wavelenghts ($\tilde{\nu} = 1/\lambda$) as well as in terms of frequencies ($\tilde{\nu} = \nu/c$, with c the velocity of light). They are measured in cm^{-1}.

2.2 The structure and Raman spectra of silicate glasses

Silicate glasses have a structure which is based on a network of SiO_4 tetrahedra (network formers), which displays a short-range order but no order at the medium and long-range due to the amorphous nature of the material, induced by the production process. Glass is in fact produced when a liquid is cooled fast enough to prevent the establishment of a thermodynamic equilibrium; in this case the viscosity increases up to the point where the liquid is "frozen" and the glass is formed.

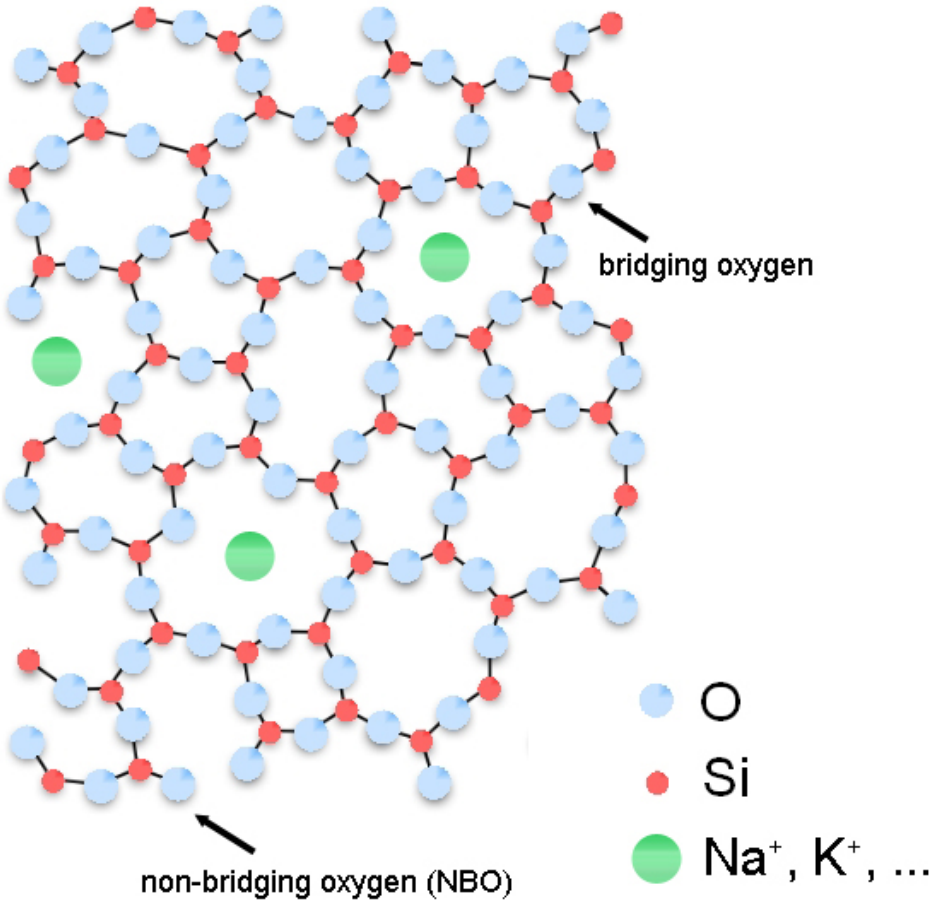

Figure 2.2: Schematic representation of the structure of alkali silicate glasses

In pure silica, the silicate network is structured in such a manner that every oxygen ion connects two tetrahedra (bridging oxygen). Incorporating into this structure cations of different nature, such as alkali or alkaline-earth metals (network modifiers), causes a

depolymerization of the network by breaking the *Si-O* connectivity, and by creating an ionic bond between the freed oxygen and the cation. Oxygens that are thus coordinated to cations in the silicate structure are called non-bridging oxygens (NBOs). A schematic representation of the structure of a basic alkali silicate glass is given in figure 2.2. In practical terms, the addition of alkali ions (Na^+, K^+) lowers the melting temperature of the glass and improves its workability by diminishing the viscosity; such elements then assume the role of "fluxes". Alkaline-earths (Ca^{2+}, Mg^{2+}) and/or aluminium ions also slightly decrease the viscosity, but their main role is to stabilize the glass against alteration, hence the name of "stabilisers" for such elements. Moreover, they can act as charge-compensating ions for cations such as Al^{3+} and Fe^{3+} which can substitute Si as network formers.

The degree of polymerization, directly linked to the amount and nature of the modifier ions, greatly affects the physical properties of the glass, and it can be quantified as the average number of NBOs per tetrahedrally coordinated cation, basically represented by NBO/Si in silicate glasses. Due to the presence of modifier species, different types of tetrahedral coordinations can be found "locally" in the glass network, and are commonly indicated by the notation Q_n, where n is the number of bridging oxygens, varying between 0 and 4. Thus the Q_4 coordination corresponds to silicate species with zero NBOs, Q_3 to species with one NBO, and so forth. These localized structures reflect those found in the different classes of crystalline silicates:

- nesosilicates, formed by isolated SiO_4 tetrahedra (coordination Q_0);
- sorosilicates, formed by couples of tetrahedra $(Si_2O_7)^{6-}$ (coordination Q_1);
- cyclosilicates, formed by rings of 3, 4 or 6 tetrahedra e.g. $(Si_6O_{18})^{12-}$ (coordination Q_2);
- inosilicates, formed by simple or double chaines of tetrahedra, in $(SiO_3)^{2-}$, $(Si_4O_{12})^{8-}$, and $(Si_4O_{11})^{6-}$ groups (coordination Q_2);
- phyllosilicates, formed by sheets of tetrahedra in hexagonal groups $(Si_4O_{10})^{4-}$ (coordinations Q_2 and Q_3, depending on the degree of substitution);
- tectosilicates, formed by a three-dimensional network of interconnecting SiO_4 tetrahedra (coordinations Q_3 and Q_4, depending on the degree of substitution).

Modelization and interpretation of the spectra

Beginning in the 1950s, a large number of articles have been published regarding the Raman spectroscopic study of silicate glasses, whose structure was interpreted in terms of a three-dimensional network of SiO_4 units (cfr. the detailed review of McMillan (1984)). The structural classification of crystalline silicates was well established, and soon silicate materials were described in terms of structural units with the concept of NBO/Si = 4, 3, 2, 1 and 0. Since 1980, the Raman spectra of glasses were decomposed following a model which saw them as the enveloping curve of a series of Gaussian-shaped bands (Mysen *et al.* 1980, 1982). Starting in 1985, studies were issued which concerned the investigation of sol-gel synthesis by means of Raman spectroscopy and Nuclear Magnetic Resonance (NMR) (Colomban 1996). It was then that the Q_n notation first appeared, but only within the description of NMR spectra of silicate glasses. It was finally in 1999-2000 that this formulation was used also for Raman spectra, in three works which appeared almost at the same time, but regarding three completely different domains (Li *et al.* 2000; Liem *et al.* 2000; Zotov *et al.* 1999).

The Raman spectrum of an amourphous material displays broad peaks owing to the distribution of local environments in its structure. More specifically, the spectra of silicate glasses are mainly due to the two most intense vibrational modes of the SiO_4 unit: the symmetric stretching ν_s, and a bending mode (δ_s). Numerous studies have in fact shown how these spectra are characterized by two "massifs", one centred at about 500 cm^{-1}, and the other at about 1000 cm^{-1}, as shown by the sample spectrum in figure 2.3. The interpretation of this kind of spectra was developed based on the assignment of the vibrational components of vitreous silica. The large "massif" in the region between 300 and 600 cm^{-1} is associated with the bending vibrations of the polymerized structure, that is the motions of the bridging oxygens in the plane bisecting the Si-O-Si bonds (δ Si-O). Another small band centered at 800 cm^{-1} is only slightly affected by compositional and structural changes, and it corresponds to the motion of silicon against its tetrahedral oxygen cage. Finally, the region between 900 and 1300 cm^{-1} is associated with the stretching vibrations of mostly depolymerized silicate species, containing different numbers of NBOs, which give rise to the appearance of an average of five bands which form the so-called "stretching massif" (ν Si-O). Each of these bands is associated with the contribution of species having different Q_n configurations. It is to be underlined that, while five spectral

components are also expected to contribute to the bending massif, our comprehension of its exact structure is not by far achieved yet.

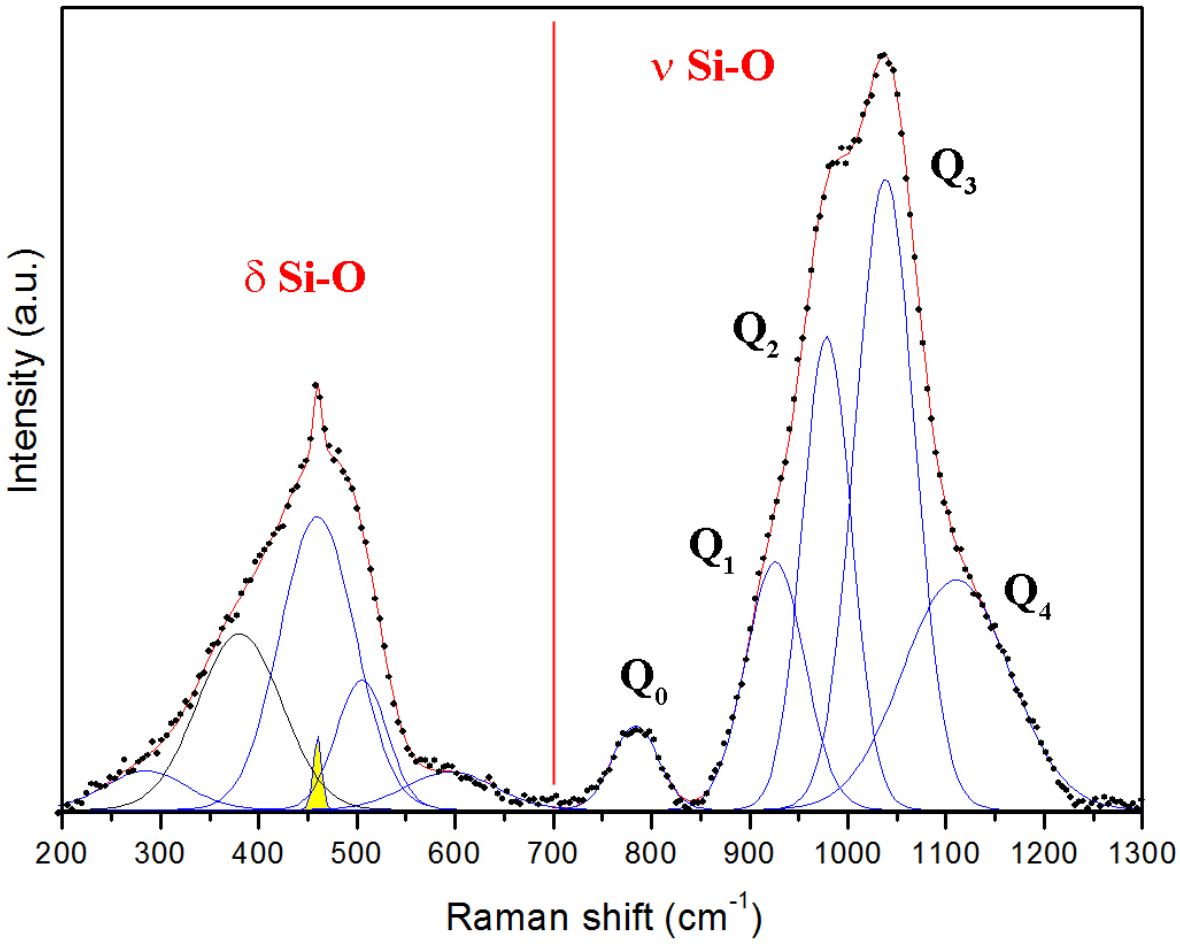

Figure 2.3: Sample Raman spectrum of a silicate glass, with indication of the bending (δ *Si-O*) and stretching (ν *Si-O*) massifs, and band deconvolution. The yellow band indicates a spectral contribution from a crystalline species.

2.3 Instrumentation, experimental conditions and data processing methods

Instrumentation used

Several different Raman spectrometers have been used during the course of this work; all but one of them belong to the LADIR and will be described in this section. The last one belongs to the Industrial Chemistry Dept. of the University of Bologna. It was used to analyze some of the pottery samples, and its characteristics will be detailed in chapter 3, in the sections devoted to the results obtained on these materials.

The availability of numerous instruments gave, among other things, the possibility to test the suitability of each of them (in terms of e.g. laser power and colour, experimental setup, ...) for the analysis of each kind of material. Different instruments bear in fact different optics, which affect the acquired spectra; moreover, the type of filter used determines the wavenumber position at which the spectrum is "cut" (in order to keep out the Rayleigh line). Finally, different colours of the laser produce varying backgrounds. All these parameters, together with the availability of different configurations (macro vs. micro) have to be taken into account when choosing the spectrometer for the analysis of a specific sample.

A Jobin Yvon Labram Infinity (LI) spectrometer was used, which is co-owned by the LADIR and the C2RMF (Centre de Recherche et de Restauration des Musées de France) and is of rather limited size and weight, allowing to move it if necessary from one lab to the other. It is equipped with a green Nd:YAG laser at 532 nm of 10 mW maximum power, a grating with 1800 lines/mm, a high sensitivity Notch filter, a CCD detector cooled to 200 K and a motorised table for mapping analyses (fig. 2.4). The instrumental resolution is of about 2.5 cm^{-1}, and the acquisition is made in a single spectral window ranging from 200 to 1600 cm^{-1}. The instrument is coupled to a microscope with several objectives, namely 5x, 10x, 50x and 100x (yielding a total magnification of 50, 100, 500 and 1000 times, respectively). Most acquisitions have been made using the 50x objective; in these case the analyzed surface area is equal to about 5×5 μm^2, for a probed depth of approximately 10 μm.

Some measures were performed with a Dilor XY spectrometer, equipped with a green Ar^+/Kr^+ laser at 514.5 nm (30 mW maximum power), a grating with 1800 lines/mm,

a CCD detector cooled to 140 K and a motorised table for cartographic analyses (fig. 2.5). This instrument can be used in macroscopic configuration, but it is also coupled with a microscope: the available objectives are the same listed above. The instrumental resolution attains 0.5 cm^{-1}, and the acquisition is made in two steps, scanning two partially overlapping spectral windows: 100-1000 and 600-1400 cm^{-1}. This instrument will be hereafter referred to as (Dilor) XY1 in order to distinguish it from a second Dilor XY spectrometer which was also used (XY2), working in macroscopic configuration. This one is equipped with a violet Ar^{+} laser at 406.7 nm (1 W maximum power at source), a grating with 2400 lines/mm, and a CCD detector cooled to 77 K (fig. 2.6). In this case the analyzed volume is about 0.3×0.3×0.3 mm^3, the resolution reaches 0.5 cm^{-1}, and the acquisition is also made scanning two spectral ranges: 30-980 and 500-1400 cm^{-1}. Spectra acquired with this instrument often present some "parasite" peaks (*plasma* peaks) at 125, 188 and sometimes 252 cm^{-1}, which are due to the laser light not being completely monochromatic. They must be correctly identified before interpreting the spectra in terms of Raman signatures of crystalline phases.

Both Dilor instruments filter out the Rayleigh line by means of a double monochromator, which yields a lower sensitivity if compared to a Notch filter, but allows reaching the low wavenumber region, down to a few cm^{-1}.

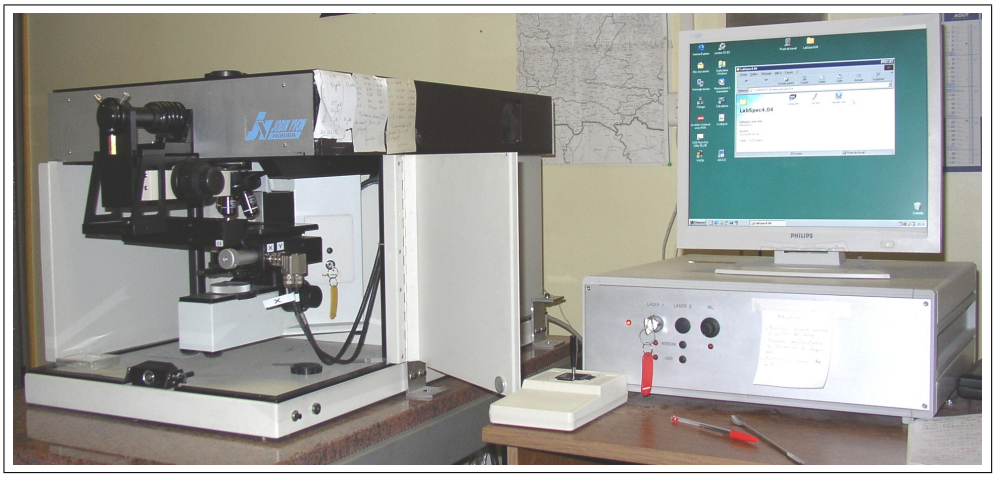

Figure 2.4: The Jobin Yvon Labram Infinity (LI) spectrometer at the LADIR, working in microscopic configuration

Figure 2.5: The Dilor XY1 spectrometer at the LADIR, suitable for working both in microscopic and macroscopic configuration

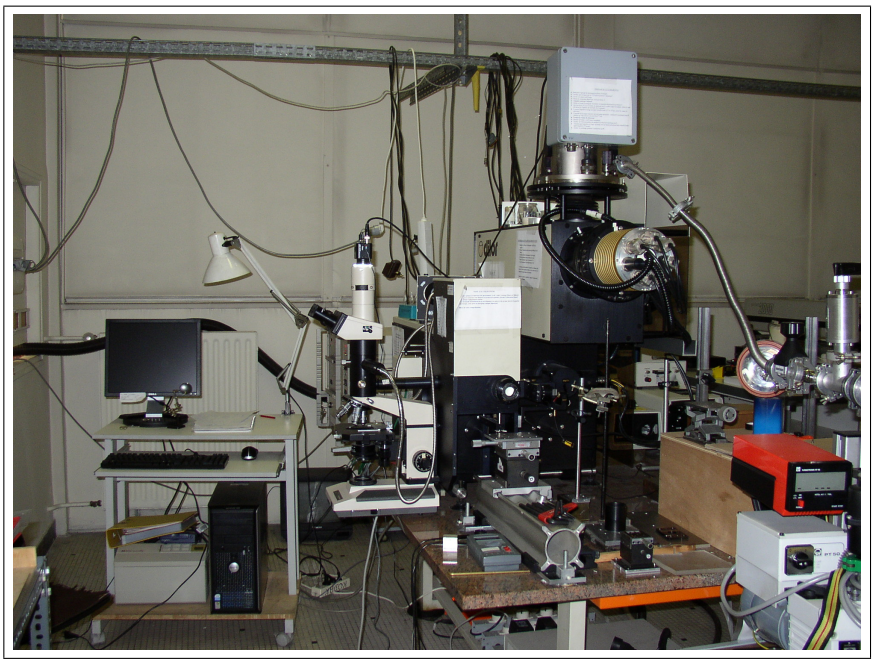

Figure 2.6: The Dilor XY2 spectrometer at the LADIR, working in macroscopic configuration

Experimental conditions

Acquisition times were always reasonably short, ranging from a few seconds to about 5 minutes for each accumulation, with the exception of measures made with the Dilor XY1, which could last up to 1 hour in order to get a good enough signal. The practical limit to exposure time is set by the so-called "spike noise", which is generated by cosmic rays as well as possible γ- and α-rays emitted from materials around the chip of the CCD detector, and which was often identified in Dilor XY1 spectra. A total of 2-16 accumulations were recorded for each spectrum, in order to reduce the relevance of background noise and fluorescence.

Thanks to the real-time acquisition of the spectra, brief tests were made on numerous spots for each sample. Only a few spectra, representative of phases which appeared to be most present in the sample material, were actually recorded, allowing a longer acquisition time, and saved to file. Spectra were also recorded when peculiar even though rare signatures were observed, which might be interesting in view of a differentiation between samples. It should be pointed out how the choice of "representative" spectra, considered as "significant" ones, is by no means straightforward. It is rather a most critical phase of the whole experimental process, whose standardization would be important in order to give Raman spectroscopy a more "quantitative" character.

Besides fluorescence, another interfering phenomenon which was observed during acquisitions with the Dilor XY1 instrument was the appearance in the spectra of bands due to the protective coating of the microscope's objective, at 844, 895 and 921 cm^{-1} (cfr. also Bouchard-Abouchacra 2001, p. 31). They were most often observed when using a high laser power, such as when analyzing porcelain glazes (intensity at source $\sim 0.5\ W$), and when analyzing poor scatterer compounds.

Finally, the low-wavenumber portion of glassy spectra is sometimes interested by the so-called "boson peak", partially visible in the spectrum of figure 2.7. It has been interpreted as being due to inhomogeneities in the structure of the glass and it is usually fitted to a Lorentzian band, but its origin and modelization are still a matter of discussion (Champagnon *et al.* 2000; McIntosh *et al.* 1997).

Figures 2.8 and 2.9 show typical experimental configurations used with the Dilor XY1 and XY2 while analyzing the 18^{th} century porcelain artefacts described in chapter 4. The spots of the green and violet lasers are clearly visible on the white surfaces of some of the objects; the "effective" laser spot is however much smaller than its visible halo.

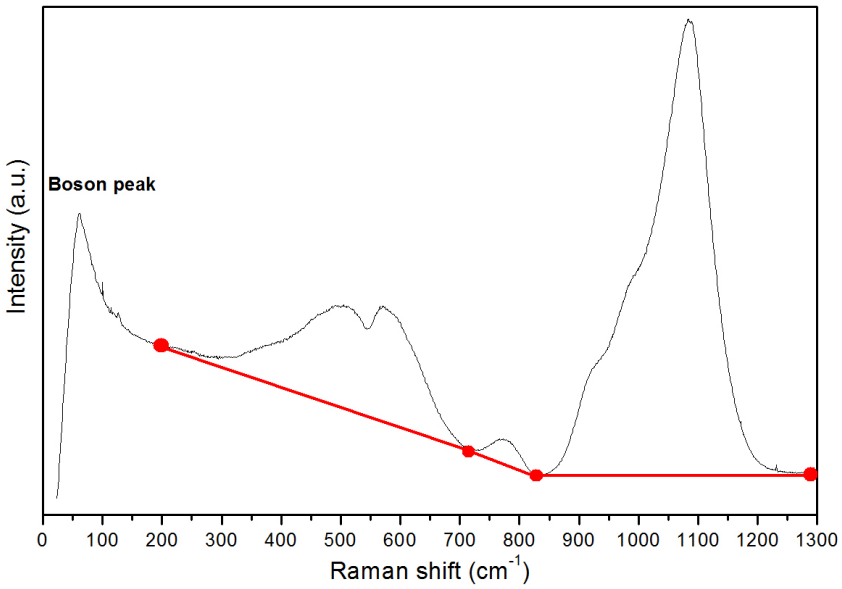

Figure 2.7: Raw Raman spectrum of an alkali-silicate glass. The boson peak is partially visible at low wavenumbers. The red segments indicate the linear baseline to be subtracted.

Data processing methods

Raman spectroscopy is mostly used as a "fingerprinting" technique, that is to say that materials, especially crystalline ones, are identified by comparing their characteristic vibrational spectra with those present in a database, similarly to the procedure employed for X-ray diffraction. Reference libraries of Raman spectra for different materials, some of which directly related to cultural heritage studies, are available in the literature (cfr. among others Bell *et al.* 1997; Bouchard and Smith 2003, 2005; Burgio and Clark 2001; Griffith 1975; Schubnel *et al.* 1992), and numerous searchable databases are offered for free consultation on the internet (Caltech; ENS Lyon; RASMIN; RRUFF Project; University College London; University of Firenze; University of Parma).

When spectra are collected in two intervals, the same Labspec software used for the acquisition is also used to combine them. Spectra relative to glasses and glazes are further treated in two successive steps: first of all, a linear baseline is subtracted in the region of interest. Such line is defined by connecting a minimum of four points (usually around

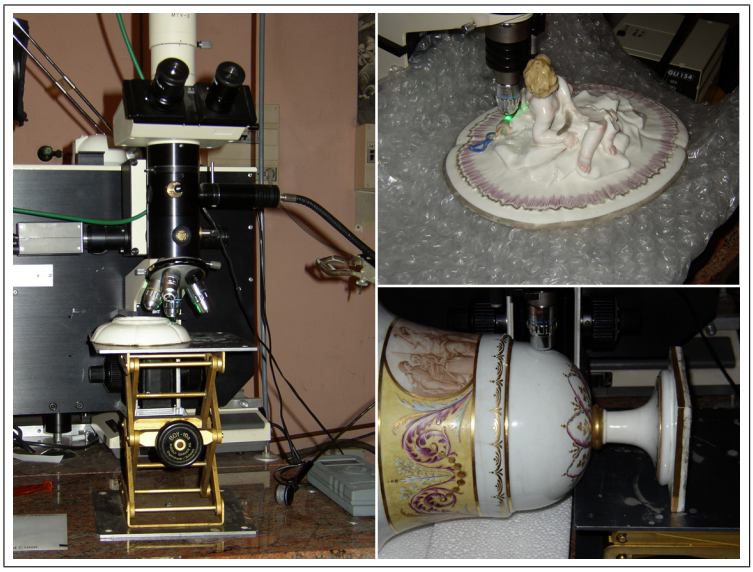

Figure 2.8: Typical experimental configurations used while acquiring Raman spectra with the Dilor XY1 spectrometer

Figure 2.9: Typical experimental configurations used while acquiring Raman spectra with the Dilor XY2 spectrometer

200, 700, 850 and 1300 cm^{-1}, cfr. fig. 2.7), where the intensity of the Raman signal is lowest, between two adjacent regions of a glassy spectrum. More points are added in between if the defined baseline crosses the spectrum. The Peak Fitting Module of the Microcal Origin software is then used to decompose the two "massifs" which make up the spectrum into a certain number of bands, following a deconvolution model based on the description of silicate glasses presented in section 2.2 (cfr. also figure 2.3), which has been already used in numerous occasions (e.g. Colomban and Milande 2006; Colomban *et al.* 2004; Ricci *et al.* 2007). A more refined version of this model has been recently developed (Robinet *et al.* 2006) especially for alkali silicate glasses, and it has been applied during this work to a series of Roman age mosaic *tesserae*, as reported in chapter 5.
Such deconvolution of the glassy spectrum allows calculating a series of "Raman parameters", which can be used effectively to compare different materials. Among the most useful are the wavenumber positions of the Q_n bands and of the maxima of the bending and stretching massifs (δ_{MAX} *Si-O* and ν_{MAX} *Si-O*, respectively). Also the so-called "polymerization index", calculated as the ratio of the areas of the two massifs ($I_p = A_{500}/A_{1000}$), has often been successfully related to the composition and structure of the analyzed glass (Colomban 2003).

> *The characteristics that make Raman spectroscopy such a well qualified technique for the analysis of cultural heritage materials include its molecular specificity, non-destructiveness, non invasivity, high spatial and spectral resolution, in situ analysis, portability, applicability to samples of large or non-uniform shape, and relative immunity to interference. Also, it can be applied to a wide range of materials, including organic and inorganic solids, and it can probe heterogeneous media or mixtures on a micrometric scale. Moreover, Raman spectroscopy is capable of differentiating between the polymorphic forms of a mineral species, and it gives at the same time some information on the physical structure and the qualitative elemental composition of the analyzed material.*
>
> *There are of course also some limitations, such as the high fluorescence signal arising in some materials, especially those who have been long buried, such as archaeological ceramics. It is not totally clear, up to now, what are the exact sources of this intense background. There are also difficulties in making this technique quantitative, due e.g. to the small surface it probes, and to the fact that its sensitivity strongly depends on the polarizability of the analyzed*

molecules. This yields, for example, an extremely good capacity to detect minimal amounts of anatase and rutile (TiO_2), and on the other hand a very low sensitivity towards cristobalite and trydimite (SiO_2). It is also not a suitable technique for the analysis of every single kind of cultural heritage material; for example nearly all pure metals are Raman silent, and some pigments are quite unstable under the local heating due to the impingement of the laser light.

2.4 References

Bell I. M., Clark R. J. H., Gibbs P. J. (1997). Raman spectroscopic library of natural and synthetic pigments (pre-∼1850 AD). *Spectrochimica Acta Part A*, **53**, 2159–2179.

Bouchard M., Smith D. C. (2003). Catalogue of 45 reference Raman spectra of minerals concerning research in art history or archaeology, especially on corroded metals and coloured glass. *Spectrochimica Acta Part A*, **59**, 2247–2266.

Bouchard M., Smith D. C. (2005). Database of 74 Raman spectra of standard minerals of relevance to metal corrosion, stained glass or prehistoric rock art. In *Raman spectroscopy in archaeology and art history*. Edwards H. G. M., Chalmers J. M. (eds.), pp. 429–464. Royal Society of Chemistry, Cambridge, UK.

Bouchard-Abouchacra M. (2001). *Evaluation des capacités de la microscopie Raman dan la caractérisation minéralogique et physico-chimique de matériaux archéologiques: métaux, vitraux et pigments*. Ph.D. Thesis, Museum National d'Histoire Naturelle, Laboratoire de Minéralogie.

Burgio L., Clark R. J. H. (2001). Library of FT-Raman spectra of pigments, minerals, pigment media and varnishes, and supplement to existing library of Raman spectra of pigments with visible excitation. *Spectrochimica Acta Part A*, **57**, 1491–1521.

Caltech. `http://minerals.gps.caltech.edu/`. Mineral spectroscopy server.

Castro K., Pérez-Alonso M., Rodríguez-Laso M. D., Fernández L. A., Madariaga J. M. (2005). On-line FT-Raman and dispersive Raman spectra database of artists' materials (e-VISART database). *Analytical and Bioanalytical Chemistry*, **382**, 248–258.

Champagnon B., Chemarin C., Duval E., Le Parc R. (2000). Glass structure and light scattering. *Journal of Non-Crystalline Solids*, **274**, 81–86.

Colomban P. (1996). Raman studies of inorganic gels and of their sol-to-gel, gel-to-glass and glass-to-ceramics transformation. *Journal of Raman spectroscopy*, **27**, 747–758.

Colomban P. (2003). Polymerization degree and Raman identification of ancient glasses used for jewelry, ceramic enamels and mosaics. *Journal of Non-Crystalline Solids*, **323**, 180–187.

Colomban P., Milande V. (2006). On-site Raman analysis of the earliest known Meissen porcelain and stoneware. *Journal of Raman Spectroscopy*, **37**, 606–613.

Colomban P., Milande V., Le Bihan L. (2004). On-site Raman analysis of Iznik pottery glazes and pigments. *Journal of Raman Spectroscopy*, **35**, 527–535.

ENS Lyon. `http://www.ens-lyon.fr/LST/Raman/index.php`. Laboratoire de Sciences de la Terre.

Griffith W. P. (1975). Raman spectroscopy of terrestrial minerals. In *Infrared and Raman spectroscopy of lunar and terrestrial minerals*. Karr, Jr. C. (ed.), pp. 299–323. Academic Press, New York.

Li H., Su Y., Vienna J. D., Hrma P. (2000). Raman spectroscopic study - Effects of B_2O_3, Na_2O, and SiO_2 on nepheline ($NaAlSiO_4$) crystallization in simulated high-level waste glasses. *Ceramic Transactions*, **107**, 467–475.

Liem N. Q., Sagon G., Quang V. X., Tan H. V., Colomban P. (2000). Raman study of the microstructure, composition and processing of ancient Vietnamese (proto)porcelains and celadons (13-16th centuries). *Journal of Raman Spectroscopy*, **31**, 933–942.

McIntosh C., Toulouse J., Tick P. (1997). The Boson peak in alkali silicate glasses. *Journal of Non-Crystalline Solids*, **222**, 335–341.

McMillan P. (1984). Structural studies of silicate glasses and melts - applications and limitations of Raman spectroscopy. *American Mineralogist*, **69**, 622–644.

Miller F. A., Kauffman G. B. (1989). C. V. Raman and the discovery of the Raman effect. *Journal of Chemical Education*, **66**(10), 795–801.

Mysen B. O., Virgo D., Scarfe C. M. (1980). Relations between the anionic structure and viscosity of silicate melts - a Raman spectroscopic study. *American Mineralogist*, **65**, 690–710.

Mysen B. O., Finger L. W., Virgo D., Seifert F. A. (1982). Curve-fitting of Raman spectra of silicate glasses. *American Mineralogist*, **67**, 686–695.

RASMIN. `http://riodb.ibase.aist.go.jp/rasmin/`. National Institute of Advanced Industrial Science and Technology.

Ricci C., Miliani C., Rosi F., Brunetti B. G., Sgamellotti A. (2007). Structural characterization of the glassy phase in majolica glazes by Raman spectroscopy: a comparison between Renaissance samples and replica processed at different temperatures. *Journal of Non-Crystalline Solids*, **353**, 1054–1059.

Robinet L., Coupry C., Eremin K., Hall C. (2006). The use of Raman spectrometry to predict the stability of historic glasses. *Journal of Raman Spectroscopy*, **37**, 789–797.

RRUFF Project. `http://rruff.geo.arizona.edu/rruff/`. University of Arizona and Caltech.

Schrader B. (ed.) (1995). *Infrared and Raman spectroscopy - methods and applications*. VCH Publishers, Weinheim, Germany.

Schubnel H. J., Pinet M., Smith D. C., Lasnier B. (1992). *La microsonde Raman en gemmologie*. Revue de gemmologie A. F. G., Numéro hors série. Association française de gemmologie, Paris.

University College London. `http://www.chem.ucl.ac.uk/resources/raman/index.html`. Chemistry Dept.

University of Firenze. `http://srv.chim.unifi.it/raman/`. Chemistry Dept.

University of Parma. `http://www.fis.unipr.it/phevix/ramandb.html`. Physics Dept.

Zotov N., Ebbsjö I., Timpel D., Keppler H. (1999). Calculation of Raman spectra and vibrational properties of silicate glasses: comparison between $Na_2Si_4O_9$ and SiO_2 glasses. *Physical Review B*, **60**(9), 6383–6397.

Chapter 3

Raman studies on ancient pottery

While the archaeometric study of pottery benefits from the availability of numerous analytical techniques, our knowledge of ancient manufacturing processes and of the sources of raw materials is far from being exhaustive. This chapter illustrates three cases in which Raman spectroscopy has been used as a complement to answer specific questions posed by different kinds of ceramic materials.

A study has been undertaken on the possibility to use the polimorphic transition of titanium dioxide as a firing temperature marker within non-calcareous ceramics. Also, the slips and decorations of Neolithic pottery from Romania have been investigated, as well as those of several samples of Renaissance "sgraffito" pottery from Italy. In both cases the aim of the study was to characterize such coating layers in a non-destructive way, in order to add some information on their production process, and on the possible sources of raw materials.

3.1 Firing temperature determination

Firing temperature determination is among the most difficult tasks in ancient pottery studies. The knowledge of the thermal treatment of ceramic artefacts provides the experts with precious information about social, economic and cultural characteristics of the society that produced them. But firing conditions in ancient times were liable to great variation even within the same production, and also not all materials carry a distinct trace of the thermal treatment they underwent during pottery making. In particular,

low fired and/or non calcareous ceramic pastes do not show the new Ca-phases which are often effectively used as temperature markers. A detailed bibliographic review shows that several different techniques have so far been used in archaeometric studies in order to evaluate firing temperatures, and more in general the firing conditions of archaeological pottery artefacts (Fabbri 1998). Amongst them, most notably are X-ray diffraction for the analysis of crystalline phases (Cultrone *et al.* 2001; Maniatis *et al.* 2002), thermal analyses (Moropoulou *et al.* 1995), SEM observations (Wolf 2002), colour measures (Mirti and Davit 2004), FT-IR analysis (Artioli *et al.* 2000; De Benedetto *et al.* 2002) and Mössbauer spectroscopy (Wagner and Wagner 2004). Phase analysis is probably the main method for studying ceramic technology; this work aims at adding different perspectives to previous well-known studies on widely used kinds of clays (Maggetti 1982, and references therein) by applying different techniques. In trying to develop a mineralogical thermometer for low fired and/or non-calcareous materials, we focused on the study of the transition between two of the polymorphs of titanium dioxide, anatase and rutile. This transition has so far been reported to take place over a range of temperatures as great as 600°C (Gennari and Pasquevich 1998; Ghosh 2001; Rodrìguez-Talavera 1997), in studies generally not dedicated to pottery analysis. The same transition has nonetheless been used as a firing temperature marker (Liem *et al.* 2000; Lofrumento *et al.* 2005). We used Raman spectroscopy for the detection of TiO_2, because this technique has long proved its great effectiveness in the detection of titanium compounds (Murad 1997, 2003). We also chose to use Mössbauer spectroscopy to follow in detail the evolution of iron compounds. This methodology has often been effectively used for detailed analysis of iron compounds modifications in raw and fired clays (Häusler 2004; Murad 1998; Nodari *et al.* 2004). Data presented in this section have been presented at the EMAC'05 conference in Lyon, and published on its proceedings (Ricciardi *et al.* 2007).

3.1.1 Test materials and analytical methodology

Two different raw materials (one illitic clay named "Sala10" and one kaolin named "C1641") were characterized and used to prepare sets of laboratory specimens. From the mineralogical point of view, the illitic clay is mainly made up of quartz and illite; accessory phases, present in small quantities, are plagioclase, K-feldspar, chlorite, kaolinite, illite-smectite mixed layers and hematite. The kaolin is mainly composed of kaolinite, with small quantities of quartz and illite. Their chemical composition is reported in table 3.1.

	SiO_2	Al_2O_3	TiO_2	Fe_2O_3	MnO	MgO	CaO	Na_2O	K_2O	P_2O_5	L.O.I.
C	62.04	22.76	1.02	6.99	0.10	1.97	1.38	0.88	2.67	0.19	12.77
K	53.68	43.09	1.09	1.29	0.01	0.14	0.16	0.08	0.41	0.05	13.54

Table 3.1: Chemical composition of the illitic clay (C) "Sala10" and of the kaolin (K) "C1641" (weight % oxides normalized to 100 without L.O.I.)

Both materials were hand shaped in small disks about 3 cm in diameter and 0.4 cm thick. Sets of three such disks were kiln fired in an oxidising atmosphere, at temperatures between 600°C and 1100°C for the illitic clay, and between 800°C and 1100°C for the kaolin, in steps of 50°C. Powders were obtained by crushing in an agate mortar a mixture of fragments taken from each of the three pieces fired at each temperature; each sample obtained was then characterized by means of XRD and Raman spectroscopy. Mössbauer analyses at $298K$ were also performed only on the illitic clay samples, because kaolinitic ones do not contain a significant amount of iron. Illitic clay samples fired at the highest temperatures ($\geq$ 1050°C) developed an extensive "black core" associated with an obvious swelling (Emiliani and Corbara 1999, p. 345, 502). In these cases, powders for Mössbauer analysis were prepared by discarding the black zones, where iron is present in a highly reduced form, because they do not represent the oxidising firing conditions. Samples of the illitic clay were also pit fired, in a first attempt to simulate ancient pottery production conditions. In order to evaluate the maximum firing temperature reached in the pit, some of these samples had been previously kiln fired respectively at 650°C, 700°C and 750°C. If the temperature reached in the pit exceeded that of the previous firing, some transformations should be observed. XRD and Raman analyses were performed on all samples.

X-ray diffraction analyses were performed with a 300 W power Miniflex instrument with Cu anode. We scanned an angular interval from 6° to 55° 2 θ, excluding the central part (26° to 30° 2 θ), which contains the main peak of quartz and has been eliminated to allow easier identification of minor peaks (cfr. figures 3.1 and 3.4). Measurements were made, with a step of 0.02° and an acquisition time of 3 sec at each point. The identification of the crystalline phases was carried out by a comparison with JCPDS data sheets. Raman analyses were made at the Industrial Chemistry Dept. of the University of Bologna, with the collaboration of Prof. G. Di Lonardo and Dr. F. Ospitali; Raman

spectra were collected using a Renishaw RM1000 spectrometer with a green Ar^+ laser (λ = 514.5 nm) and maximum power of 3.5 mW. A small quantity of powder from each sample was optically examined through the microscope coupled to the instrument and then analyzed in 10 to 20 spots, from which a few representative spectra were collected for data analysis. Mössbauer spectra were collected at the Chemical Science Dept. of the University of Padova by Dr. L. Nodari and Prof. U. Russo. Mössbauer data were collected at $298K$ by means of a conventional instrument with constant acceleration velocity and a ^{57}Co source in a Rh matrix, using a proportional counter as a γ-ray detector. The spectra were fitted with a procedure which interpolates experimental data by means of Lorentzian functions. A small quantity of powder (about 80 mg) from each sample was mixed with vaseline and inserted into the sample holder. Each measurement took one to two days; therefore only a limited number of samples could be studied by this method.

3.1.2 Results on illitic clay samples

A comparative plot of X-ray diffractograms of the illitic clay (fig. 3.1) shows that quartz seems only slightly affected by the temperature rise, and that clay minerals disappear by 900°C, while cristobalite starts forming above 950°C and mullite around 1050°C. The traces of hematite which were present in the raw material become more evident as the temperature (T) increases, most notably above 800°C. The spinel-type phase which is weakly visible by XRD at the highest firing temperatures most likely corresponds to hercynite, whose presence is not interesting, because it has to be related to the "black core".

The evolution of Fe-compounds can be followed in greater detail by examining the Mössbauer spectra shown in figure 3.2; the one corresponding to the raw material shows a sextet due to a well crystallized oxide (hematite), together with paramagnetic absorption peaks which have been fitted with one $Fe(III)$ and one $Fe(II)$ sixfold sites. At 600°C the complete oxidation of $Fe(II)$ promotes the formation of a new $Fe(III)$ site which disappears above 850°C, when there is a rearrangement of the silicate framework. In the spectra shown, this phenomenon is first indicated by the widening of the central doublet between these two temperatures. The amount of hematite grows clearly between 800°C and 1000°C.

A synthesis of the experimental data on the illitic clay, including those from Raman

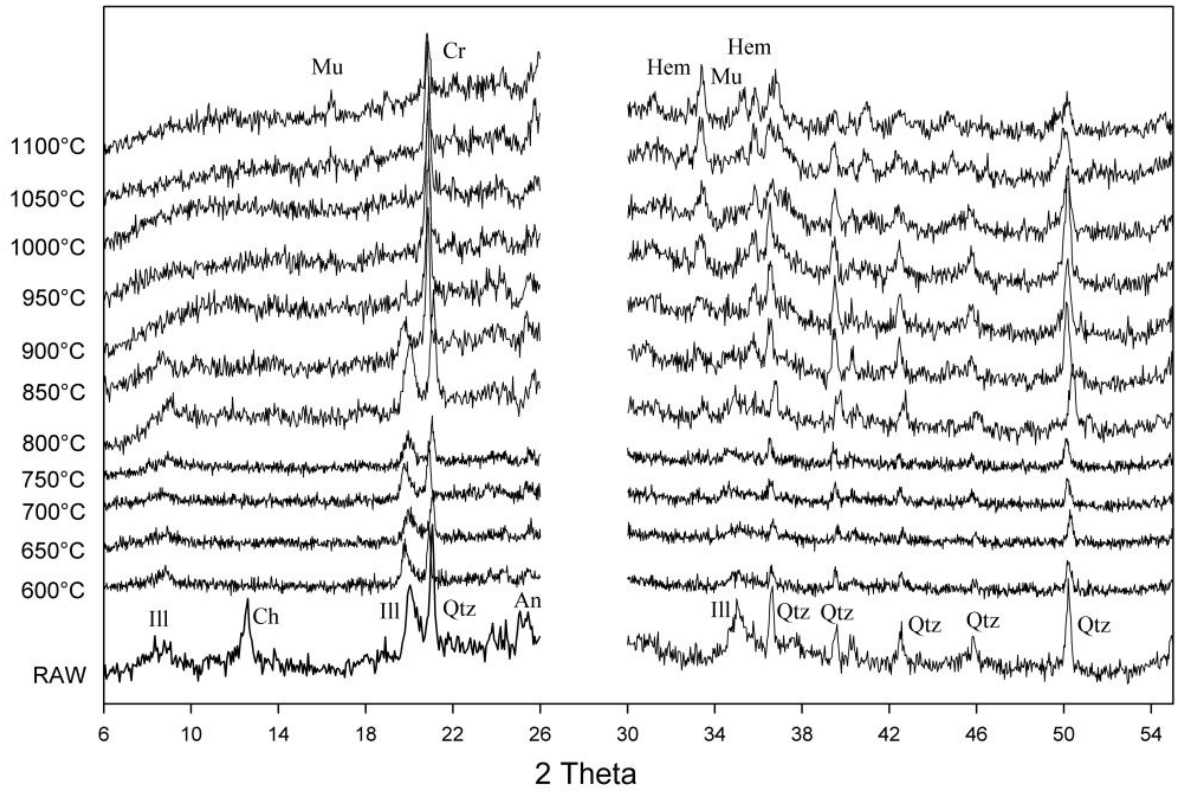

Figure 3.1: Comparative plot of XRD analyses on the illitic clay samples (Qtz: quartz, Ill: illite, Ch: chlorite, An: anatase, Hem: hematite, Mu: mullite, Cr: cristobalite)

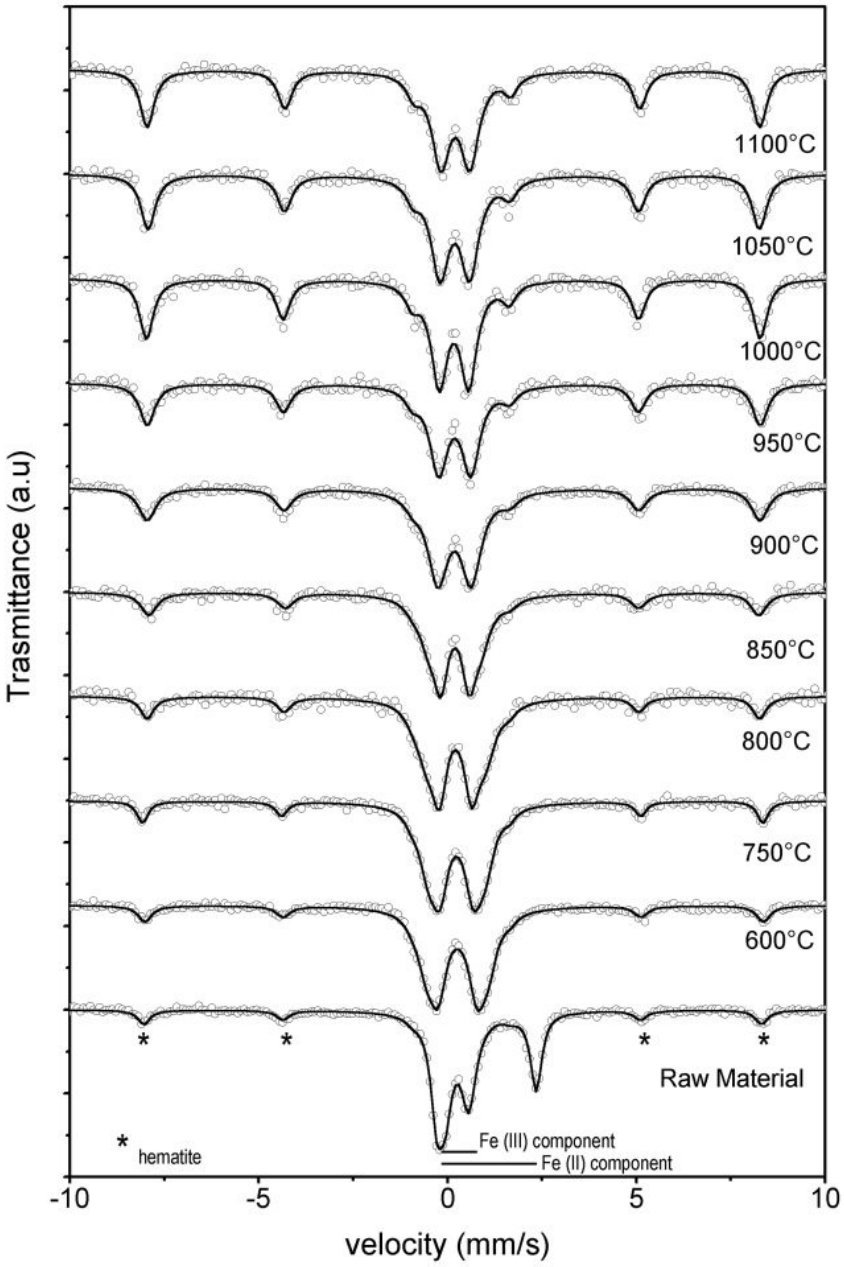

Figure 3.2: Mössbauer spectra of the illitic clay samples fired at different temperatures

spectra, is presented in figure 3.3; the results mostly confirm literature data about the mineralogical changes occurring in clays during firing (Cultrone *et al.* 2001; Riccardi *et al.* 1999). The combined use of XRD and Raman results shows the transition between anatase and rutile taking place around 1050°C. This is too high a temperature if one wants to use the transition as a mineralogical thermometer for prehistoric/low fired artefacts. Diffractograms of the pit fired samples show that the firing temperature in the pit cannot have exceeded 700°C. The Raman spectra are very different from those of the kiln fired samples, in that they only show a high fluorescence background, which masks any traces of peaks and often saturates the detector. This phenomenon is probably due to the presence of "contaminants" within the samples, which are in turn likely related to the interaction between ceramics and soil during burying. In support of this statement, we observed the same feature in the Raman spectra of a few ceramic sherds belonging to prehistoric (6^{th}-4^{th} millennium B.C.) archaeological contexts in Italy and Romania. Further investigations are necessary to better specify the nature of such an interaction.

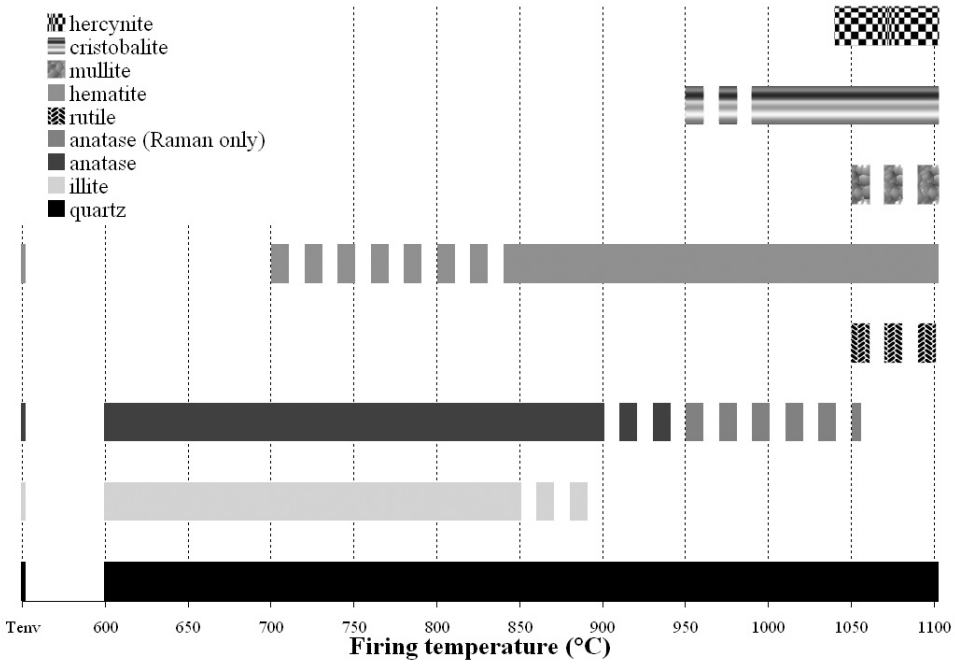

Figure 3.3: Synthesis of experimental data on the illitic clay samples

3.1.3 Results on kaolin samples

A comparative plot of X-ray diffractograms of the fired kaolin samples (fig. 3.4) shows the presence of a high background signal between 15° and 35° 2 θ, which is due to the great quantity of amorphous material deriving from the destruction of kaolinite well below 800°C. Two large peaks are observable above 950°C, which correspond to γ-alumina that forms, in a scarcely crystalline structure, following the collapse of metakaolin. Quartz is hardly affected by the temperature increase, while illite disappears by 950°C and mullite starts forming above 1000°C; these results confirm data in literature about the evolution of kaolinitic clays during firing (Lee *et al.* 1999). Anatase is present in all the fired samples without significant variations. Raman analyses show the coexistence of anatase and rutile in the whole temperature range, as well as in the raw material (cfr. as an example the spectrum in fig. 3.5); this is therefore another case in which the transition between the two polymorphs cannot be used as a temperature marker. Figure 3.6 shows a synthesis of the experimental data on the kaolin.

> *The anatase/rutile transition was observed only in the illitic clay, both with Raman spectroscopy and XRD, at a temperature of about 1050° C. In the kaolin, both polymorphs coexist in the raw material and in the whole range of temperatures (up to 1100° C), and no significant changes can be observed in their relative amounts. Experimental data therefore show that this transition is strongly dependent on the composition of the clay, and that it can hardly be used as a mineralogical thermometer in the archaeometric study of pottery. Some applications could perhaps be found in studies on ceramic typologies fired at temperatures above 1000° C. It still seems interesting to investigate more deeply the dependence of this transition on the composition of the raw material in a systematic manner; the use of a macro- rather than a micro-Raman approach seems to be advisable in order to obtain quantitative data. Mössbauer data collected at 298K suggest that a deeper understanding of the evolution of iron compounds, particularly the formation and size increase of iron oxide crystals, is needed. This can be achieved by undertaking Mössbauer measures at low temperatures (80 and if necessary 10K). Such data, together with further analyses on materials with different oxide concentrations and particle sizes, might allow a "calibration curve" for a fast comparison with the ancient pottery spectra to be developed.*

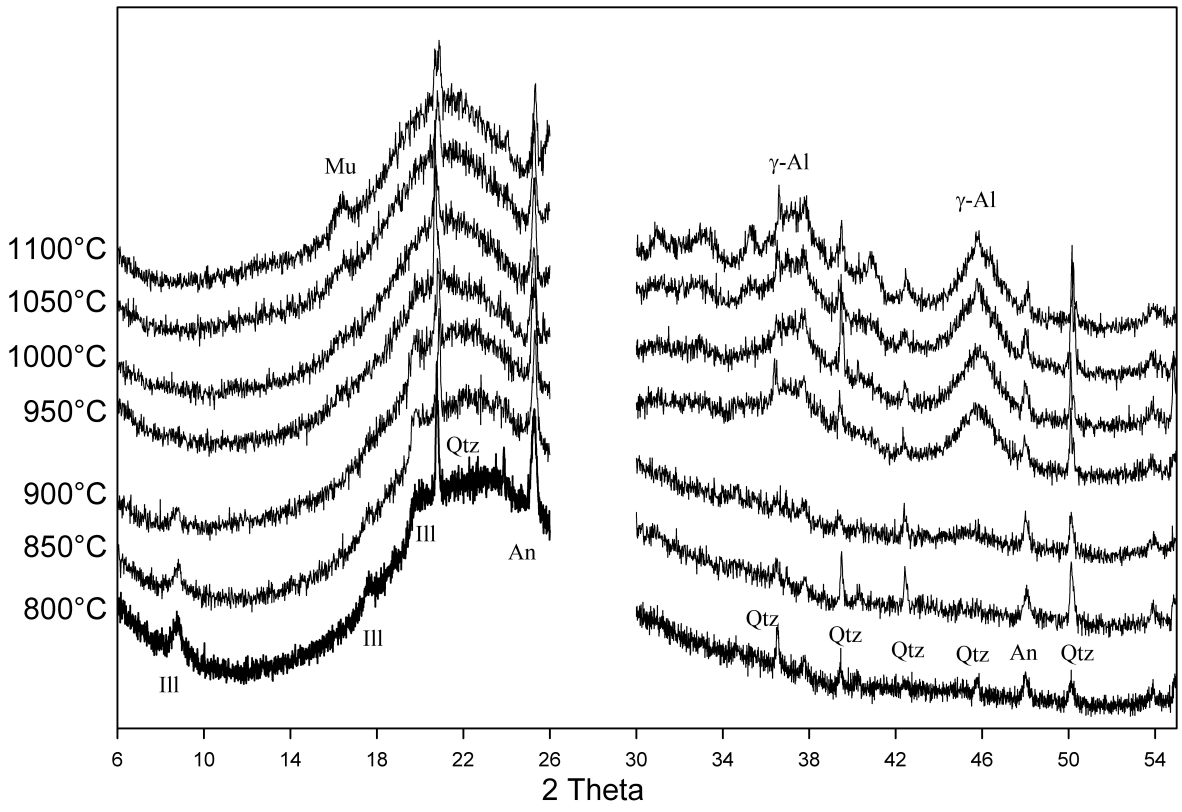

Figure 3.4: Comparative plot of XRD analyses on the kaolin samples (Qtz: quartz, Ill: illite, An: anatase, Mu: mullite, γ-Al: γ-alumina)

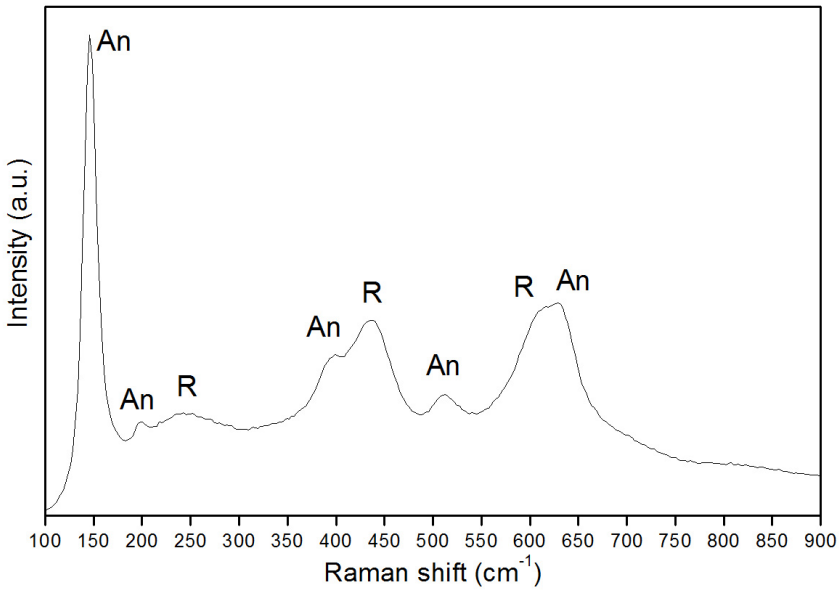

Figure 3.5: Sample Raman spectrum of kaolin fired at 1100°C , in which both anatase (An) and rutile (R) can be identified

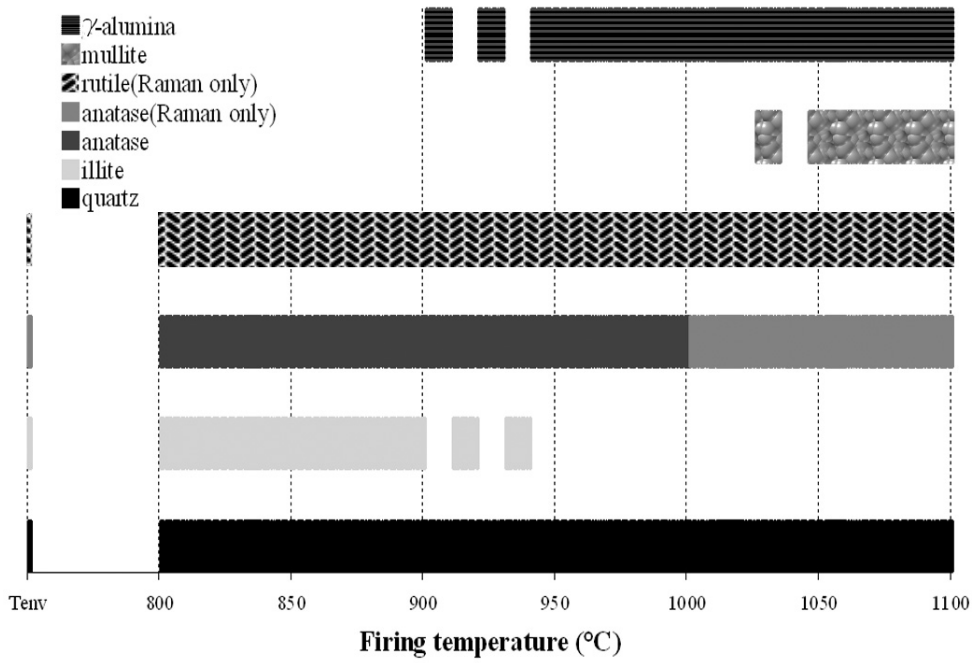

Figure 3.6: Synthesis of experimental data on the kaolin samples

3.2 Slips and decorations of Neolithic pottery

A micro-Raman spectroscopic analysis was performed in order to identify and characterize non-destructively the white slips and coloured pigments applied on the surface of some Neolithic potsherds from excavations in Romania. These experiments were a complement to a wider study on Romanian Neolithic pottery, undertaken jointly between the CNR-ISTEC and the Systemic Archaeology Institute of the "1 Decembrie 1918" University of Alba Iulia, and partly within the framework of the SEEPAST project, financed by the Culture 2000 Programme of the European Union (`www.seepast.net`). This research benefitted also of a Short Term Scientific Mission Grant from the COST G8 Action "Non-destructive analysis and testing of museum objects" (Varvara 2005), and its results have been diffused by means of several oral and poster presentations during the past two years (cfr. appendix B).

3.2.1 Historical background and analytical methodology

In the last years, one of the most interesting and controversial issues of Romanian archaeology was related to a Neolithic painted ceramic material belonging to the "Lumea Noua" culture (first half of the 4^{th} millennium B.C.). Lumea Noua pottery was found in relatively small quantities in few archaeological excavations (e.g. Limba, Alba Iulia-Lumea Noua, Zau de Campie, Tartaria, Cheile Turzii) in Transylvania, Romania (Paul 1981). The painted decoration patterns of Lumea Noua pottery from Transylvania show strong analogies with the ceramic finds from Slovakia (Bükk and Raškovce cultures), Hungary (Esztár and Bükk cultures) and Ukraine (Diakovo culture). Moreover, the development of the Lumea Noua painted pottery groups from Transylvania takes place at a similar chronological level with that of the above-mentioned cultures from Slovakia, Hungary and Ukraine.

The aforementioned research focused on the investigation of Lumea Noua pottery and of the potential raw materials from Transylvanian settlements by different physical and chemical techniques in order to: (i) identify the type of raw materials used for the ceramic bodies, the slips and the painted decorations; (ii) to distinguish imported vs. locally made finds and to hypothesize the provenance of investigated Lumea Noua pottery; (iii) to identify all the stages and techniques used for the artefacts' manufacturing. A total of twenty-one pottery sherds belonging to the Lumea Noua culture were selected

for analysis by means of X-ray fluorescence, optical microscopy and X-ray diffraction in order to obtain chemical, petrographical and mineralogical information. In addition, the chemical composition of the slips and decorations was determined by means of SEM-EDS (STEREOSCAN 360 Cambridge Instruments microscope coupled with an INCA Energy 300 spectrometer). Macroscopically, all the potsherds are covered with a white or a white-yellowish slip and all except for one (Rom 13) are decorated with red, red-orange to purple or brown bands or geometrical models. In some cases (e.g. Rom 3) parallel black lines are also drawn on the slip. Some samples are characterised by a paste with a typical "sandwich structure" (i.e. black or grey core and reddish outer layers).

To obtain a better insight into the nature of the slips and pigments used for decorations, five representative potsherds were selected for non-destructive Raman spectroscopic analyses. Raman analyses were again carried out at the Industrial Chemistry Dept. of the University of Bologna, using a Renishaw RM1000 spectrometer with a green Ar^+ laser ($\lambda = 514.5\ nm$). The spectra were acquired directly on the samples in microscopic configuration, without any preparation or cleaning. A synthetic description of the samples is presented in table 3.2, and photographs are shown in figure 3.7).

Sample	Type of artefact	Slip colour	Decoration
ROM3	fragment of lid	white-yellowish	red band, thin brown bands
ROM7	pot fragment	light yellow	red bands
ROM10	fragment of lid	light yellow	beige bands
ROM34	pot fragment	light yellow	red bands
ROM36	pot fragment	light yellow	light brown bands

Table 3.2: Synthetic description of Neolithic pottery samples from Romania

3.2.2 Characterization of slips and decorations

The Raman characterization of the white slips and decorations of these samples was hindered by an extremely high fluorescence background, which often saturated the detector, and in most cases made the identification of specific signatures extremely hard, when not impossible. We did not succeed in recording a satisfying number of useful spectra, therefore the results presented here are necessarily only partially significant and do not allow drawing substantial conclusions.

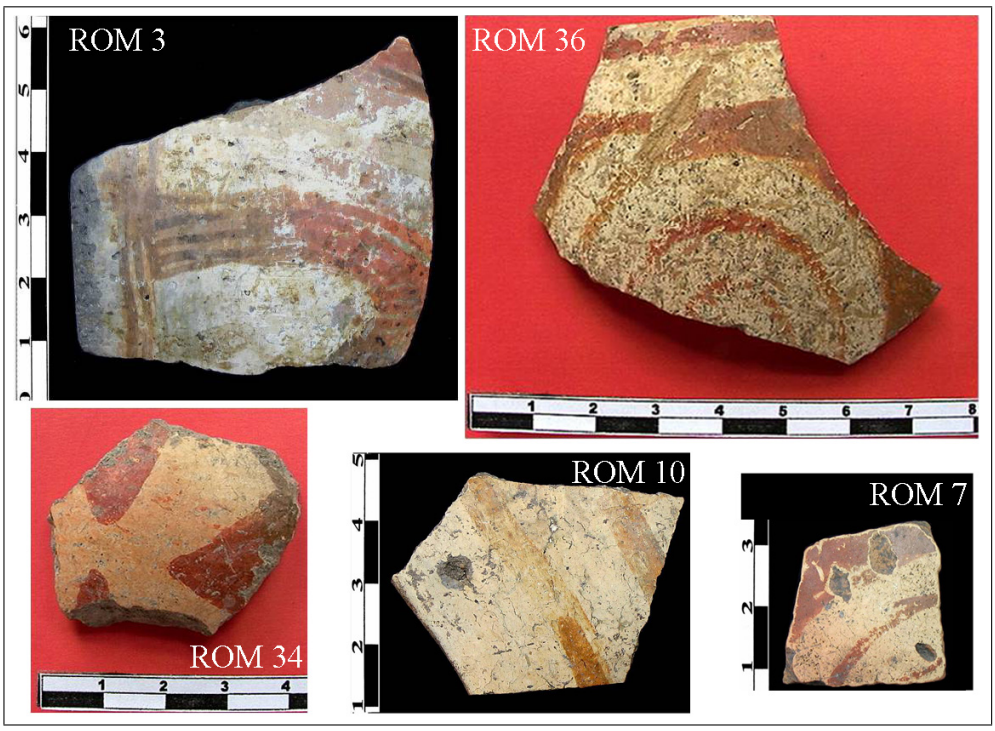

Figure 3.7: The analyzed Neolithic pottery samples from Romania

The Raman spectra of red and brownish crystals in the decoration layers (figure 3.8) mostly revealed the presence of hematite (α-Fe_2O_3), identified by peaks at 230, 290, 405, and 608 cm^{-1}. Such wavenumbers are slightly down-shifted with respect to the band positions usually assigned to this phase when pure; this could relate to a disordered, non perfectly stoichiometric structure of hematite (Zoppi *et al.* 2006, 2007). Yellow and reddish crystals in the decorative layers of two samples give spectra containing also a weak band centered around 720 cm^{-1} and related to a spinel-like structure, possibly magnetite. All these results are in good agreement with the EDS analysis, which shows a high concentration of iron in the decorations of all samples (cfr. as a reference the chemical composition of the paste, slip and decoration of sample ROM3, reported in table 3.3). Finally, white crystals in the decorations yield the Raman signature of quartz. Raman spectra of the white slips (fig. 3.9) yield mostly the signatures of quartz and anatase, and occasionally of calcite, the latter characterized by a peak at 1085 cm^{-1} together with a low intensity band at 280 cm^{-1}. Traces of hematite in the spectra of the samples' slips could be due to the spread of the red pigments over the white layer. Careful examination of the samples showed that the slips and decorations are much fractured and traces of

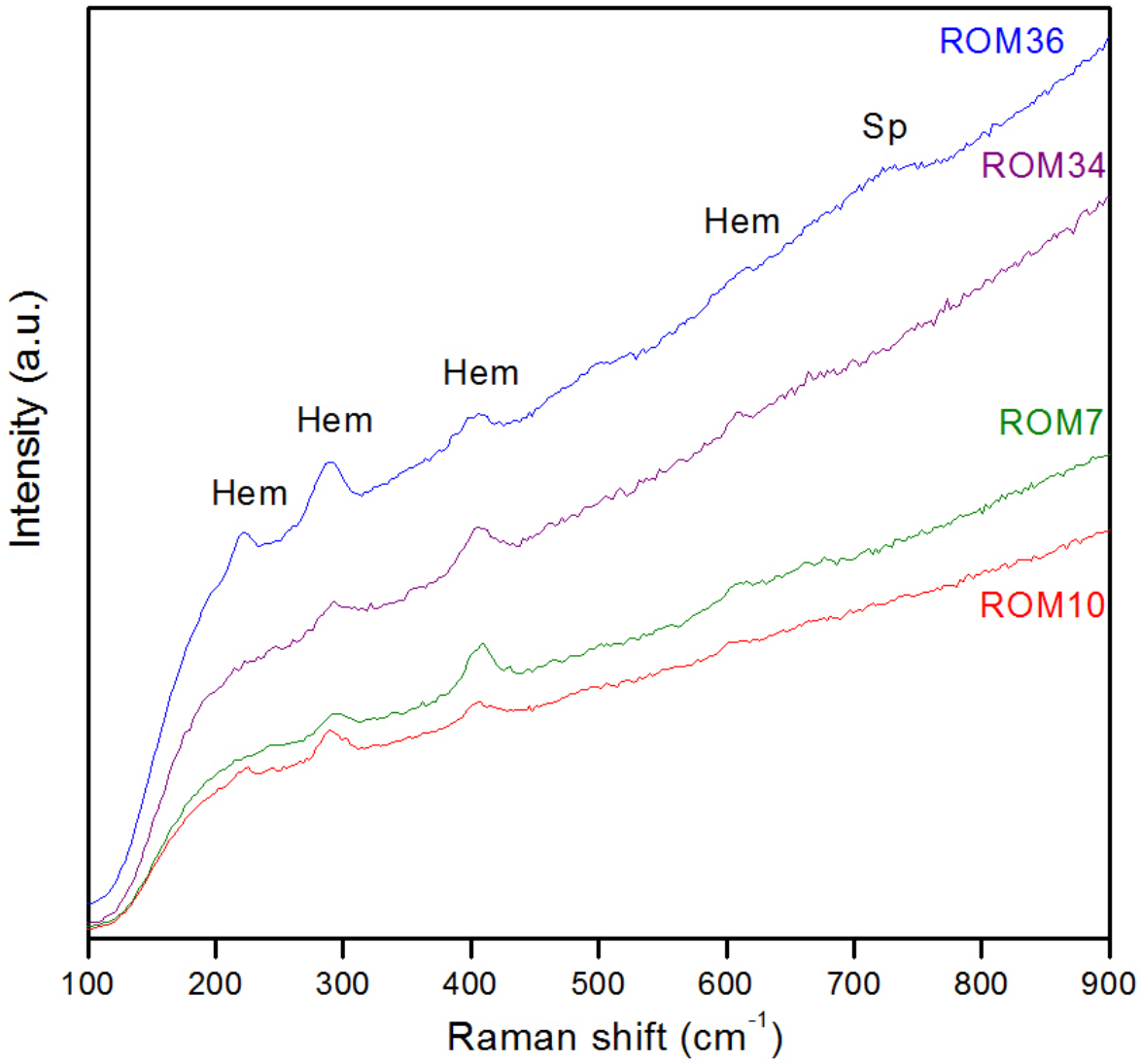

Figure 3.8: Raman spectra of red and brownish crystals in the decoration layers (Hem: hematite, Sp: spinel)

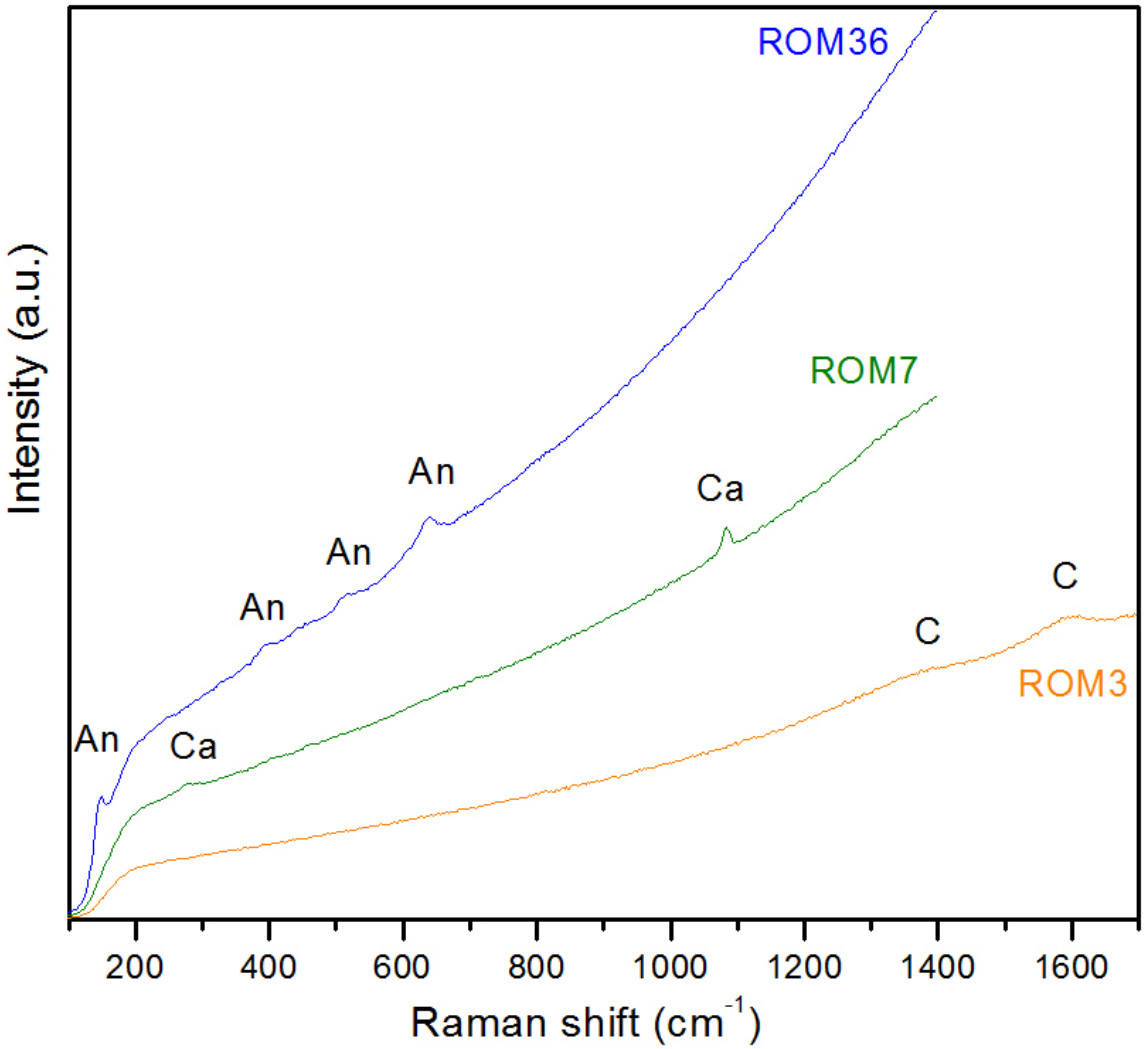

Figure 3.9: Representative Raman spectra of the white slips (An: anatase, Ca: calcite, C: carbon)

carbon, probably due to the burial period, have been often identified while acquiring the Raman spectrum inside these fractures.

	SiO_2	Al_2O_3	TiO_2	Fe_2O_3	MnO	MgO	CaO	Na_2O	K_2O
Paste (XRF)	67.36	18.51	0.77	6.39	0.12	1.86	1.62	0.64	2.73
Slip (EDS)	44.41	12.66	0.03	12.91	0.80	1.81	23.85	0.06	3.47
Decoration (EDS)	42.87	6.71	0.38	22.36	0.77	1.6	17.09	0.52	3.85

Table 3.3: Chemical composition of the paste, white-yellowish slip and red decoration of sample ROM3 (weight % oxides normalized to 100)

Raman analyses provided valuable complementary information regarding the composition of the slips and decorations of the Lumea Noua Neolithic pottery samples, which complete and support the results of other kinds of analysis, which had allowed to characterize these materials and to reconstruct the production stages of these pieces. The slip was obtained probably with a fine-grained carbonate clay with high contents of illite, which was applied on the unfired body, smoothened and/or polished, and painted using iron-rich materials before being fired at a temperature comprised between about 600 and 900° C. One comment can be made, regarding the suitability of Raman spectroscopy for the study of archaeological materials such as these Neolithic potteries: in many cases, obtaining a "good" spectrum was quite a difficult task, due to a high fluorescence background which could mask the Raman peaks completely, and often saturated the detector.

3.3 Engobes and glazes of "sgraffito" Renaissance ceramics

"Sgraffito" ceramics are usually characterized by a red paste, covered by a white slip called "engobe" and by a transparent glaze, and were produced in Europe since the medieval period. The word "sgraffito" refers to the most common type of decoration present in the vessels: scratched lines or areas realized by means of different tools (tips or cutters) and

enriched sometimes with yellow, green or brown brush touches. The term "sgraffito" is commonly used also to indicate vessels which are engobed, painted and glazed, but not necessarily incised or scratched.

This research complements a more comprehensive study of a diffused production of "sgraffito" ceramics attested in a large number of small artisan furnaces in several sites in Tuscany since the 15^{th} century (Amato *et al.* 2004, 2006). The chemical composition of coatings of a large number of pottery fragments was determined on carbon-coated polished sections by means of a scanning electron microscope (SEM - Stereoscan 360 Cambridge Instruments) combined with an energy dispersive spectrometer (EDS Inca Energy 300). Average values were calculated on a minimum of ten measures on each sample. Raman analyses were carried out with the Dilor XY2 and the Labram Infinity instruments (cfr. section 2.3) on the engobes and glazes of a few representative samples from several sites (7 from Borgo San Lorenzo, 5 from Cafaggiolo, 8 from Castelfiorentino and 4 from Empoli), in order to verify the possibility to obtain complementary information about raw materials and production technology of the artefacts in a completely non-destructive way. Pictures of representative samples from all the provenance sites are presented in figure 3.10; the analyzed pieces are representative of open shapes (plates, cups, bowls), and present all kinds of decorative typologies: painted (e.g. BSL2), incised with a tip (e.g. CF6, CFT8, PF1), scratched with a cutter producing a "champlevé" effect (e.g. EM4).

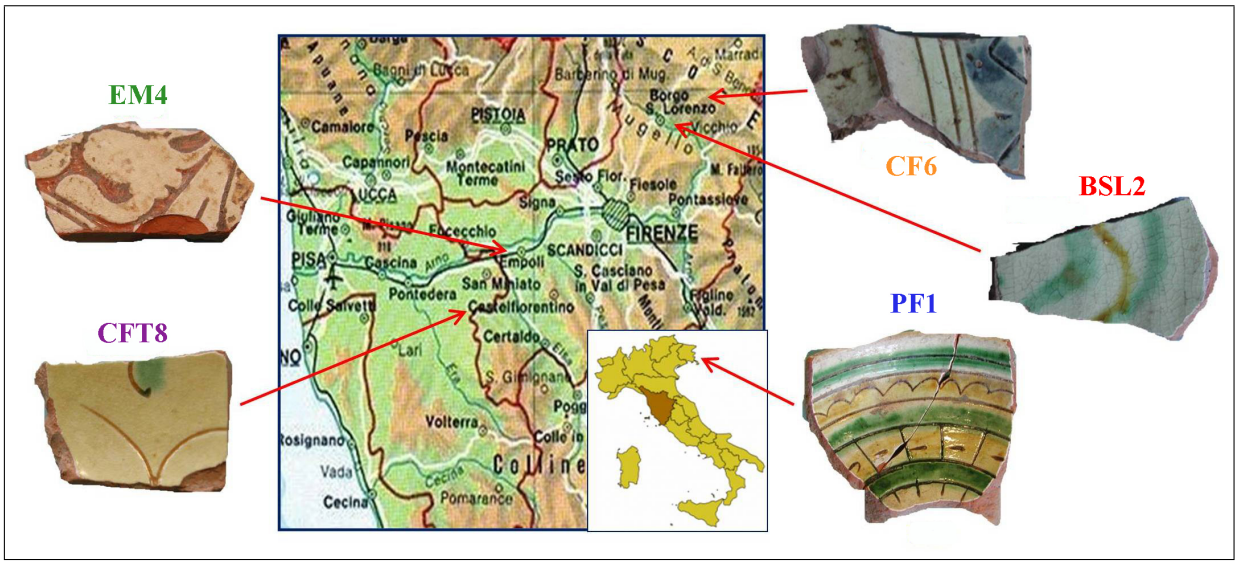

Figure 3.10: Representative samples of "sgraffito" pottery from sites in Tuscany and Friuli Venezia Giulia

Some of the samples are first or second-firing kiln wastes. Four shards from Udine (Friuli Venezia Giulia, N-E Italy) were also analyzed for comparison purposes. In oder to perform a totally non-destructive Raman analysis of the engobes, measures were limited to artefacts where the engobe was exposed due to a chipped portion of the glaze, in the case of glazed samples (second-firing wastes). Therefore only 22 out of 28 samples were subject to engobe analysis; likewise, glaze analysis was obviously not undertaken on first-firing wastes, but limited to the 21 glazed fragments. The main results of this study have already been presented in the form of a poster at the European Meetings on Ancient Ceramics in Budapest (October 2007, cfr. appendix B).

3.3.1 Characterization of the engobes

Representative Raman spectra of the engobes relative to pottery from the different production sites are shown in figure 3.11, while tables 3.4 and 3.5 present in detail the mineral phases identified and the chemical composition of each sample.

Almost all the engobes from Tuscany are characterized by the presence of feldspars, linked to the high potassium content (5-10% K_2O), and of rutile. Mg-containing phases, namely enstatite ($MgSiO_3$) and forsterite (Mg_2SiO_4), are detected in most spectra of samples from Borgo San Lorenzo and Cafaggiolo, although their magnesium content (7-9% MgO) does not substantially differ from that of the other engobes from Tuscany (4-8% MgO). Feldspars and rutile are never observed in the spectra of samples from Udine, while quartz and anatase are always present. The low content of magnesium (<2% MgO) is reflected in the absence of Mg-containing phases in the spectra.

3.3.2 Characterization of the transparent glazes

The Raman spectra of all the glazes indicate them as belonging to the family of Pb-silicate glasses, as shown also by the variation range of their chemical compostion, reported in table 3.6 (Si:Pb$\simeq$1:1.5). Four samples differ from the others from the chemical point of view, having Si:Pb$\simeq$1:1 (CF5, CF6, CFT5), or even Si:Pb$\simeq$1.5:1 (CFT6). Figure 3.12 shows the deconvolution of a representative Raman spectrum of a glaze, together with the spectra relative to the glazes of the four aforementioned "peculiar" samples. Almost all glazes contain traces of undissolved feldspars, visible in their Raman spectra. Crystalline enstatite was also detected in two of the glazes from Tuscany (CF6 and CFT6) and corresponds to higher values of Mg as found by the EDS analysis (table 3.6).

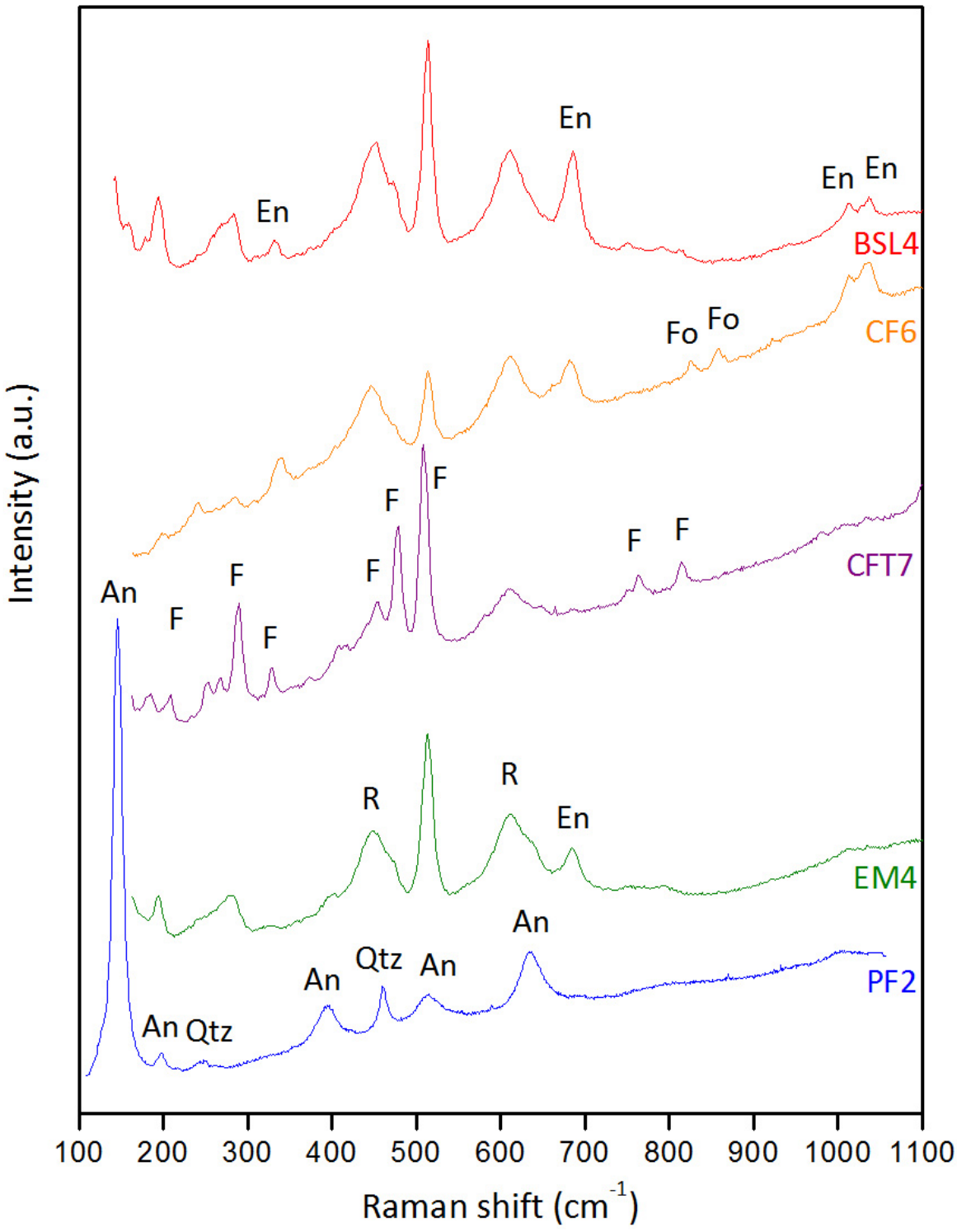

Figure 3.11: Representative Raman spectra of the engobes of samples from all the production sites (En: enstatite, Fo: forsterite, F: feldspars, R: rutile, An: anatase, Qtz: quartz)

	Quartz	Feldspars	Enstatite	Forsterite	Anatase	Rutile
Borgo San Lorenzo						
BSL1		X	X			X
BSL2	X	X				X
BSL4		X	X			X
BSL6	tr.	X		X		X
BSL7					X	X
Cafaggiolo						
CF2	tr.	X	tr.			X
CF5		X	X			X
CF6		X	X	X		X
CF7	X	X	X			X
Castelfiorentino						
CFT1		X			X	X
CFT2	X	X				X
CFT3		X			X	
CFT4	X	X				X
CFT5	tr.	X	tr.			X
CFT7		X				X
CFT8	X					X
Empoli						
EM2		X				X
EM3	X	X				X
EM4	X	X	tr.			X
Udine						
PA1	X				X	tr.
PF1	X				X	
PF2	X				X	

Table 3.4: Mineral phases detected in the Raman spectra of the analyzed engobes

	SiO_2	Al_2O_3	TiO_2	Fe_2O_3	MgO	CaO	Na_2O	K_2O
Borgo San Lorenzo								
BSL2	62.13	18.88	0.76	1.07	7.03	3.21	1.16	5.75
BSL4	55.84	22.58	0.55	0.66	7.48	1.67	3.08	8.13
BSL6	62.48	17.98	0.47	0.67	6.90	0.96	1.04	9.49
BSL7	55.89	20.46	0.87	1.11	8.30	5.44	0.93	7.00
Cafaggiolo								
CF5	60.50	18.62	0.86	0.74	8.30	1.20	0.74	8.89
CF6	57.59	20.75	0.86	1.00	8.49	1.95	0.81	8.55
Castelfiorentino								
CFT5	62.53	19.90	0.93	0.81	7.64	1.61	0.88	5.69
CFT7	58.04	24.37	1.01	1.49	4.40	3.76	1.35	5.57
CFT8	55.34	29.53	0.75	0.68	5.63	0.54	1.31	6.22
Empoli								
EM2	50.85	24.16	0.63	1.26	6.03	6.65	3.00	7.42
EM4	55.38	22.58	1.15	0.71	8.07	2.84	1.59	7.68
Udine								
PF1	58.45	28.22	0.30	1.36	1.83	2.38	0.39	7.07
PF2	59.21	28.39	0.39	0.94	1.40	2.94	0.20	6.52

Table 3.5: Chemical composition of the engobes of "sgraffito" pottery samples (weight % oxides normalized to 100)

	SiO_2	Al_2O_3	TiO_2	Fe_2O_3	MgO	CaO	Na_2O	K_2O	PbO
Var. range (15 samples)	34-40	2.7-5	0-0.5	0.3-1	0.4-1.7	0.5-1.7	0-0.8	0.4-1.7	51-61
CF5	43.00	4.99	0.47	0.99	1.40	1.04	0.29	1.37	46.46
CF6	43.14	5.75	0.31	0.68	2.30	1.23	0.29	2.01	44.28
CFT5	46.61	5.18	0.16	0.68	1.40	1.16	0.33	1.60	42.89
CFT6	50.28	7.90	0.28	0.41	2.83	0.70	0.67	2.76	34.16

Table 3.6: Chemical composition of the transparent glazes of "sgraffito" pottery samples (weight % oxides normalized to 100)

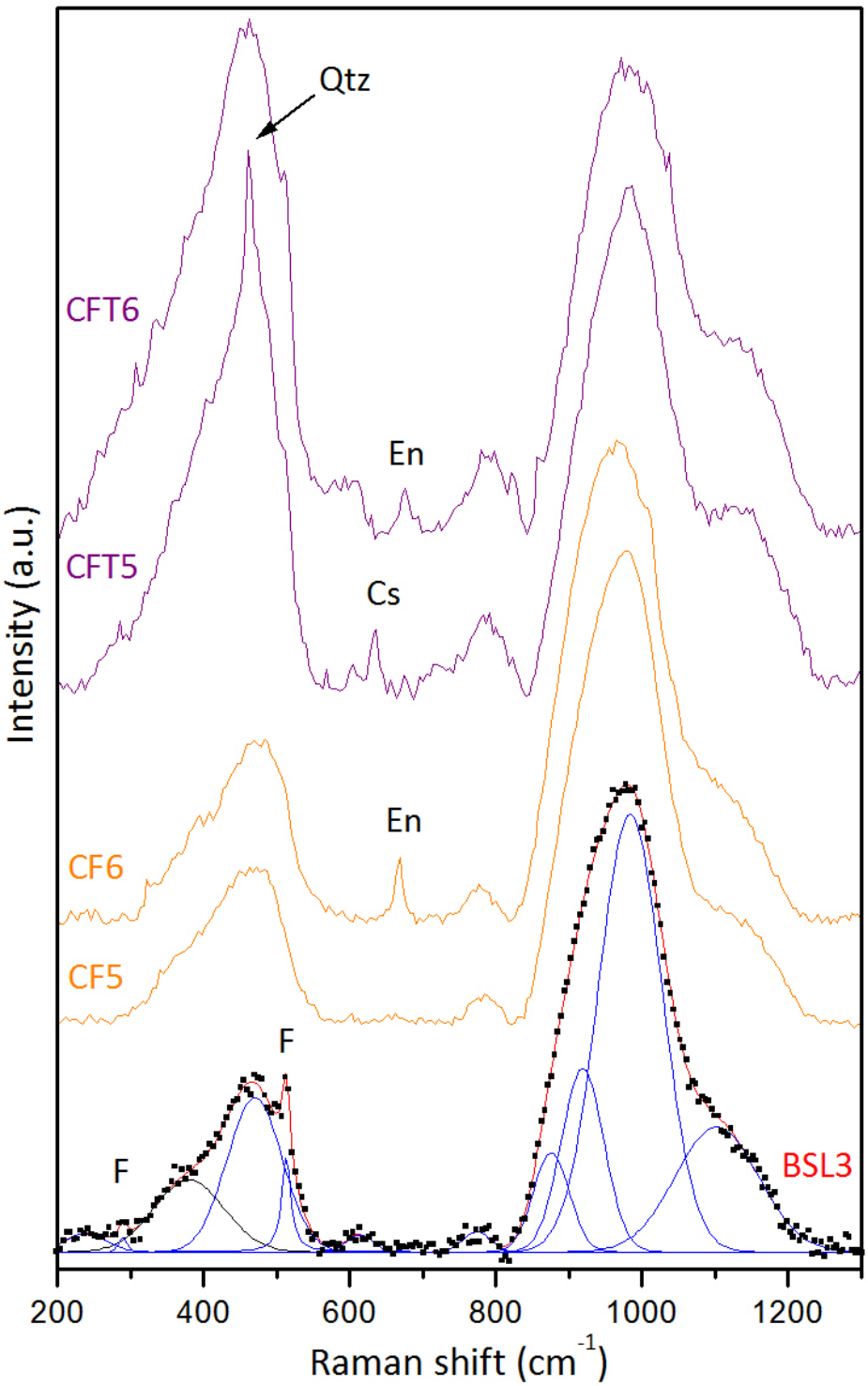

Figure 3.12: Representative deconvolution of one glaze spectrum (sample BSL3), and Raman glaze spectra of the four "peculiar" samples (F: feldspars, En: enstatite, Cs: cassiterite, Qtz: quartz)

The plot of the SiO_2 content vs. total fluxes (PbO+Na_2O+K_2O) shows the narrow compositional variation range of most glazes and points out the four "anomalous" samples already mentioned (fig. 3.13). A good correlation can be observed in the plot of I_p vs. total fluxes (fig. 3.14), which shows how the polymerization index is a good "technological marker" as it is directly linked to the total amount of fluxing agents in the glaze. This correlation can be quite well fitted with a polynomial regression curve ($y = 0.001x^2 - 0.155x + 4.874, R^2 = 0.879$).

Raman spectroscopy proved once again to be a good complementary technique for the analysis of ceramics, with the advantage of being non-destructive; some conclusions could in fact be drawn on the analyzed productions, regarding both raw materials and manufacturing technology. Engobes from Tuscany are characterized by their high Mg content, never identified thus far in local clay deposits, and therefore suggesting an intentional addition, possibly of talc ($Mg_3Si_4O_{10}(OH)_2$), as already pointed out by Casellato et al. *(2007). The presence of Mg-containing phases (enstatite and/or forsterite) only in the spectra of samples from Borgo San Lorenzo and Cafaggiolo might indicate a different production technology for these two sites, in terms of processing of raw materials and/or of thermal treatment. Raman analyses give further indications to differentiate the engobes from Udine, thanks to the absence of feldspars in their spectra. The constant presence of anatase, as opposed to the frequent identification of rutile in those from Tuscany, may suggest a higher firing temperature for the latter, unless in both cases the identified polymorph was already present in the raw material.*

Analytical results on glazes do not allow distinguishing among production sites, indicating in all cases the use of a typical "recipe" for transparent glazes, based on Pb-oxide (minium) and a quartz-rich sand, seemingly mixed in different proportions. A good correlation can be established between the total amount of fluxes in each glaze and the value of the polymerization index, calculated on representative spectra on the basis of non-destructive Raman analyses.

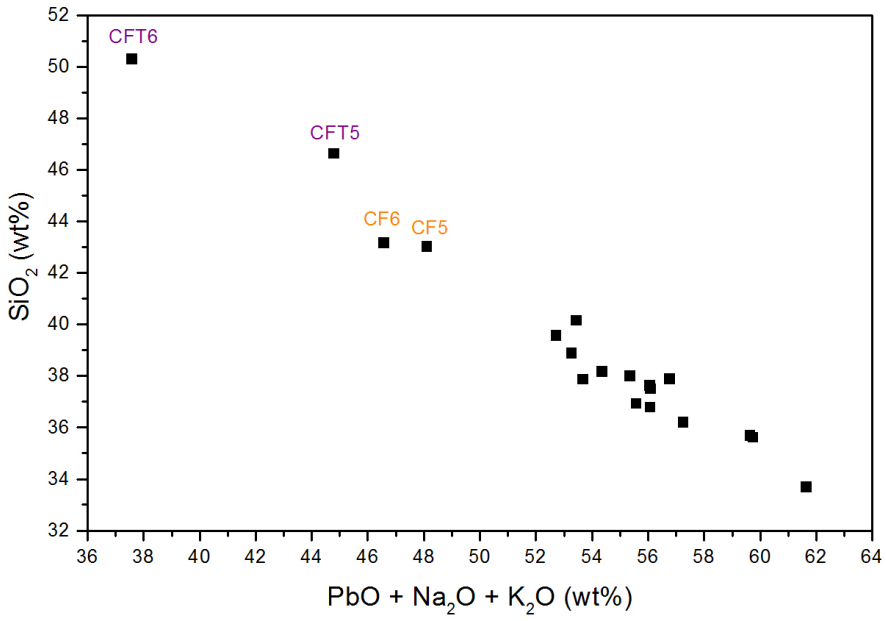

Figure 3.13: Plot of the SiO_2 content vs. total fluxes (PbO+Na_2O+K_2O) for the analyzed transparent glazes

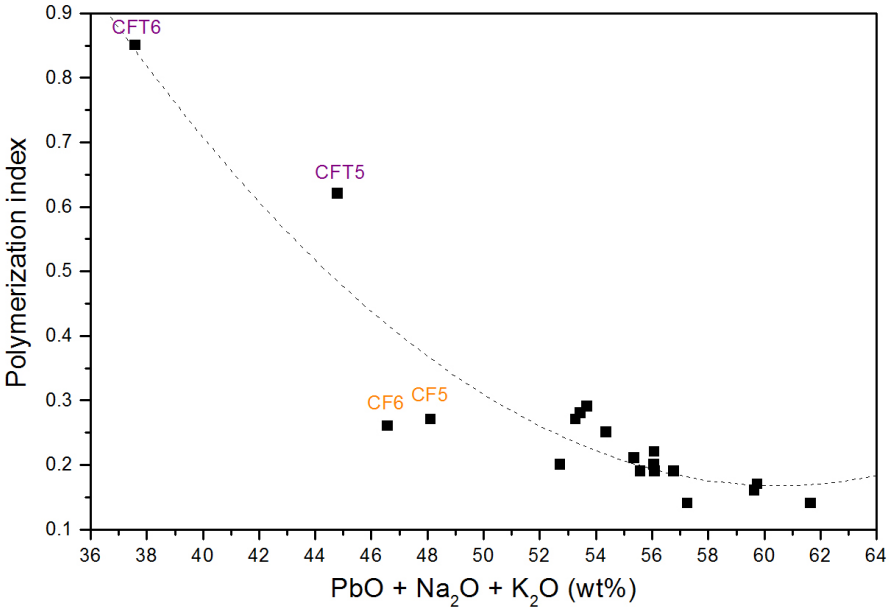

Figure 3.14: Plot of I_p vs. total fluxes for the analyzed transparent glazes. The dashed line is the polynomial regression curve (cfr. text)

3.4 References

Amato F., Fabbri B., Gualtieri S. (2004). Studio archeometrico. In *Ceramiche rinascimentali di Castelfiorentino - L'ingobbiata e graffita in Toscana*. Valeri Moore A. (ed.), pp. 77–80. Ed. Polistampa, Firenze.

Amato F., Fabbri B., Gualtieri S., Ruffini A., Valeri Moore A. (2006). Sgraffito ceramics from Florentine area (XVI century): archaeometric characterization of paste and coating. In *Proceedings of the 34th International Sympostium on Archaeometry 2004*, pp. 365–370. Zaragoza.

Artioli G., Gianni G. B., Bruni S., Cariati F., Fermo P., Morin S., Russo U. (2000). Studio spettroscopico della tecnologia di cottura di ceramiche etrusche dagli scavi di Tarquinia. In *Proceedings of the I Congresso nazionale di archeometria*. Martini M. (ed.), pp. 335–349.

Casellato U., Fenzi F., Mendera M., Peruzzo L., Riccardi M. P., Vigato P. A. (2007). La produzione di ceramica ingobbiata e graffita a Castelfiorentino (Fi): il sito di Via Bertini tra XV e XVII secolo. In *Atti della 11^{a} Giornata di Archeometria della Ceramica*. To be published.

Cultrone G., Rodriguez-Navarro C., Sebastian E., Cazalla O., De la Torre M. J. (2001). Carbonate and silicate phase reactions during ceramic firing. *European Journal of Mineralogy*, **13**, 621–634.

De Benedetto G. E., Laviano R., Sabbatini L., Zambonin P. G. (2002). Infrared spectroscopy characterization of ancient pottery. *Journal of Cultural Heritage*, **3**, 177–186.

Emiliani G. P., Corbara F. (1999). *La tecnologia ceramica 2. La lavorazione*. Faenza editrice, Faenza.

Fabbri B. (1998). The problem of defining the firing temperature of ceramic artefacts. In *Proceedings of the XIII UISPP Congress - Forlì, 8-14 sept. 1996 - Volume I.* Ariao C., Bietti A., Castelletti L., Peretto C. (eds.), pp. 207–214. Ed. A. B. A. C. O., Forlì.

Gennari F. C., Pasquevich D. M. (1998). Kinetics of the anatase-rutile transformation in TiO_2 in the presence of Fe_2O_3. *Journal of Materials Science*, **25**, 1571–1578.

Ghosh S. K. (2001). Influence of different additives on anatase-rutile transformation in titania system. *British Ceramic Transactions*, **100**(4), 151–154.

Häusler W. (2004). Firing of clays studied by X-ray diffraction and Mössbauer spectroscopy. *Hyperfine Interactions*, **154**, 121–141.

Lee S., Kim Y. J., Moon H. (1999). Phase transformation sequence from kaolinite to mullite investigated by an energy-filtering transmission electron microscope. *Journal of the American Ceramic Society*, **82**(10), 2841–2848.

Liem N. Q., Sagon G., Quang V. X., Tan H. V., Colomban P. (2000). Raman study of the microstructure, composition and processing of ancient Vietnamese (proto)porcelains and celadons (13-16th centuries). *Journal of Raman Spectroscopy*, **31**, 933–942.

Lofrumento C., Zoppi A., Castellucci E. M. (2005). La spettroscopia micro-Raman: un "termometro mineralogico" nello studio delle ceramiche archeologiche. In *Tecnologia di lavorazione e impieghi dei manufatti*. Fabbri B., Gualtieri S., Volpe G. (eds.), Atti della 7^{a} Giornata di Archeometria della Ceramica, Lucera 10-11 Aprile 2003, pp. 21–28. EDIPUGLIA, Bari.

Maggetti M. (1982). Phase analysis and its significance for technology and origin. In *Archaeological Ceramics*. Olin J., Franklin A. D. (eds.), pp. 121–133. Smithsonian Institution Press, Washington D. C.

Maniatis Y., Facorellis Y., Pillali A., Papanthimou-Papaefthimiou A. (2002). Firing temperature determinations of low fired clay structures. In *Modern trends in scientific studies on ancient ceramics - BAR Int. Series 1011 - Proceedings of the 5th EMAC, Athens 1999*. Kilikoglou V., Hein A., Maniatis Y. (eds.), pp. 59–68. Archaeopress, Oxford, England.

Mirti P., Davit P. (2004). New developments in the study of ancient pottery by colour measurement. *Journal of Archaeological Science*, **31**, 741–751.

Moropoulou A., Bakolas A., Bisbikou K. (1995). Thermal analysis as a method of characterizing ancient ceramic technologies. *Thermochimica Acta*, **269-270**, 743–753.

Murad E. (1997). Identification of minor amounts of anatase in kaolins by Raman spectroscopy. *The American Mineralogist*, **82**, 203–206.

Murad E. (1998). Clays and clay minerals: what can Mössbauer spectroscopy do to help understand them? *Hyperfine Interactions*, **117**, 39–70.

Murad E. (2003). Raman and X-ray diffraction data on anatase in fired kaolins. *Clays and Clay minerals*, **51**, 689–692.

Nodari L., Maritan L., Mazzoli C., Russo U. (2004). Sandwich structures in the Etruscan-Padan type pottery. *Applied Clay Science*, **27**, 119–128.

Paul I. (1981). Der gegenwärtige Foschungsstand zur Petresti-Kultur. *Prähistorische Zeitschrift*, **56**(2), 197–234.

Riccardi M. P., Messiga B., Duminuco P. (1999). An approach to the dynamics of clay firing. *Applied Clay Science*, **15**, 393–409.

Ricciardi P., Nodari L., Fabbri B., Gualtieri S., Russo U. (2007). Contribution for a mineralogical thermometer to be applied to low fired and/or non-carbonate ceramics. In *Archaeometric and Archaeological approaches to ceramics - BAR Int. Series 1691 - Proceedings of the 8th EMAC, Lyon 2005*. Waksman S. Y. (ed.), pp. 13–18. Archaeopress, Oxford.

Rodrìguez-Talavera R. (1997). Modification of the phase transition temperatures in titania doped with various cations. *Journal of Materials Research*, **12**(2), 439–443.

Varvara S. (2005). Scientific report on Short Term Scientific Mission in the frame of the project "Archaeometric investigations on the provenance and technological aspects of the Neolithic painted pottery (4th millennium b.C.) from Transylvania (Romania)". Unpublished (reference COST-STSM-G8-01426).

Wagner F. E., Wagner U. (2004). Mössbauer spectra of clays and ceramics. *Hyperfine Interactions*, **154**, 35–82.

Wolf S. (2002). Estimation of the production parameters of very large medieval bricks from St. Urban, Switzerland. *Archaeometry*, **44**(1), 37–65.

Zoppi A., Lofrumento C., Castellucci E. M., Dejoie C., Sciau P. (2006). Micro-Raman study of aluminium-bearing hematite from the slip of Gaul *sigillata* wares. *Journal of Raman Spectroscopy*, **37**, 1131–1138.

Zoppi A., Lofrumento C., Castellucci E. M., Sciau P. (2007). Al-for-Fe substitution in hematite: the effect of low al concentrations in the Raman spectrum of Fe_2O_3. *Journal of Raman Spectroscopy*. In press (D.O.I. 10.1002/JRS.1811).

Chapter 4

Raman characterization of 18^{th} century porcelain

4.1 The Bourbon porcelain factories: Capodimonte and Buen Retiro

> *"Capodimonte has well deserved its former reputation as the most distinguished of the Italian factories. In artistic quality its useful wares and figures stand high among the 18^{th} century porcelains of Europe, to which they make a unique and original contribution" (Lane 1954, p. 52).*

Such was the opinion of Arthur Lane, the renowned director of the ceramics section of the Victoria & Albert Museum of London during the 1950s. The uniqueness of Capodimonte does not only relate to the artistic qualities of its production, but also to the most peculiar history of the manufacture itself, whose short-lived activities lasted only sixteen years (Minieri Riccio 1878c). Documents regarding the Neapolitan factory are scarce and fragmentary, due to a combination of reasons: the manufacture archives were transported to Madrid in 1759 and were lost when the building which hosted them was destroyed during war time (cfr. section 4.1.2). An extensive correspondence between the factory staff and providers of raw materials, which remained in the State Archives of Naples, also burned down almost completely during a fire of the town in 1943. The latter documentation had luckily been examined by the historian Camillo Minieri Riccio, who produced an accurate report on the information he had thus found about the history, raw materials

used, workers, and artefacts produced in Capodimonte (Minieri Riccio 1878a,b,c,d). Our knowledge of these subjects is largely based on his account, along with an interesting volume on Italian porcelain written by Arthur Lane (1954), and on another report which benefits from more recent researches (Pepe 1995).

4.1.1 Historical background: early porcelain manufacturing in Europe

Porcelain production in Europe has a long and complex history, which will only be outlined here, while it has been extensively recounted by Kingery (1987). Beginning in the 16^{th} century, the Portuguese and then the English and Dutch brought large amounts of beautiful translucent porcelain from China into Europe. There are many reports of Venetian efforts to reproduce such materials, but no regular production was established and there exist no examples of any obtained success. A truly pioneer work was that of the Italian production of the so-called "Medici's porcelain", for a short period at the end of that same century (1575-1587), which took place in Florence under the auspices of Duke Francesco I de' Medici. Its composition seems to be an adaptation of a Persian recipe to Italian methods. A few precious examples of this production have survived and some have also been analyzed by means of several techniques, including Raman spectroscopy (Colomban *et al.* 2004b; Kingery and Vandiver 1984).
After this near-success, another hundred years passed, with increasing importation of Chinese ware and increasing pressure for a European production of something equivalent. Soft-paste porcelain, based on a frit, was probably first developed around 1680 at Rouen (France), by Louis Poterat. However, the first established manufacture for which we have reliable examples seems to have been near Paris at St. Cloud (∼1700). Similar productions soon began in several locations near Paris, and then spread around Europe during the 18^{th} century. It was then only in 1710 that "real" (i.e. kaolin-based) porcelain first made its first official appearance in Europe, with the foundation of a manufacture at Meissen, in present-day Germany. The recipe for this much sought-after material was carefully kept secret, but sooner or later the technology spread and many manufactures were established all over Europe, and new compositions were formulated.

> *Much of the European porcelain production since the 18^{th} century has been classified into the two main typologies of "soft" and "hard" paste already men-*

tioned, and yet quite a few "hybrid" or peculiar productions exist, which do not fit in either of these categories (e.g. English bone-ash porcelain). Due to their quite special composition, Capodimonte products can also hardly be defined as belonging to either of the two main types of porcelain, and this fact makes them quite an interesting object for archaeometric analyses.

4.1.2 A brief history of the Bourbon manufactures

In 1739 Charles of Bourbon, king of Naples, following the example of Royal Courts all over Europe, promoted the establishment of a porcelain manufacture, at first housed in the Royal Palace. He had been highly fascinated by the tableware made of Meissen porcelain that his wife, Maria Augusta of Saxony, had brought him as dowry. Those of his kingdom were years of flourishing cultural and artistic activities in Naples, where a number of manufactures were set up, producing among other things crystals, cut gemstones, textiles and tapestries. After a few years devoted to the search for suitable raw materials and to experimentations of different recipes for the porcelain paste, in 1743 the porcelain manufacture officially started its work, and was relocated in the Royal woods of Capodimonte, in the so-called "Guardiamaggiore" building. During the following sixteen years, the factory produced high quality porcelain, often in the form of decorative objects, which served as gifts from the king to Italian and foreign noblemen, and were commercialized since 1745. The factory mark used all along the manufacture's activity was a fleur-de-lis painted in underglaze blue, or sometimes impressed under the bottom of the artefact, mostly in the case of figurines (cfr. figure 4.1a,b,d,e).

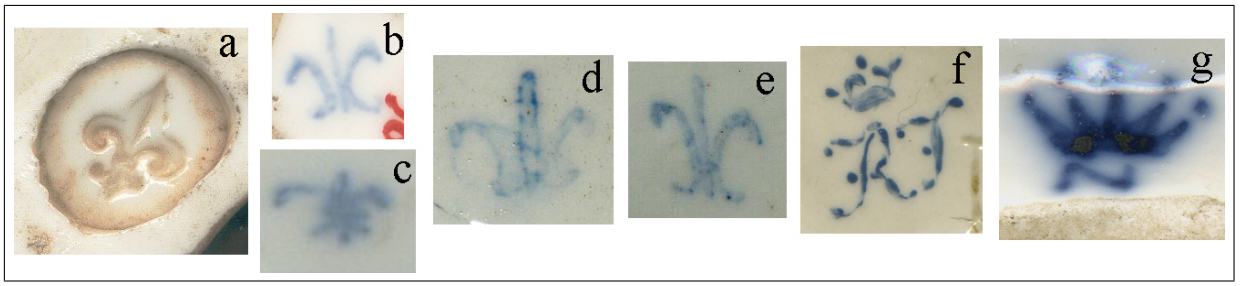

Figure 4.1: Factory marks as found on objects from Capodimonte (a,b,d,e), Buen Retiro (c), and the Real Fabbrica Ferdinandea (f,g). Images are not to scale

Starting up the manufacture was by no means an easy task, especially in terms of finding a good recipe for the porcelain paste. Raw materials arrived in Naples from several locations in Northern and Southern Italy (mostly Vicenza, Fuscaldo (CZ), Tuscany, and Sicily) , and already in 1743 at least two different paste compositions had been devised by the manufacture's chemist Livio Vittorio Schepers and his son Gaetano, both initially yielding a high number of mediocre pieces and kiln wastes. Along with the search for materials throughout the kingdom, a recognition was also conducted among the Courts which already produced porcelain, looking for recipes and skilled workers in order to accelerate the experimental phase. Help had been requested in Wien, Turin, and from the Ginori and Vezzi factories, often trying to bribe experienced labourers talking them into giving away manufacturing secrets. Finally, it is clear from historical sources that during the short life of the manufacture the quest for raw materials and the experimentations never ceased. Each and every element which could serve to improve the whole manufacturing cycle was taken into consideration: from the wood used to feed the kilns, to the minerals and raw materials used for pigments, pastes and glazes. Experimenting really stopped only when the factory closed down (Musella Guida 1993).

In 1759, when he rose to the Spanish throne becoming Charles III of Spain, the king decided to move the porcelain production to Madrid, completely dismantling the Neapolitan factory. Three small ships (the Vergine del Lauro, the Madonna delle Grazie, and the Santa Lucia) were charged with most artisans, workers, moulds, machinery and even about 400 myriagrams ($4\text{x}10^3$ kg) of porcelain paste, and left Naples on October 7^{th}, 1759, to land in Alicante the following November 12^{th}. Soon after, a new manufacture was established, called "la China", within the royal garden of Buen Retiro. The king followed its work with great interest, not disdaining to get personally involved in the hand labour, until his death in 1788 (Le Breton 1879, p. 17), when his son Charles IV inherited the kingdom. The Buen Retiro production is usually divided into three periods, to which correspond different kinds of products (Casanovas 1995). The early production (1760-1783) is similar, in composition and style, to that of Capodimonte, and even the factory mark did not change right away (fig. 4.1c). The second period (1783-1803) is characterized by the transition to a neoclassic style. In the last years (1803-1808), under the direction of Bartolomé Sureda who had been sent to study at the Sèvres Manufacture, a new magnesian paste was used and the mark was changed to an "M" (for "Madrid"),

and later to "SMR" (for "Sureda, Madrid, Retiro"). This later production was reported to the french chemist Vauquelin by his colleague Joseph Proust, who managed the manufacture's laboratory under Charles IV, as having an exceptional quality and a harder paste than that of Sèvres (Le Breton 1879, p. 19). Since the french invasion of Spain in 1808, Napoleon's troops used the Buen Retiro palace as barracks and for weapon storage. When they finally cleared out of it in 1812, a large part of the building was in ruins, and the rest was demolished in 1868; the land was handed over to the municipality of Madrid to serve as a public garden, and this is still its use today (Elliott 2000). Porcelain manufacturing was resumed in 1817 at La Moncloa, still directed by Sureda until 1820, but it never reached again the splendours of Buen Retiro, its products being rather a witness of the decadence of the Spanish court and of Spain itself at that time (Almagro 1966).

Meanwhile in Naples Ferdinand IV, son of the original founder, had restarted a porcelain factory in 1771, better known since as "Real Fabbrica Ferdinandea" (or Naples manufacture), which operated until 1807 and whose products are often mistakenly called "Capodimonte" even if they bear a different mark, usually a crowned "N" or the letters "RFR" in underglaze blue (cfr. figure 4.1f,g).

4.1.3 Research aims

Due to this unique history, products from Capodimonte (hereafter indicated as CdM) and from the first period of Buen Retiro (indicated as BR) show high similarities, and distinction between them is not always straightforward by simple visual examination, as generally done by curators. There remain, up to this day, quite a few objects unattributed between the two manufactures, e.g. those shown in the recent catalogue of Trinity Fine Art (2007, pp. 24, 26, 30, 32). Moreover, these two peculiar productions have not so far been the object of extensive archaeometric studies. Prof. Orazio Rebuffat was the first, in 1905, to provide chemical data regarding Capodimonte pastes and glazes (Rebuffat 1905). Only in 1995 more data were published regarding the chemistry, mineralogy, density and microstructure of some porcelain fragments found during excavations in the 1950s in the area formerly occupied by the manufacture (Istituto G. Caselli 1995; Mascolo 1995). Pepe (1995) reports two possible compositions for the typical Capodimonte paste, the first based on a frit, therefore more similar to soft-paste technology, and containing quartz, earths as plastic component, and fluxes in the form of soda, calcinated potassium carbonate,

and gypsum. The second possible composition does not envisage the use of a frit, and is therefore most similar to a hard-paste technology, including one ingredient containing pegmatitic rocks and acting both as flux and as a vitrifying agent, and again earths as the plastic element. The author thinks the first hypothesis more likely, but also acknowledges that definitive proofs will only come by a further rielaboration of the historical data, as well as by future analytical results.

In the past few years a more comprehensive interdisciplinary study has been undertaken on some of the mentioned excavation samples, which has included their characterization by means of SEM-EDS, XRD, optical microscopy on thin sections, and porosimetry. Such study has been carried out within the framework of a bilateral project between the Italian CNR and the Spanish CSIC on "the Bourbon porcelain from Capodimonte to Buen Retiro: continuity or innovation", whose results have been presented in various occasions and are being partly published (Amato *et al.* 2007). Tables 4.2 and 4.3 report chemical compositions of the pastes and glazes of the Capodimonte samples which have been the object of this study. As already mentioned, it is easily inferred from the data regarding the pastes, that Capodimonte porcelain can still neither be exactly defined as a "soft-paste" nor as a "hard-paste". The high silica content ($\geq$79% SiO_2) and the low values of alumina (4-9% Al_2O_3) and calcium oxide (<2% CaO) make its composition anomalous with respect to the standards of late 18^{th} century European manufactures, and more similar from the chemical point of view to the early production of "Medici porcelain". So far, the Capodimonte paste has usually been identified as a "mixed" or hybrid porcelain, having a melting point of about 1200°C (Musella Guida 1993).
The Spanish production has also been the object of some analytical investigations, mostly focused on materials from the Sureda's period, whose composition is different from any other porcelain of the time, and characterized by the use of local sepiolite (a Mg-containing silicate) as a raw material (De Aza *et al.* 2004; Pascual *et al.* 2006), which yields a final product rich in enstatite ($MgSiO_3$).

This research conducted by means of Raman spectroscopy aims at completing the characterization of the Capodimonte production and, most of all, at laying the basis for a correspondence between the results of destructive and non-destructive analyses on porcelains. In addition to the mentioned excavation samples, we have in fact analyzed a few porcelain artefacts, belonging to the Sèvres Museum, which could not have been sampled for destructive analyses.

4.2 Materials and methods

4.2.1 Excavation fragments from Capodimonte

The sixteen samples which are the object of this study belong to pieces which have been selected among the 2000 which were recovered during the mentioned excavations in the surroundings of the former factory. They can be recognized as belonging to different shapes (cups, saucers, bases of figurines), and their complete description can be found in table 4.1, while figure 4.2 shows photos of a few selected excavation samples, together with the fragments detached for analytical purposes, and the chemical composition of all bodies is reported in table 4.2.
All pastes are white or lightly coloured (in blue, purple, or brown). Eight out of the 16 detached fragments are covered, on one or both surfaces, by a colourless glaze ("couverte"); some are also glazed in green or blue, and one sample (P185) has a flowery decoration in underglaze blue. Table 4.3 reports the chemical composition of all (colourless and coloured) glazes.

4.2.2 Excavation fragments from Buen Retiro

The six samples which are the object of this study are shown in figure 4.3 and belong to pieces which have been selected among the several hundreds which were recovered during archaeological excavations in the Buen Retiro park, as well as in the Aranjuez Palace, near Madrid (Memoria del proyecto de investigación 2005; Pascual *et al.* 2006). Their description is reported in table 4.4.

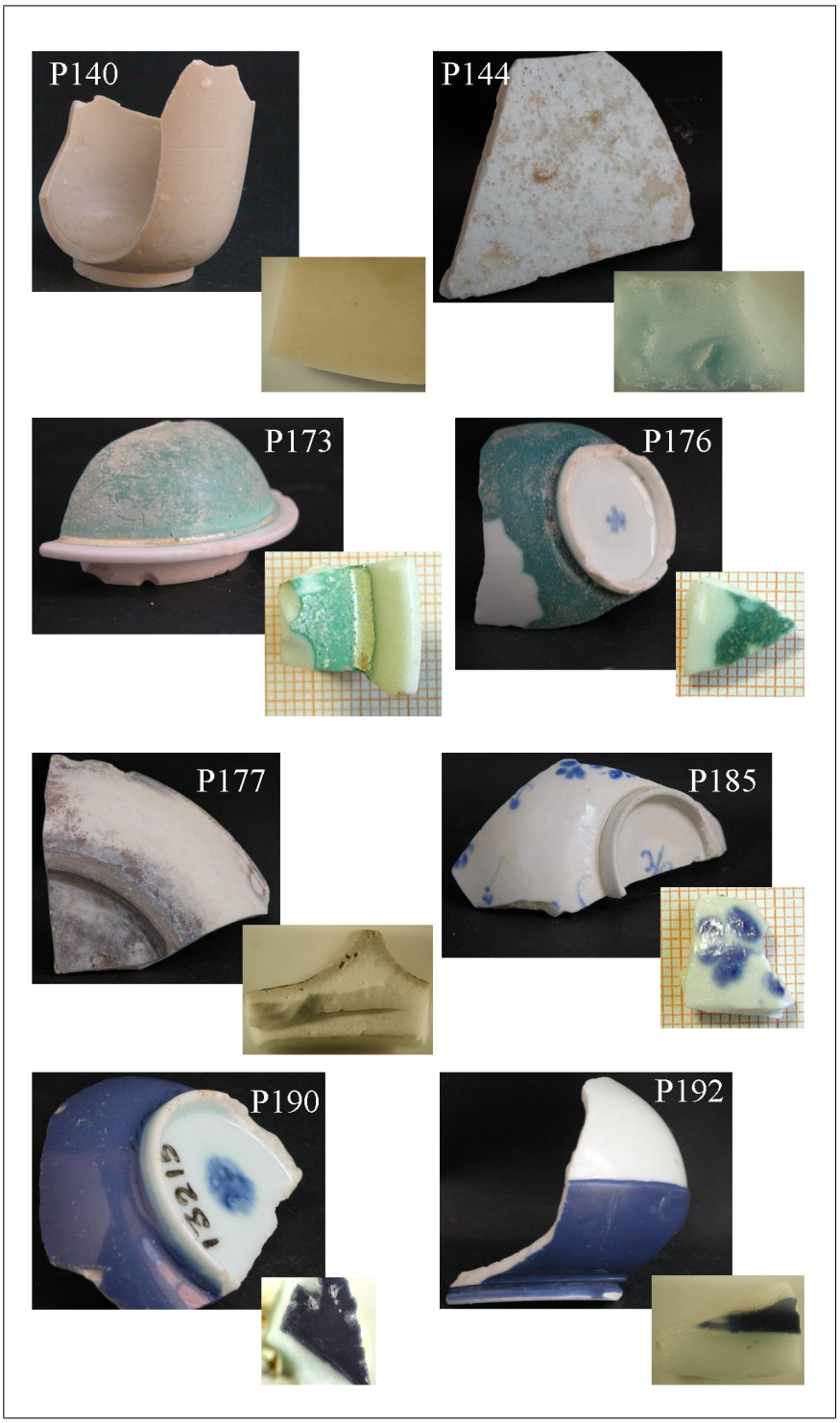

Figure 4.2: Selected excavation samples from Capodimonte, and corresponding fragments detached for analytical purposes (images not to scale)

Sample	Paste colour	Colourless glaze	Coloured glaze or decoration	Possible shape attribution
P27	white	yes		lid of sugar bowl
P42	light blue	no		vase lid
P140	light brown	no		cup
P144	light blue	no		n.d.
P161	white	no		small tray
P172	white	(yes)	turquoise	n.d.
P173	white	yes	green/golden rim	lid of coffee pot
P176	white	yes	green	base of tall cup
P177	white	no ?	greyish (degraded)	tall saucer
P180	white	no		decorative ornament
P182	white	yes	(coloured flowers)	dish
P183	white and light purple	no		base of figurine
P185	white	yes	flowery decoration in underglaze blue	small bowl
P190	light blue	yes	blue glaze	base of cup
P191	white	yes	blue multilayer glaze	n.d.
P192	white	yes	blue glaze	lower portion of milk-jug or pitcher

Table 4.1: Description of the analyzed excavation samples from Capodimonte (glazes and decorations in parentheses indicate that they were not present on the fragments used for Raman analyses)

	SiO_2	Al_2O_3	TiO_2	Fe_2O_3	MgO	CaO	Na_2O	K_2O	PbO	SnO_2	P_2O_5	SO_3
P27	84.26	6.48	0.11	0.34	0.35	1.76	2.80	2.96	0.00	0.00	0.31	0.17
P42	85.53	6.43	0.11	0.49	0.39	1.30	2.26	2.70	0.00	0.23	0.13	0.14
P140	81.67	8.55	0.11	0.53	0.50	0.55	1.45	2.81	0.82	1.34	0.33	0.19
P144	82.32	7.57	0.12	0.37	0.35	1.19	4.15	2.55	0.00	0.19	0.35	0.18
P161	84.75	7.48	0.23	0.39	0.51	1.19	1.97	2.92	0.00	0.29	0.25	0.00
P172	84.84	5.94	0.03	0.50	0.33	1.82	2.74	3.22	0.00	0.20	0.16	0.17
P173	84.70	5.55	0.21	0.32	0.41	1.46	3.46	2.45	0.00	0.66	0.39	0.19
P176	83.84	6.09	0.11	0.38	0.40	1.60	2.60	2.81	0.19	1.37	0.34	0.10
P177	84.27	5.45	0.16	0.52	0.50	1.61	3.15	2.71	0.00	1.04	0.24	0.21
P180	84.31	6.04	0.20	0.21	0.41	1.20	3.76	2.35	0.00	0.72	0.40	0.21
P182	83.95	6.48	0.13	0.42	0.44	1.69	2.50	2.74	0.00	0.84	0.32	0.32
P183	82.28	5.25	0.08	0.32	0.42	1.54	1.31	5.16	1.13	0.46	0.37	0.26
185	79.72	3.55	0.18	0.27	0.49	1.81	3.16	3.41	2.82	3.50	0.22	0.40
P190	82.93	7.64	0.15	0.34	0.35	1.19	3.76	2.75	0.00	0.35	0.28	0.25
P191	84.83	6.33	0.03	0.39	0.33	1.47	2.11	2.98	0.00	0.00	0.36	0.09
P192	84.67	6.20	0.10	0.41	0.36	1.76	2.61	2.86	0.00	0.55	0.27	0.21

Table 4.2: Chemical composition of Capodimonte and Buen Retiro porcelain pastes, as reported by Amato *et al.* (2007) (weight % oxides normalized to 100; tr. = traces; n.d. = not determined). Minor amounts of Cl are included in the normalization but not reported in the table

	SiO_2	Al_2O_3	TiO_2	Fe_2O_3	MgO	CaO	Na_2O	K_2O	PbO	SnO_2	CoO	CuO	Cl
Colourless glazes													
P27	53.07	3.69	0.12	0.40	0.21	1.14	5.47	2.29	32.93	0.29	0.00	0.00	0.34
P173	51.50	1.42	0.28	0.21	0.38	2.61	5.86	1.61	34.10	1.54	0.00	0.00	0.47
P176	57.55	3.34	0.27	0.10	0.26	1.23	6.77	2.65	21.72	5.22	0.00	0.19	0.37
P182	53.03	2.49	0.16	0.14	0.37	1.40	5.68	2.10	33.24	1.00	0.00	0.00	0.30
P185	55.51	1.56	0.12	0.34	0.37	1.78	6.76	3.52	27.61	1.26	0.00	0.00	0.41
P190	50.83	3.33	0.09	0.19	0.23	1.16	7.75	1.72	30.00	3.99	0.00	0.00	0.48
P191	50.87	1.92	0.38	0.38	0.12	1.70	4.44	1.86	36.75		0.25	0.30	0.35
P192	50.55	3.24	0.07	0.16	0.24	1.26	6.10	2.01	35.41	0.58	0.00	0.00	0.36
Green glazes													
P173	37.78	2.26	0.20	0.06	0.32	1.04	7.34	1.46	36.88	6.31	0.00	5.25	0.81
P176	43.24	1.72	0.04	0.31	0.40	1.64	7.15	1.57	32.12	7.06	0.00	3.89	0.82
Blue glazes													
P190	54.63	2.25	0.12	1.08	0.32	2.38	10.45	3.48	13.50	8.47	0.70	0.00	1.18
P191	57.92	2.12	0.15	0.96	0.33	2.00	8.16	3.88	10.47	10.37	0.69	0.97	0.61
P192	58.05	2.13	0.01	1.18	0.22	1.97	8.57	3.31	11.52	9.96	0.40	0.36	0.75

Table 4.3: Chemical composition of Capodimonte porcelain glazes, as determined by the researchers of CNR-ISTEC (unpublished data) (weight % oxides normalized to 100; tr. = traces; n.d. = not determined). Minor amounts of Sb, As and Ni, mostly linked to the presence of Co, are included in the normalization but not reported in the table

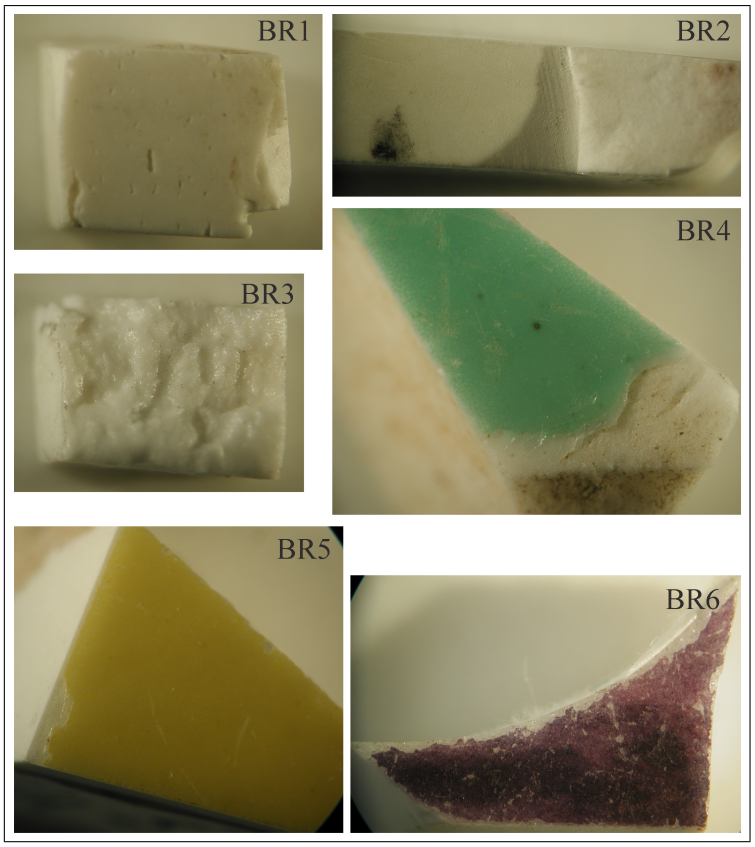

Figure 4.3: The analyzed excavation samples from Buen Retiro (images not to scale)

Sample	Inventory number	Period	Glaze	Shape attribution
BR1	219/124	1760-1783	unglazed	n.d.
BR2	329/20	1760-1783	thin colourless glaze (degraded)	n.d.
BR3	226/3	1803-1808	unglazed	sculpture
BR4	133	1803-1808?	green glaze	floor tile?
BR5	457	1803-1808	yellow glaze	floor tile (Huerto del Francés)
BR6	L6P3	1803-1808	purple glaze	floor tile (Casita del Labrador)

Table 4.4: Description of the analyzed excavation samples from Buen Retiro

4.2.3 Museum objects

Artefacts attributed to both manufactures have been selected within the collections of the National Ceramics Museum of Sèvres, and are described in tables 4.5 and 4.6. The most impressive one is a large fragment belonging to the tabletop of a pedestal table from Capodimonte (GUE), entirely made in porcelain, and decorated with oriental-looking motifs. It has been recently restored at the Sèvres Museum in the occasion of its display in an exhibition at the Musée Cernuschi in Paris ("Pagodes et dragons: exotisme et fantaisie dans l'Europe Rococo 1720-1770" february 23^{rd} to june 24^{th}, 2007). Figure 4.4 shows it along with all the other analyzed objects from Capodimonte: two pairs of cups and saucers (TB, SCB, T_Or and SC_Or), a small figurine of a fisher (SH), and a pitcher decorated with a variety of coloured insects (CRU). Objects attributed to Buen Retiro are shown in figure 4.5; they are the lid of a soup bowl (COUV), a cup decorated with a landscape of archaeological ruins (TA), and a couple of tall bell-shaped vases decorated with a brownish camaïeu (V1BR and V2BR). The museum records tentatively attribute the latter to the first period of the Retiro production, but their decoration in a typical Neoclassical style would more likely assign them to the second period. Additionally, a description made by Arthur Lane (Lane 1954, p. 56: *"From the Madrid collections one gains the impression that the ornamental Buen Retiro vases which show the greatest technical accomplishments are those in a pronounced neo-classical style. They were evidently made under the regime of the two younger Gricci (1784-1803)* [...]. *A brilliant, glassy white paste was used for open bell-shaped vases on pedestal feet* [...]) seems to refer to the exact same kind of vases as those which have been analyzed. All these Buen Retiro objects also bear the Capodimonte mark, as was often the case at the beginning of the Spanish production.

All samples except the golden saucer (SC_Or) presented portions of broken/chipped surface or absence of the glaze on the base of the footring, which allowed paste analysis in a completely non-destructive way, with no need of sampling the object or preparing it for the Raman analysis.

4.2.4 Analytical methodology

Raman spectra have been collected on pastes, glazes and pigments using all three instruments described in section 2.3: the Dilor XY2 for macroscopic analyses, and the Jobin Yvon Labram Infinity and Dilor XY1 for microscopic investigations (mostly with a 50x objective, which yields a total magnification of 500 times). Each sample has been ana-

Sample	Inventory n.	Dimensions	Mark	Notes
GUE: fragment from the tabletop of a pedestal table	MNC 4423	Tabletop: 1 m x 61 cm		Label: "Console, porcelaine tendre Capo di Monte, vers 1756-1758 Acquis 1853 à Londres Auteur GRICCI décorateur FISCHER"
TB and SCB: white cup and saucer	MNC 5390	Cup: h. 6.4 cm Ø 6.4 cm, ø 3.2 cm Saucer: h. 2.5 cm Ø 14 cm, ø 8 cm	Blue fleur-de-lis	White flowery decoration in relief Acquired in 1860
T_Or and SC_Or: golden cup and saucer	MNC 13578	Cup: h. 7.4 cm Ø 6.8 cm, ø 3.2 cm Saucer: h. 2.6 cm Ø 13.5 cm, ø 7 cm	Blue fleur-de-lis	Golden decoration in the so-called "Meissen style" Gift from the Marquis de Grollier 1908
CRU: pitcher	MNC 13579	h. 20 cm	Blue fleur-de-lis	Handle is missing Decorated with insects
SH: figurine (fisher)	MNC 13527	h. 15 cm base 7 x 5 cm	Impressed fleur-de-lis	Broken arm Gift from the Marquis de Grollier 1908

Table 4.5: Description of the analyzed Capodimonte artefacts from the collections of the Sèvres Museum

Figure 4.4: The analyzed objects from the Capodimonte manufacture (images not to scale); the analyzed fragment of the tabletop is shown in the white rectangle on the top left corner (Tabletop photo: V. Milande, Sèvres Museum). Inventory numbers and object descriptions can be found in table 4.5

Sample	Inventory n.	Dimensions	Mark	Notes
COUV: lid of soup bowl	MNC 3091-3	length 28 *cm*	Impressed fleur-de-lis	One child missing Label: "porcelaine tendre?, Buen Retiro, Madrid, 18^{th} century"
TA: tasse	MNC 16316	h. 7 *cm*	Blue fleur-de-lis?	Painted decoration of a landscape with ruins gift from M. Pape 1917
V1BR, V2BR: couple of bell-shaped vases	MNC 3091-1/2	h. 28 *cm*	Blue fleur-de-lis	Decoration in Neoclassical style Label: "1775/1780?" Acquired in 1843 from M. Barscia, spanish merchant

Table 4.6: Description of the analyzed Buen Retiro artefacts from the collections of the Sèvres Museum

Figure 4.5: The analyzed objects from the Buen Retiro manufacture (images not to scale). Inventory numbers and object descriptions can be found in table 4.6

lyzed in an average of 4-5 points, in order to gain a view as complete as possible of the composition, especially in the case of pastes which are usually less homogeneous than the glazes. In the case of the museum objects, microscopic investigations of glazes and pigments has been undertaken only with the Dilor XY1, again mostly with the 50x objective. Also in this case a few points have been analyzed on each sample, when possible. It has not always been easy to find large areas for paste analysis, which has forcedly been confined to chipped or unglazed portions of the artefacts.

4.3 Results and discussion

4.3.1 Characterization of pastes

Excavation fragments from Capodimonte

All Capodimonte fragments contain large quantities of crystalline α-quartz (peaks at 200, 262, 353, 462, 1080 and 1160 cm^{-1}), sometimes together with more or less abundant cristobalite (225 and 415 cm^{-1}), and trydimite (290, 350 and 430 cm^{-1}), the latter phases being characteristic of a high firing temperature. The presence of some glassy phase can also be identified in some cases, due to the traces of large bands centered around 500, 800 and 1000 cm^{-1} (the latter almost completely obscured by the background). In the spectra of eight samples the characteristic peaks of β-wollastonite, at 637 and 971 cm^{-1}, can be identified. Some samples show also a small peak around 965 cm^{-1}; this position corresponds to the main peak of phospates, which are usually found in Bone China pastes (Edwards *et al.* 2004; Leslie 2003), but we do neither have enough data at the moment to confirm this attribution, nor to propose a valid alternative.
The 16 fragments have been grouped on the base of the Raman spectra of pastes, by considering the presence and abundance of the different silica polymorphs and of glassy phase, and also the presence or absence of β-wollastonite. These criteria yield a classification into three groups, whose typical spectra are shown in figure 4.6:

- group 1 (quartz, cristobalite, tr. trydimite): samples P42, P140, P161;

- group 2 (quartz, cristobalite/trydimite, glassy phase[1]): samples P144, P176, P180,

[1]The presence of small amounts of glassy phase can be hypotesized in all the analyzed samples. However, its constant presence is more evident in the spectra of group 2 samples; this is why it is considered as a "characteristic" signature for this group

P185, P190;

- group 3 (quartz, β-wollastonite, tr. cristobalite/trydimite): samples P27, P172, P173, P177, P182, P183, P191, P192.

Besides the mineral phases already mentioned, which are the most meaningful for making compositional and technological comments, Raman spectra also showed the presence in some samples of accessory phases such as iron oxides, traces of feldspars and sulphates, and titanium dioxide in the form of both anatase and rutile. They are naturally present in clays or can derive from transformations which take place during firing.

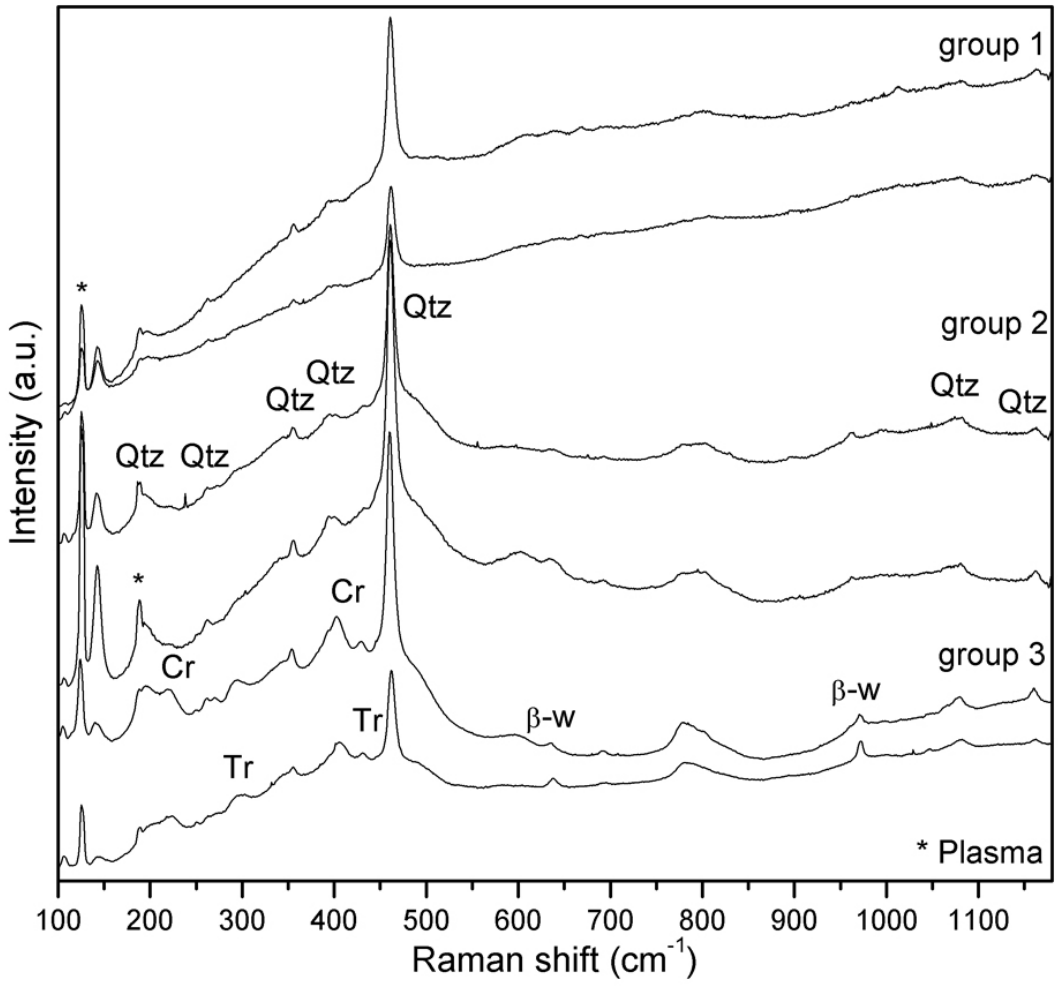

Figure 4.6: Representative Raman spectra of the three paste groups identified within the Capodimonte samples (Qtz: quartz, Cr: cristobalite, Tr: trydimite, β-w: β-wollastonite)

This classification can be further discussed in the light of the chemical composition of pastes, reported in table 4.2. These data show a certain chemical homogeneity among the 16 samples but we can observe, for example, that group 2 samples are characterized by a high sodium content, with an average of 3.5% Na_2O vs. average values of 1.9 and 2.6% Na_2O for groups 1 and 3, respectively. This can justify the abundance of cristobalite and trydimite, whose formation is favoured by the high sodium values, as it is evident from the phase diagram of the Na_2O-Al_2O_3-SiO_2 system (Levin *et al.* 1974). The absence of wollastonite in group 1 spectra is probably due to the low CaO/Al_2O_3 ratio in the samples ($\sim$0.14 vs. 0.26-0.28 in the other groups), and possibly also to a lower firing temperature. Finally, the absence of wollastonite in samples of group 2 can be due to a different "form" in which calcium was introduced in the paste. In fact, if CaO and SiO_2 are finely ground, wollastonite will more easily crystallize during firing.

Moreover, traces of diopside ($CaMgSi_2O_6$) were detected in a total of six samples (2 from group 1, 3 from group 2, 1 from group 3). Unfortunately, there does not seem to be any relationship between the presence of this phase and the chemical composition of the samples, neither in terms of calcium content nor of the Ca/Mg ratio.

Excavation fragments from Buen Retiro

Chemical analyses were only performed on samples BR1 and BR2 by the researchers of the Spanish CSIC-Instituto de Céramica y Vidrio (unpublished data), but Raman spectra were acquired of all six samples (fig. 4.7). All pastes contain variable amounts of quartz, almost always together with variable amounts of cristobalite. The samples can be grouped as follows, on the basis of the mineral phases identified in their spectra:

- BR2 and BR4 contain cristobalite and also show a peak at about 638 cm^{-1}, which can probably be attributed to SnO_2. These samples are therefore almost fully comparable to those of group 1 samples from Capodimonte;

- BR1 does not contain cristobalite, but it contains diopside ($CaMgSi_2O_6$, peaks at 669 and 1015 cm^{-1}), which is compatible with its Ca and Mg content, considerably higher than in the other first period sample (2.57 vs. 0.75 CaO and 2.44 vs. 0.36 MgO). Also the presence of (clino)enstatite can be hypothesized, linked to two small peaks at 687 and 1031 cm^{-1}. A Raman spectrum very similar to that of BR1 has been acquired by Leslie (2003, p. 194) on a mid-eighteenth century soapstone porcelain sample from the Chaffers (Liverpool) manufacture, and interpreted as

containing both diopside and enstatite. The peak at 340 cm^{-1}, visible in the spectra of BR1, would further support the presence of enstatite in this sample;

- BR3, BR5 and BR6 contain variable amounts of cristobalite, traces of trydimite and relevant amounts of (proto)enstatite ($MgSiO_3$, peaks at about 334, 674, 1014 and 1038 cm^{-1}); there is no evident difference between the paste of the figurine (BR3) and those of the two tiles (BR5 and BR6).

It can be observed that this grouping coincides only partially with the chronological one, the main discrepancy being the absence of enstatite in BR4, which makes it different from a "typical" third period sample. Further comments are possible on this sample's attribution, following glaze analysis (cfr. section 4.3.2). Moreover, there are some differences between samples BR1 and BR2, even though they are both attributed to the same production period.

Museum objects

Figure 4.8 shows representative Raman spectra recorded on exposed areas of the pastes of the museum artefacts. Capodimonte objects have rather homogeneous Raman signatures. They all show the main peaks of crystalline α-quartz, together with cristobalite and trydimite in variable amounts, and some glassy phase, and are therefore comparable to group 2 pastes of the Capodimonte fragments.

The spectra of the Buen Retiro lid (COUV) and cup (TA) contain the same phases, and additionally the main peaks of β-wollastonite; this makes these two samples fully similar to group 3 fragments from Capodimonte. Finally, the paste spectra of the ornamental vases contain quartz, traces of crisobalite and trydimite, relevant amounts of α-wollastonite, and a series of well defined peaks (at 269, 455, 534 and 785 cm^{-1}) which can tentatively be attributed to a mineral of the scapolite family[2]. This pastes therefore show a very peculiar Raman signature, never so far identified in other porcelain materials.

It needs to be pointed out that in most of these spectra, the fluorescence background is very high, to the point that most peaks are only weakly superimposed to it. The importance of such a background might be linked to the fact that the analysis is made

[2]Scapolites are complex silicates; further investigations on their stability range would be needed, in order to validate the hypothesized identification. Moreover, these minerals always contain small amounts of chlorine, sulphates and/or carbonates, whose presence would not be common in a porcelain paste

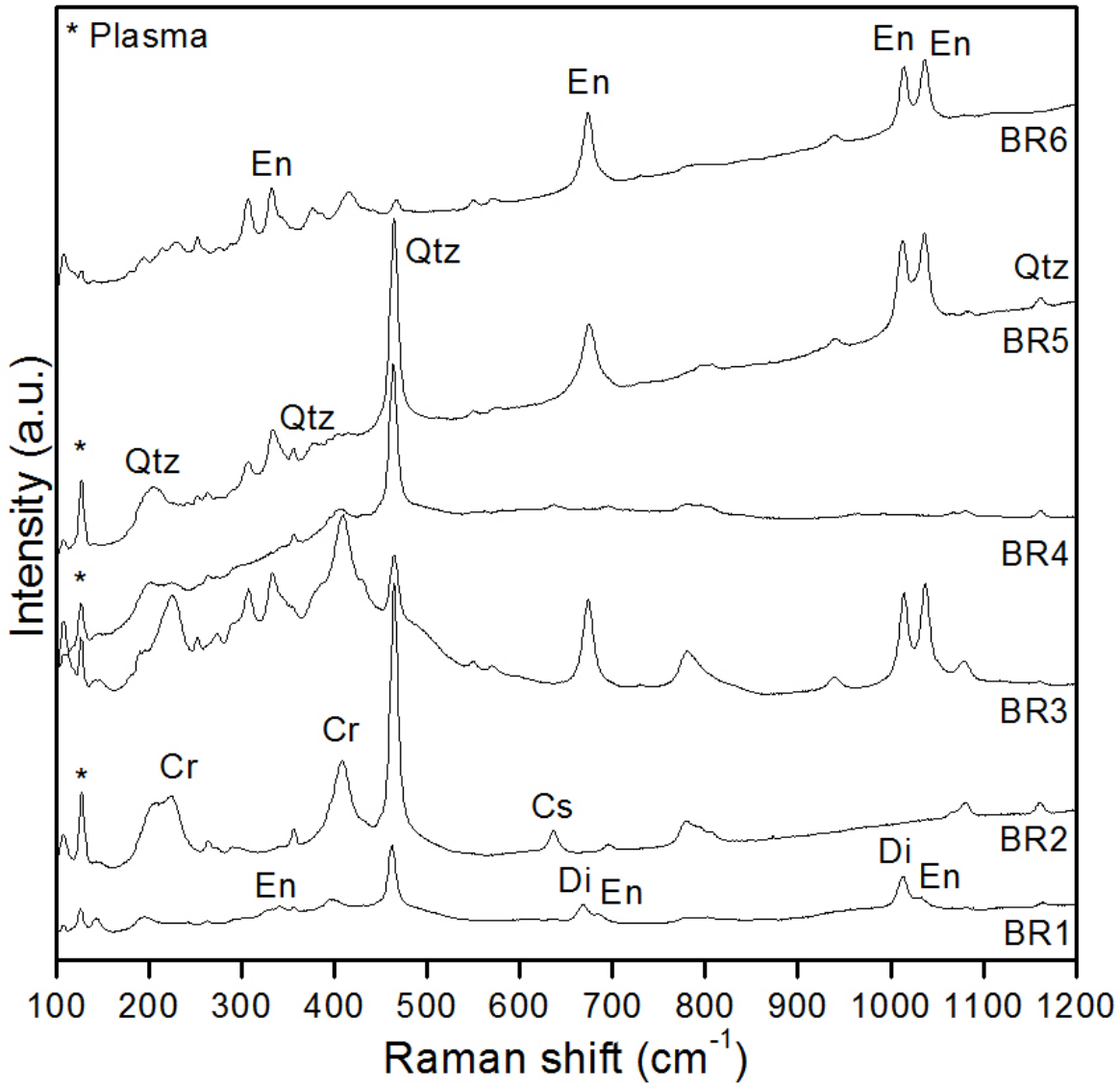

Figure 4.7: Representative Raman spectra of the pastes of the excavation samples from Buen Retiro (En: enstatite, Qtz: quartz, Cr: cristobalite, Cs: cassiterite, Di: diopside)

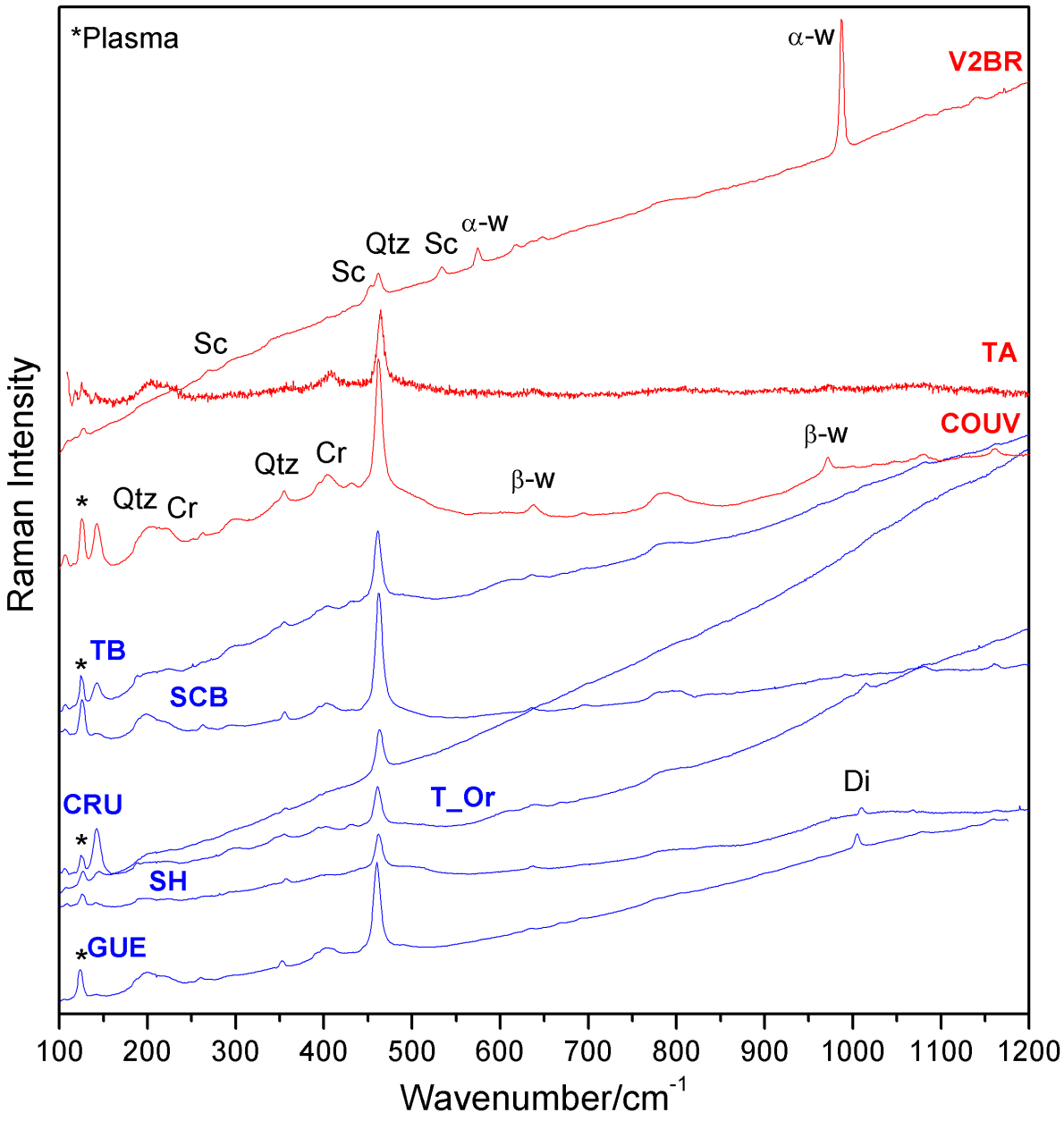

Figure 4.8: Representative Raman spectra of the pastes of all museum objects from the Sèvres collection (Qtz: quartz, Sc: scapolite, α-w: α-wollastonite, Cr: cristobalite, β-w: β-wollastonite, Di: diopside)

on surfaces which are not freshly fractured, so dust and other contaminants may have spread over them. This makes it very hard to evaluate the amount of glassy phase in the pastes, and the overall comparison with the Capodimonte excavated fragments becomes of course more difficult.

> *Paste analysis showed that all the Capodimonte objects have Raman signatures which are compatible with those of the excavation fragments. The presence of crystalline α-quartz, cristobalite, trydimite and occasionally of β-wollastonite is in agreement with the average chemical composition of Capodimonte pastes. This allows considering the obtained spectra as a good reference for future analysis of porcelains possibly attributed to this manufacture. The presence of different Raman signatures, obtained from the analysis of samples of the same provenance and relative to such a short time interval (the sixteen years of activity of the manufacture), well agrees with documentary evidence of the fact that testings for suitable raw materials and production technologies, started in 1740, went on at least until 1752, and were resumed when the Real Fabbrica opened (Minieri Riccio 1878d). Buen Retiro pastes seem to have developed a more complex mineralogical composition, especially in the last part of the production, as indicated by the presence of scapolite in the vases, and enstatite in the third period samples. Further analyses would be useful, especially on first and second period excavation samples, in order to better define the Raman signature of this production; it is clear in fact that the raw materials and the production technology have been very varied during the three periods of this manufacture's life. Table 4.7 summarizes the results of the Raman analysis of all the pastes.*
>
> *From the methodological point of view, the use of a macro- rather than a micro-Raman approach seems sufficient in order to obtain data as representative as possible of the overall composition of each paste. In addition, the use of a high-energy laser, such as that of the XY2 spectrometer, helps "cleaning" the sample's surface and thus reducing to some extent the spectral background. Microscopic measures can also become useful, for example when the visual inspection of a sample reveals the existence of marked inhomogeneities within the material.*

Group	Samples	Characteristic Raman signatures
1	3 Cdm exc.	Quartz
1b	1 BR exc. (1^{st} period)	Quartz, (clino)enstatite
2	5 CdM exc., GUE, SH, CRU, TB, SCB, T_Or, 2 BR exc. (1^{st} and 3^{rd}? period)	Quartz, cristobalite, tr. trydimite, glassy phase
3	8 CdM exc., COUV, TA	Quartz, cristobalite, trydimite, β-wollastonite
4	3 BR exc. (3^{rd} period)	Quartz, cristobalite, tr. trydimite, (proto)enstatite
5	V1BR, V2BR	Quartz, tr. cristobalite, tr. trydimite, α-wollastonite, scapolite

Table 4.7: Schematic representation of the results of Raman analysis on the pastes of CdM and BR excavation samples and museum objects (exc.: excavation samples, tr: traces)

4.3.2 Characterization of colourless glazes

The colourless glazes ("couvertes") present on almost all the studied samples have been characterized by acquiring a series of spectra using all three of the LADIR's instruments (cfr. section 2.3), with the exception of museum objects, which have not been analyzed with the Labram Infinity. Calculation of the Raman parameters has been made by choosing *a posteriori* a representative spectrum per sample, always obtained in microscopic configuration with the Dilor XY1 spectrometer. Macroscopic analysis in fact yields spectra which are "disturbed" by a high number of peaks due to crystalline phases, mostly located at the interface between glaze and paste, or in the paste itself; this makes it harder to execute a correct decomposition of the spectra. Additional comments on this subject are reported in section 4.3.5.

Excavation fragments from Capodimonte

The glazes of the Capodimonte fragments show a general homogeneity which does not allow subdividing them into groups, let alone reproducing the same grouping made for the corresponding pastes. Representative spectra are presented in figure 4.9, and the corresponding Raman parameters are reported in table 4.8. Some spectral features can

however be highlighted:

- on the basis of their spectral shape and calculated parameters, all the colourless glazes can be attributed to the family of *Na-Pb* silicate glasses;

- all glazes contain undissolved quartz crystals, as shown by the peak at 462 cm^{-1} which also corresponds to the position of the maximum of the first massif;

- two samples (P190 and especially P176) show a more or less pronounced "shoulder" around 530 cm^{-1}; these glazes contain a great amount of Na_2O, and their spectral shape consequently tends to have some of the typical features of soda silicate glasses. The same spectra contain also the main peak of cassiterite (635 cm^{-1}), which is in accordance with the high tin content measured (greater than 4% SnO_2, as opposed to an average of 0.78% in the remaining fragments).

	I_p	Q_0	Q_1	Q_2	Q_3	Q_4	δ_{MAX} *Si-O*	ν_{MAX} *Si-O*
P27	0.82	792	921	972	1033	1122	461	1035
P173	0.69	791	917	978	1044	1109	463	1043
P176	0.76	785	923	977	1039	1087	463[1]	1047
P182	0.60	787	922	980	1047	1122	460	1049
P185	0.83	788	919	982	1054	1110	462	1057
P190	0.70	783	934	978	1030	1096	460	1034
P191	0.59	789	921	971	1033	1125	460	1034
P192	0.54	784	927	976	1032	1105	460	1032

[1]This is the only case in which the maximum of the first massif is not represented by the main peak of crystalline quartz

Table 4.8: Raman parameters extracted from the XY1 spectra of colourless glazes of the CdM excavation samples (wavenumber positions in cm^{-1})

Museum objects

Regarding the museum artefacts, all of their glazes show a general homogeneity in spectral shape, Q_n band wavenumbers and maxima of the bending and stretching massifs, with few exceptions, and from their Raman spectra they can also easily be attributed to the family of *Na-Pb* glasses (cfr. figure 4.10 and table 4.9). On the other hand, values

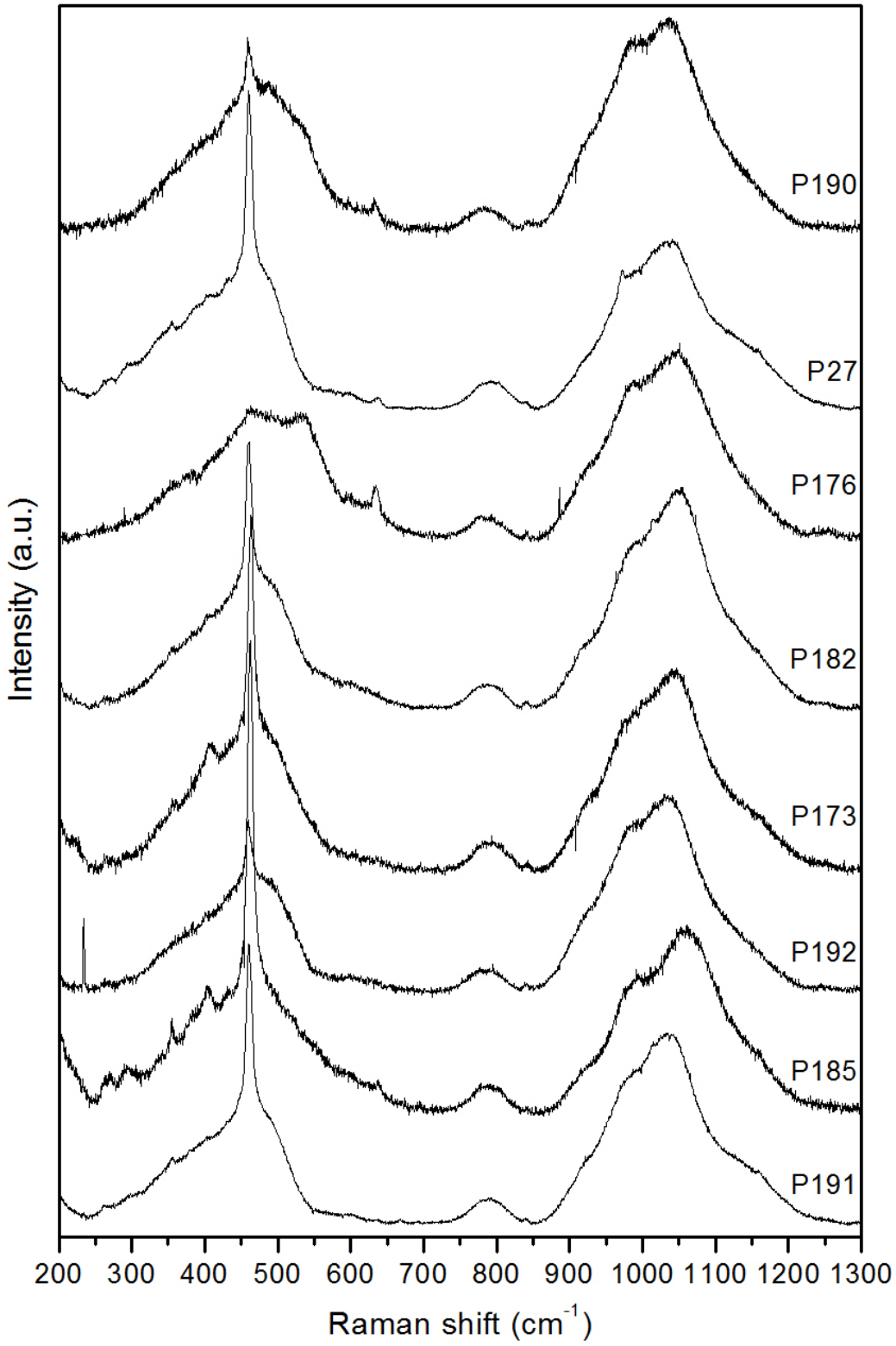

Figure 4.9: Representative Raman spectra of the colourless glazes of the CdM excavation samples (microscopic analysis - XY1)

of the polymerization index show some variations, which so far do not seem correlated to the attribution to one or the other manufacture (Capodimonte and Buen Retiro).
It can finally be observed in figure 4.10 that the glazes of the two saucers (SCB and SC_Or) yield spectra which contain a higher amount of crystalline silica (in the form of its three polymorphs) than the other glazes. This is compatible with a more siliceous and therefore more refractory composition, which yields also high values of I_p.

Some more comments can be made about two of the objects, namely the pitcher (CRU) and the golden cup (SC_Or). In addition to the previously mentioned signatures, the glaze spectra of these objects, acquired in macroscopic configuration, show also the peaks of β-wollastonite, which is neither visible in the paste spectra nor in the glaze spectra acquired in microscopic configuration. This would indicate that this phase is present at the interface between paste and glaze; in fact, molten *Pb*-containing glazes act as a very active flux and may lead to phase crystallization at the interface.

	I_p	Q_0	Q_1	Q_2	Q_3	Q_4	δ_{MAX} *Si-O*	ν_{MAX} *Si-O*
GUE	1.58	784	916	973	1040	1105	461	1037
SCB	1.53	790	931	989	1048	1130	462	1056
SC_Or	1.28	780	912	976	1055	1156	462	1056
CRU	0.95	785	922	983	1050	1124	462	1047
SH	0.66	786	927	976	1031	1107	462	1032
V1BR	0.52	774	920	975	1026	1119	461	1024[1]
COUV	1.92	781	913	975	1042	1118	463	1044
TA	0.41	786	919	977	1047	1124	463	1049

[1]Actually the highest point of this second massif is at 988 cm^{-1}, corresponding to the main peak of crystalline α-wollastonite

Table 4.9: Raman parameters extracted from the XY1 spectra of colourless glazes of the museum objects (wavenumber positions in cm^{-1})

It can be noted that the glazes of CdM museum artefacts are evidently comparable with those of the excavation samples, and a good agreement between the values of the polymerization index can also be observed. The Raman spectrum

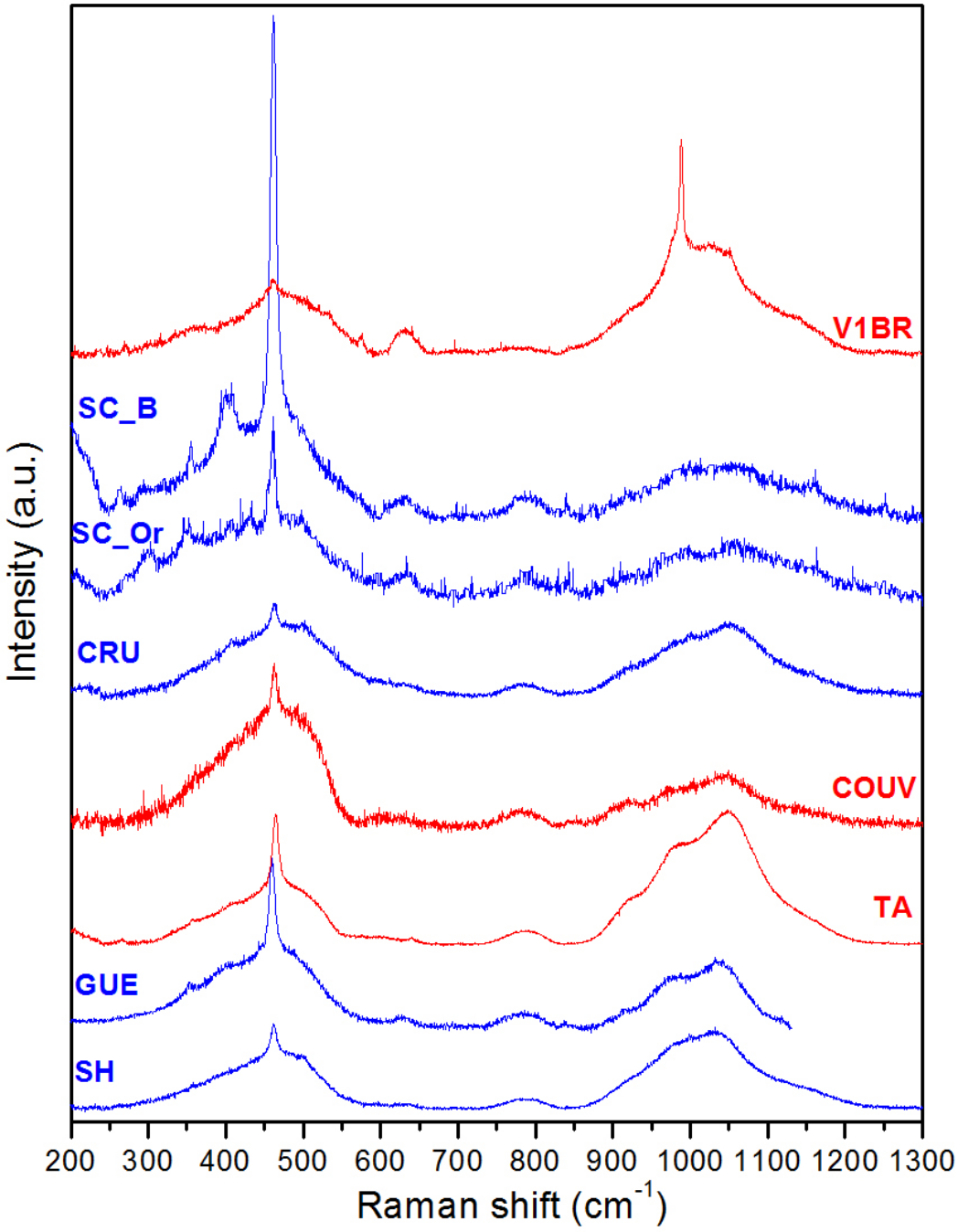

Figure 4.10: Representative Raman spectra of the colourless glazes of the museum objects from Capodimonte, in blue, and Buen Retiro, in red (microscopic analysis - XY1)

of the glaze of the Buen Retiro cup (TA) is very similar to those of Capodimonte, as is that of the lid (COUV), which however has a higher I_p*, possibly indicative of a higher firing temperature. The glazes of the two vases (V1BR and V2BR) show some differences from all the other ones (slightly lower position of* ν_{MAX} *Si-O, presence of* α*-wollastonite). Finally, all the analyzed glazes have Raman signatures and* I_p *values which are similar to those observed in samples from other* 18^{th} *century soft-paste manufactures (Colomban* et al. *2004a).*

It also seems that a more accurate interpretation of the macroscopic spectra of the glazes, together with a thorough comparison with the corresponding microscopic spectra would yield interesting information on the composition of the interface between paste and glaze. This would in turn give technological indications about the production process of the artefacts.

4.3.3 Characterization of coloured glazes and pigments

Excavation fragments from Capodimonte

Two of the Capodimonte fragments are covered by a green glaze (P173 and P176), while three of them have a multi-layered blue glaze (P190, P191 and P192). Thin sections of two coloured glazes are shown in figure 4.11, along with the thin section of a colourless glaze for comparison. In addition to this, one sample presents a blue underglaze decoration (P185, cfr. figure 4.2). Representative Raman spectra of all of these coloured glazes are shown in figures 4.12 and 4.13; they are all characterized by the presence of cassiterite

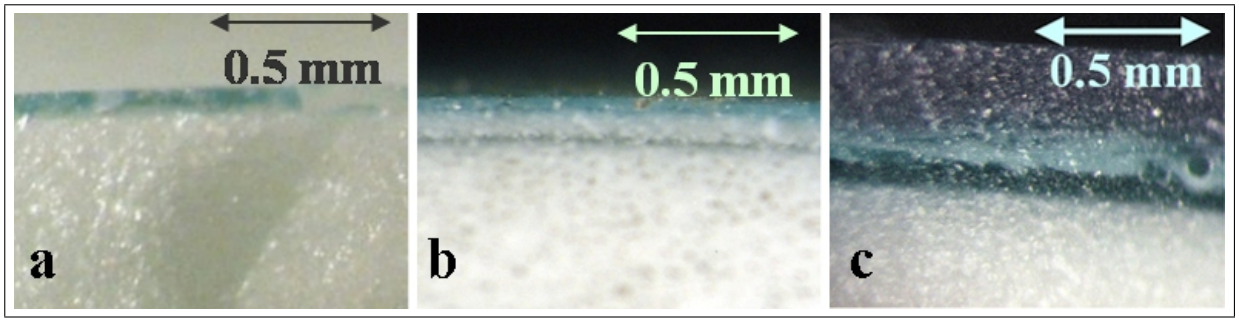

Figure 4.11: Thin sections of CdM excavation fragments with: (a) colourless glaze, sample P27, (b) green glaze, sample P176 and (c) layered blue glaze, sample P191

(peaks at about 635 and 780 cm^{-1}). On the base of their spectra, the green glazes can be assigned to the family of *Na-Pb* silicate glasses (just like the couvertes), while blue glazes belong to the family of soda silicate glasses. The spectrum of the blue decoration is clearly different, referring in effect to the colourless glaze of this sample, but including also the signature of the pigment, originated in the layer right underneath the couverte. The spectra of the green glazes also show very intense peaks at 125 (not shown in the figure) and 508 cm^{-1}, linked to the presence of whitish small crystals recognizable as a lead oxide, which contributes to the opacification of the glaze itself and most of all to a whitening of the colour. This itself is due to the interaction of *Pb* with *Cu* ions dissolved within the glass, which as expected do not yield a Raman signature, but whose presence is confirmed by the chemical analysis (cfr. table 4.3). The spectra of the blue glazes and pigment are characterized by an intense peak at 995 cm^{-1}, which we tend to attribute to a *Ca* and/or *Al*-silicate, containing also cobalt ions, which are certainly (seen the results of chemical analyses) responsible for the deep blue colour of these materials. So far it has unfortunately not been possible to find suitable standard Raman spectra of *Co* oxides or silicates which would allow to validate this hypothesis.

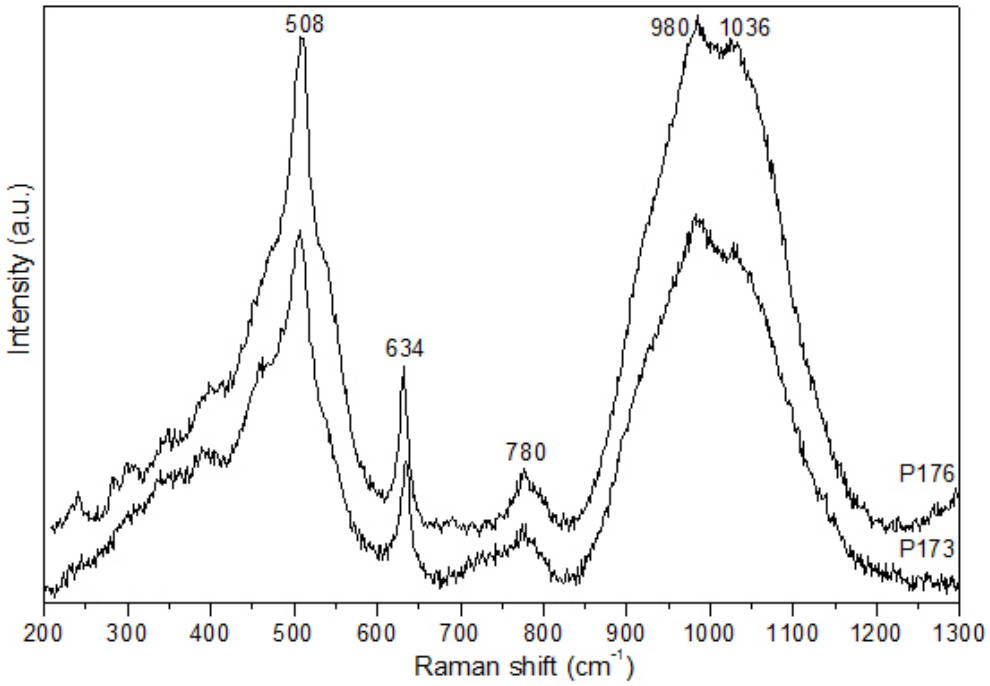

Figure 4.12: Representative Raman spectra of the green glazes on samples P173 and P176

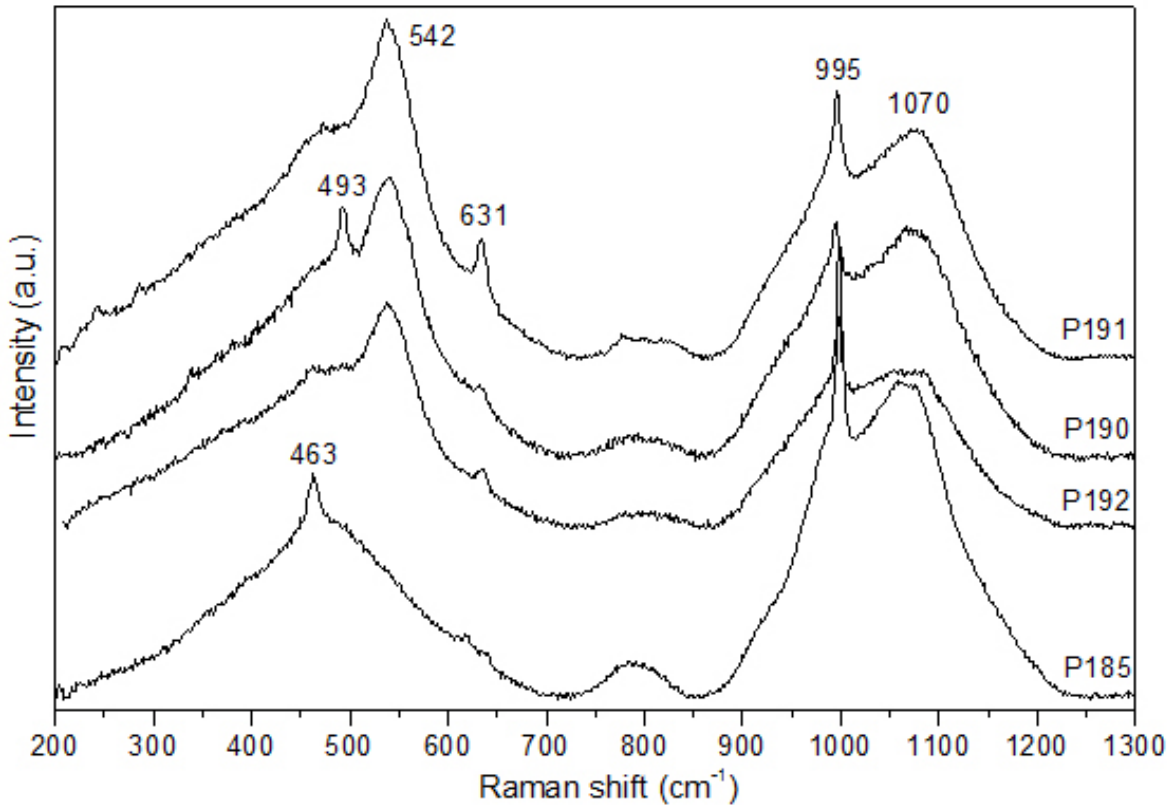

Figure 4.13: Representative Raman spectra of the blue glazes on samples P190, P191 and P192, and spectrum of the blue underglaze pigment on sample P185

Excavation fragments from Buen Retiro

The three coloured glazes of the BR samples, respectively green (BR4), yellow (BR5) and purple (BR6), have also been analyzed and Dilor XY1 spectra (Fig. 4.14) have also in this case been chosen for deconvolution, because of the absence of pigment and/or enstatite peaks superimposed to the massifs, which were instead visible in most of the spectra collected with other instruments. Spectra of the green glaze (BR4) show the main peak of quartz, and have a shape typical of *Na-Pb* silicate glasses; they are clearly different from the spectra of the yellow and purple glazes (BR5 and BR6). These two are very similar, and show the features of glasses rich in aluminium, calcium and potassium (*K-Ca-Al* silicate glasses). Most of the BR6 spectra show also peaks due to crystalline enstatite. The Raman parameters extracted from these spectra are presented in table 4.10. The differences with the Capodimonte couvertes can hardly be attributed only to the colour of these glazes. By the way, previous analyses conducted on Sureda's period

BR glazes (Pascual *et al.* 2006) show that they are feldspatic, sometimes enriched in CaO and always very low in Pb; this description is compatible with our attribution of BR5 and BR6 glazes but not with BR4, whose glaze is much more similar, as regards the spectral shape and Raman parameters, to some CdM couvertes. This information, together with the absence of enstatite in the paste, points out the differences existing between BR4 and the other two floor tiles, and allows questioning the provenance/dating of this sample. Pascual *et al.* (2006) also state in their work that small amounts of the paste were sometimes mixed with the glaze materials, in order to facilitate the accord between paste and glaze during firing; this could explain the intensity and sharpness of the enstatite peaks revealed in the microscopic spectra of the glaze of sample BR6.
These two Sureda's samples (BR5 and BR6) then show Raman features which are quite similar to hard-paste typical glazes, as shown by a comparison with e.g. the spectra of Meissen glazes (Colomban and Milande 2006, figs. 1 and 2).

	I_p	Q_0	Q_1	Q_2	Q_3	Q_4	δ_{MAX} *Si-O*	ν_{MAX} *Si-O*
BR4	0.38	781	932	978	1031	1105	462[1]	1028
BR5	2.45	795	915	978	1051	1129	486	∼1100
BR6	2.42	799	920	997	1053	1127	485	∼1100

[1]Main peak of crystalline quartz

Table 4.10: Raman parameters extracted from the XY1 spectra of coloured glazes of the BR fragments (wavenumber positions in cm^{-1})

The pigment used in both the green and yellow glazes has been identified as being Naples' yellow ($Pb_2Sb_2O_7$, peaks at 137, 331, 453, and 506 cm^{-1}). On the contrary, the purple glaze does not contain specific signatures which can be assigned to a colouring phase, so that the use of Cassius' purple can be proposed, in agreement with what was found by other analythical techniques during the recent research project on the tiles of Aranjuez (Memoria del proyecto de investigación 2005).

Museum objects

Some pigmented areas of the glazes of the museum artefacts were also analyzed, which showed a variety of colours: yellow, green, red, purple, brown, black and blue. The

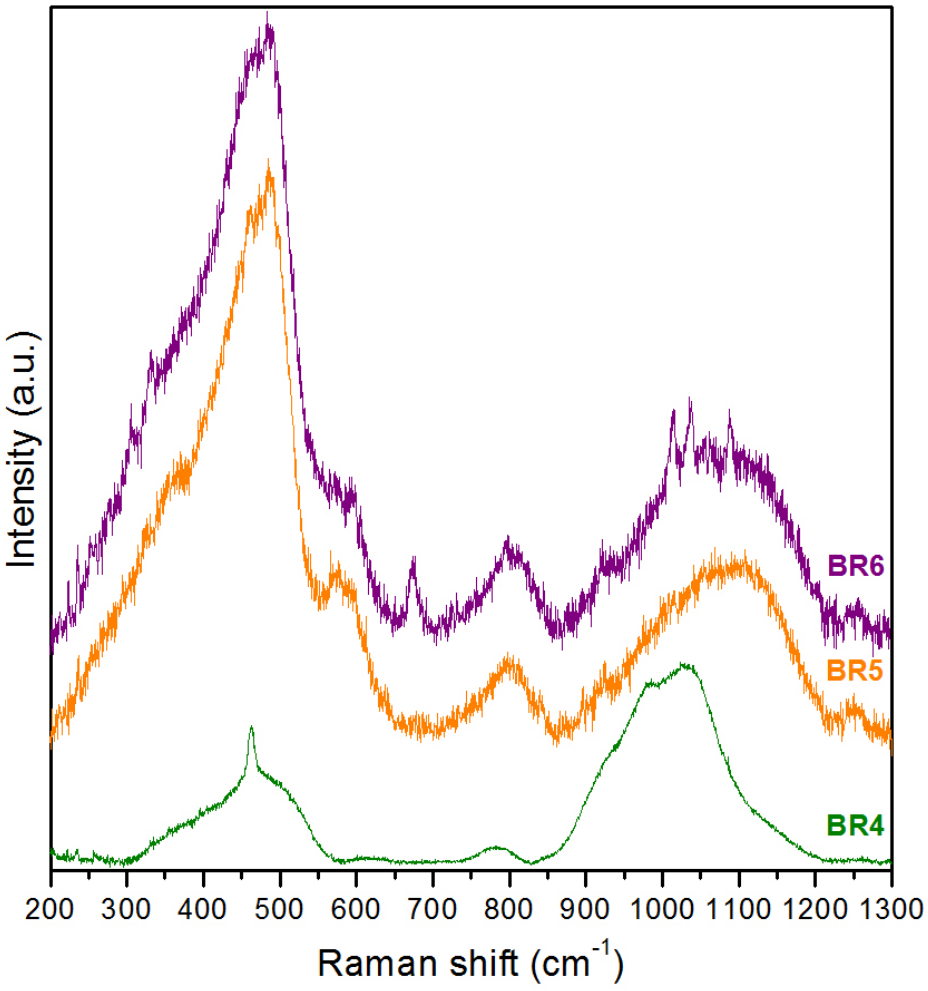

Figure 4.14: Representative Raman spectra of the coloured glazes of BR excavation samples (microscopic analysis - XY1)

Raman signatures of pigments/colourants identified on all the objects are summarized in table 4.11; they mostly belong to pigments which were of common use in pottery and porcelain production during the 18^{th} century, such as hematite for red, Cassius' purple, and manganese oxides for brown and black. Yellow and green areas show signatures which can be attributed to different combinations of Pb, Sn and Sb oxides (such as Naples' yellow and lead-tin yellow). The peak around 460 cm^{-1} in some of these spectra is most probably masked by the main peak of quartz (within parentheses in the table). Searching through several databases, it seems that the presence of an intense peak around 200 cm^{-1} can lead to the attribution of a pigment to lead-tin yellow (type I), while the position of the peak around 320-350 cm^{-1} seems to shift progressively to higher wavenumbers, depending on the increasing amount of Sn in the mixture. It is mostly on these two bases that the attributions of yellow and green pigments have been made. In the case of blue pigments, identification was not always straightforward; the presence of Co-based colourants can be hypothesized in most cases, but a more complete database of blue glaze pigments would be useful for a clearer identification. As an example, details of pigment analyses are reported, relatively to the CdM tabletop (MNC 4423), as its rich flowery decoration allowed studying a wide range of colours; the analyzed points are indicated in figure 4.15, and representative spectra are shown in figure 4.16.

Figure 4.15: Detailed view of the points chosen for pigment analysis on the tabletop

Colour	Object	Peaks (cm^{-1})	Pigment assignment
Yellow	tabletop	136, 200, 341, 459, 506	Lead-tin yellow (type I)
	pitcher	139, 343, (464), 510	*Pb-Sn-Sb* triple oxide yellow
	figurine	141, 340, (463), 500	*Pb-Sn-Sb* triple oxide yellow
	vase	140, (462), 505	Naples' yellow ($Pb_2Sb_2O_7$)[1]?
	lid	348, 450, 510	*Pb-Sn-Sb* triple oxide yellow?
Green	tabletop	136, 328, 453	Naples' yellow ($Pb_2Sb_2O_7$)[1]
	pitcher	140, 342, (463), 511	*Pb-Sn-Sb* triple oxide yellow
	figurine	138, 334, 451, 511	Naples' yellow ($Pb_2Sb_2O_7$)[1]
	lid	139, 340, 451, 509	*Pb-Sn-Sb* triple oxide yellow
Blue-green	tabletop	137, 328, 455	Naples' yellow ($Pb_2Sb_2O_7$)[1]
Blue	tabletop	822	*Co*-silicate (olivine-type)
	pitcher	-	Cobalt ions
	lid	- / 1350br , 1590br	Cobalt ions / carbon
Red	tabletop	223, 290, 407, ∼1300	Hematite
	pitcher	224, 406	Hematite
	lid	217, 282, 400br	Hematite
Purple	tabletop	608, 648 / 290, 409	*Mn*-oxyde / Hematite
	pitcher	224, 1294br	Hematite
	vase	-	Cassius' purple[2]
	lid	-	Cassius' purple[2]
Brown	figurine	band 810-870 (max. at 837)	CrO_4^{2-} containing compound
Black	tabletop	375, 520, 625	*Mn*-oxyde (MnO_2 structure)
	figurine	band 600-650, 678	Spinel ($Fe/Mn/$)

[1]Green is traditionally obtained by mixing a yellow pigment with a *Co*-containing glaze; *Co* ions are dissolved within the glassy network, so that no specific signature is observed

[2]obtained by dissolution of *Au* ions in the glaze, yielding no Raman signature

Table 4.11: Raman signatures of the pigments identified on all the museum objects

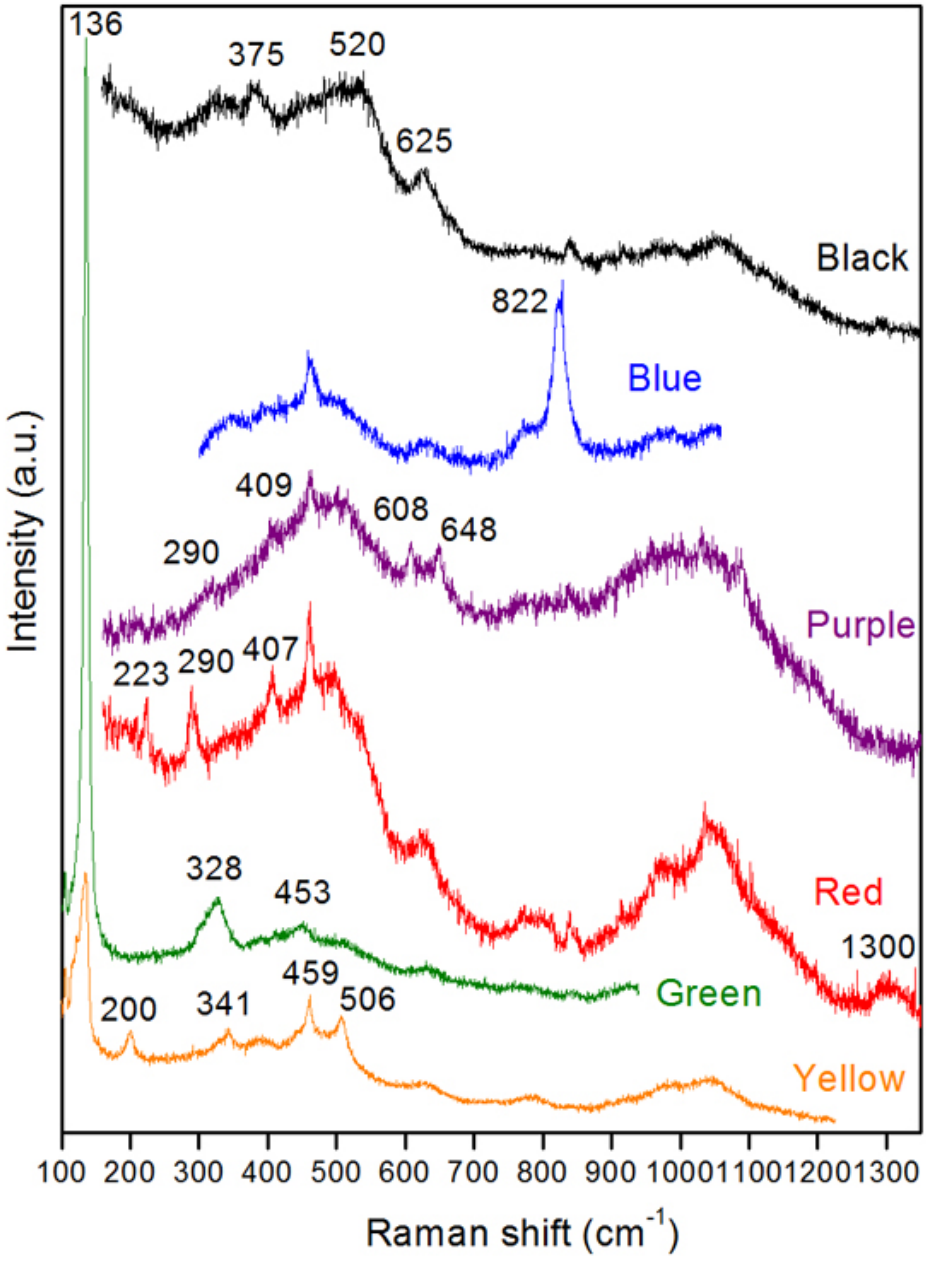

Figure 4.16: Representative Raman spectra of pigments on the tabletop (top to bottom): black (8), blue (4), violet (6), red (7), green (1) and yellow (9). Numbers in parentheses refer to the point of analysis (cfr. figure 4.15); the peak at about 464 cm^{-1} can be attributed to α-quartz

4.3.4 Correlations between chemistry and the Raman spectra of glazes

A comparison among the spectra of the colourless and coloured glazes of the Capodimonte fragments has been carried out, in order to point out how the relative abundance of certain chemical elements does have clear effects on the shape and intensity of the Raman bands of the glassy phase. The spectra of figure 4.17 can be looked at by keeping in mind the chemical compositions reported in table 4.3, yielding the following remarks:

- the wide band centered at 530 cm^{-1} is correlated to the sodic component of the glass; it is in fact very intense in the spectra of blue glazes ($Na_2O > 8\%$), slightly visible in those of the colourless glazes with relatively high sodium content, and totally absent in all other cases;

- the Raman signature of cassiterite (peaks at about 634 and 780 cm^{-1}) is present only in the spectra of the coloured (opaque) glazes, and in those of the two colourless glazes with highest Sn content;

- the position of the maximum of the stretching massif shifts from about 1040 to about 1065 cm^{-1} as a function of the drastic decrease in lead content in the blue glazes (about 12% PbO, compared to the 20-35% of the other glazes).

One last remark can be made, regarding the relationship between the polymerization index with the total amount of fluxes; the value of I_p changes in fact from about 0.6-0.7 in colourless and green glazes (total amount of fluxes > 40%) to 1.4 in blue glazes, which contain only about 27% of fluxes. It is once again clear, then, how closely this parameter is related to the chemical composition of glass (cfr. also section 3.3.2).

The multi-layered glaze of sample P191 is also interesting, as it allows following the evolution of its Raman spectra acquired in section on the different layers (fig. 4.18), in parallel with the changes in chemical composition (table 4.12). Spectra a and b are identical from the point of view of glass structure, and show the typical shape of Na-Pb glazes. The greater evidence of cassiterite in spectrum b is probably due to having acquired the spectrum on or very close to some SnO_2 crystals. Cassiterite shows intense peaks also in spectrum c, reflecting the high amount of tin contained also in the intermediate layer.

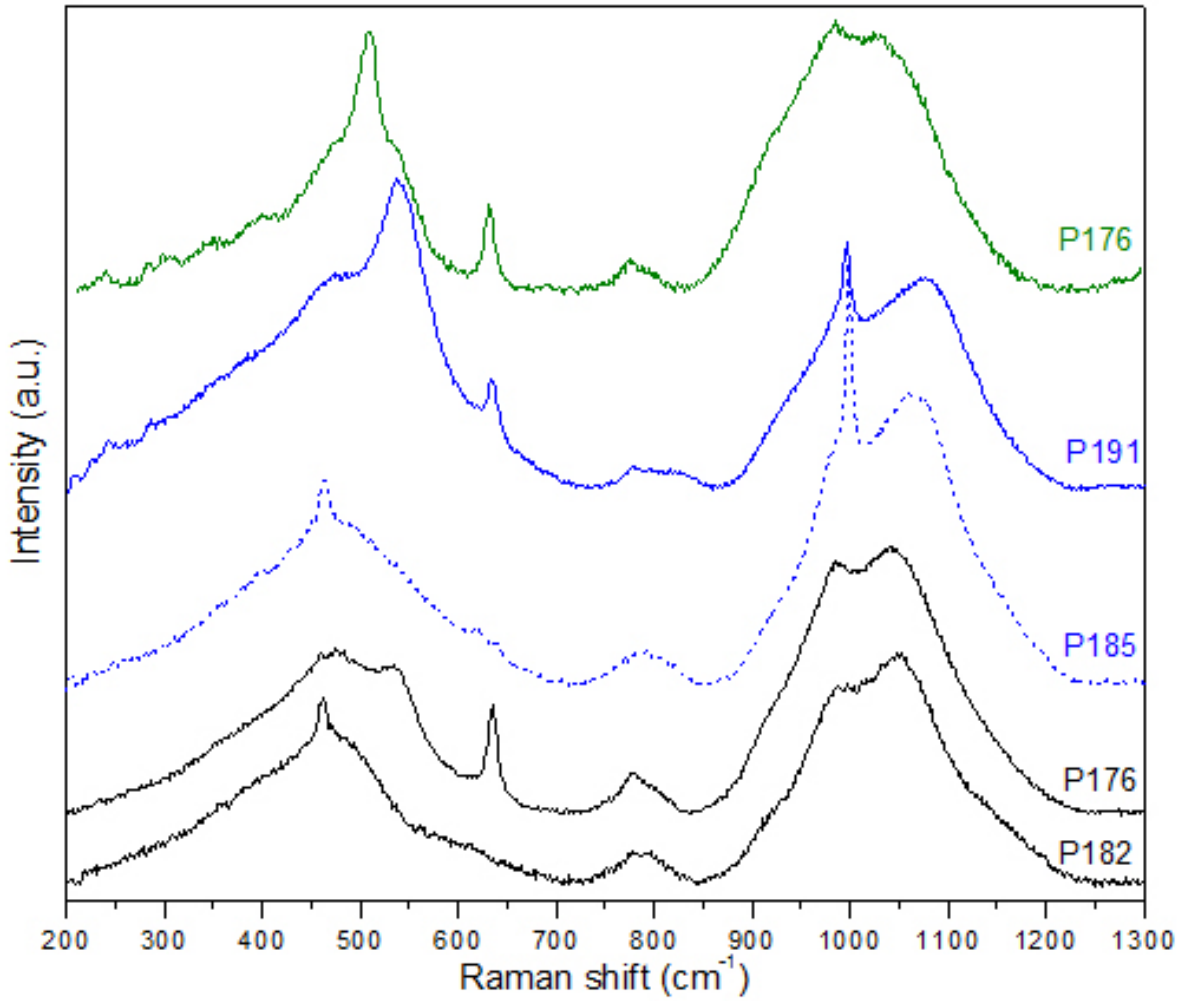

Figure 4.17: Representative Raman spectra of, top to bottom: green glaze, blue glaze, blue underglaze pigment, two colourless glazes

The progressive decrease in sodium content, together with the increase in Pb while moving from the outer layer towards the inner one, are clearly marked by the decreased intensity of the band at 530 cm^{-1}, along with the shift of the maximum of the second massif from 1065 to about 1040 cm^{-1}.

Finally, these spectra seem to confirm the hypothesis that the peak at 995 cm^{-1} may be linked to the Co content of the glaze. It is in fact very intense within the outermost layer, where the measured cobalt amounts to almost 0.7% CoO. It is instead much smaller, or not visible, in the other two layers, with a concentration just above 0.1% CoO. The peak at 840 cm^{-1}, which might at first seem correlated to the one at 995 cm^{-1}, is most probably rather due to the coating of the microscope's objective (cfr. section 2.3).

Glaze layer	SiO_2	Al_2O_3	Fe_2O_3	CaO	Na_2O	K_2O	PbO	SnO_2	CoO
Outer	57.92	2.12	0.96	2.00	8.16	3.88	10.47	10.37	0.69
Intermediate	51.08	2.73	0.37	1.80	6.68	3.08	20.17	10.42	0.13
Inner	57.61	3.22	0.60	1.41	6.61	3.16	23.27	0.53	0.13

Table 4.12: Partial chemical composition of the multi-layer blue glaze on sample P191 (weight % oxides normalized to 100). Only the major elements and those which show relevant differences among layers are presented

> *Silicate melts and glasses of binary and ternary compositions have been the object of many Raman studies, aimed at identifying the observed Raman bands and at "justifying" them from the point of view of glass structure (McMillan 1984, and references therein). The effect of modifier cations on the position and intensity of Raman bands of such "simple" glasses has also been investigated. Further work has been carried out on more complex glassy materials, such as those that can be found in cultural heritage (e.g. mosaic and stained-windows glass, pottery and porcelain glazes, ...), and some relationships have been established between glass composition and the parameters which can be extracted from the Raman spectra (Colomban 2003; Colomban and Paulsen 2005). Most recently, a "guide" to the recognition of glass type on the base of Raman data has been tentatively proposed, which provides useful indications about the correlations existing between glass composition (nature and*

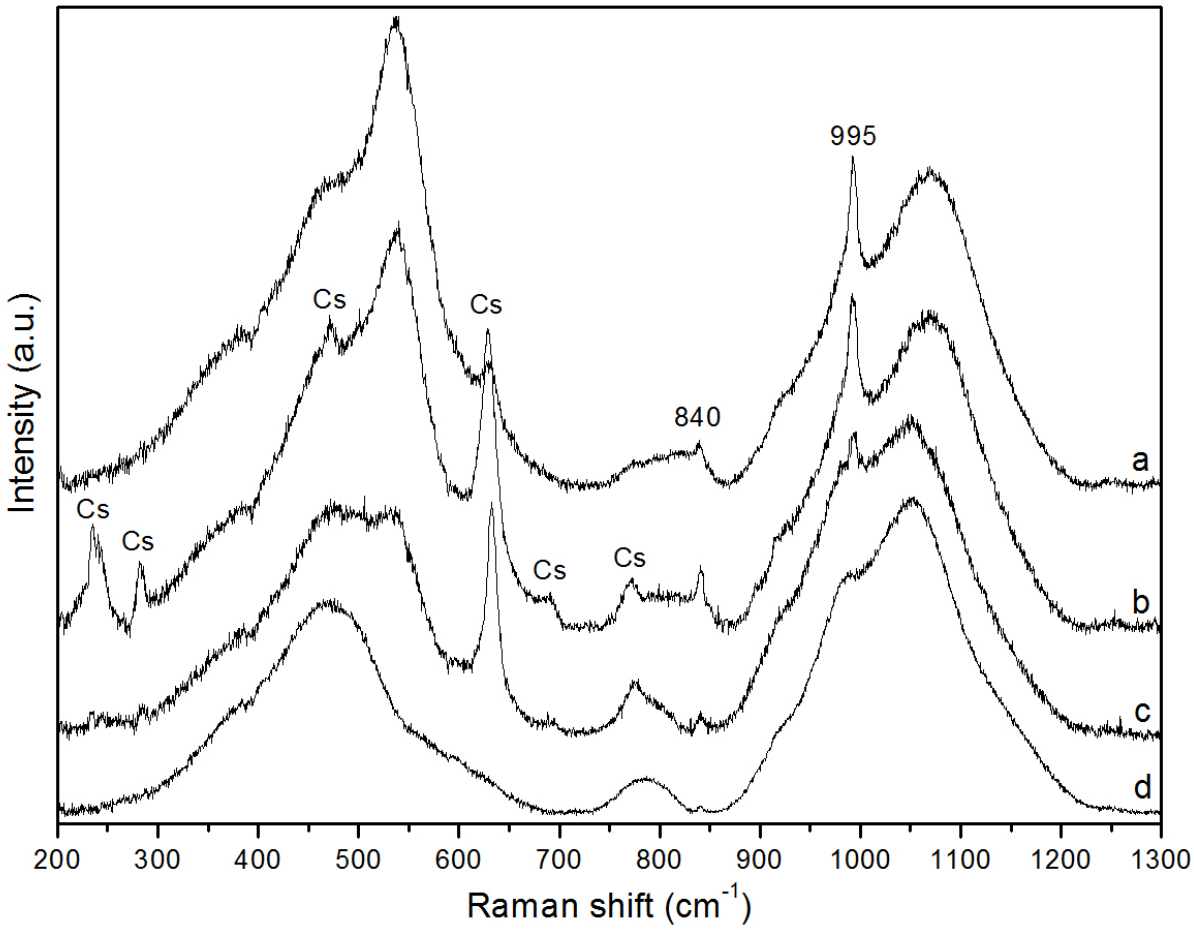

Figure 4.18: Representative Raman spectra of the different layers of the glaze of sample P191, acquired (a) on the surface, and in section on (b) the outer, (c) the intermediate and (d) the inner layer (Cs: cassiterite)

total amount of modifiers, processing temperature) and its Raman signature (Colomban et al. *2006). However, such correlations are far from being quantitative and unambiguous, due to the combination of effects that a complex chemistry brings about. Expanding the existing corpus of samples of historic glasses and glazes of which both the Raman spectrum and the chemical composition are known will certainly help to improve our knowledge of their relationship. It will also provide further tools for the non-destructive characterization and classification of these materials.*

4.3.5 Suitability of different instruments for glaze analysis

During the last period of this research, a preliminary study has been undertaken on the possibility to compare spectra acquired with different instruments, taking advantage of the availability of several spectrometers, in order to acquire a deeper comprehension of the reproducibility, and therefore the significance, of Raman data relative to ceramic glazes.

One most important difference between the macroscopic and microscopic analysis is the analyzed depth, which in the case of the macroanalysis ($\sim 300\ \mu m$) is greater than the average thickness of Capodimonte glazes ($\sim 100\ \mu m$). Thus the collected signal in this case will also be originated by the underlying paste, and by any interface between paste and glaze. Microscopic analyes therefore give Raman signatures more representative of the glaze layer alone, as opposed to macroscopic spectra which may yield useful information on its interaction with the paste, and consequently on the production technology. From this point of view, comparisons between macro- and micro-Raman analyses are less interesting in the case of thicker samples of bulk glass such as mosaic *tesserae*.

A comparison can be made between spectra acquired on a same sample with three spectrometers (LI, XY1 and XY2), first on a visual basis (fig. 4.19) and secondly by considering the calculation of some Raman parameters. Preliminary comments include the following:

- the spectral shape of *Na-Pb* silicate glasses is only recognizable with LI and XY1;

- crystalline phases (mostly different polymorphs of SiO_2) are identified in all cases, but are more evident when using XY2 (as mentioned, the greater depth of analysis

accounts for signal coming also from the paste and the interface, which are richer in crystalline phases);

- the abundant peaks due to crystalline phases make deconvolution harder for XY2 spectra, and the calculation of Raman parameters less straightforward and precise.

It can easily be observed in fact how parameters calculated on the basis of XY2 spectra have more widespread values when compared to those deriving from other (microscopic) spectra; table 4.13 lists, as an example, calculated values of the polymerization index, which are plotted in figure 4.20. Mean values and dispersions (the latter calculated as the standard deviation) have been computed taking into account the extreme homogeneity of the 8 considered glazes, which allows hypothesizing the same "true value" for the polymerization index of all of them. The arithmetic mean of the 8 calculated I_ps can then be considered a good estimate for the expected value, and the standard deviation can be worked out. For spectra acquired with LI and XY1, the dispersion equals about 15% of the mean of absolute values. On the other hand, in the case of macroscopic analysis the dispersion reaches 50% of the mean value. It is also true, however, that when redoing the calculations excluding the value obtained for sample P182 with XY2, which is clearly an "outlier", the mean of the I_ps equals 0.90 ± 0.30, which is much closer to the average values relative to the other spectrometers.

	P27	P173	P176	P182	P185	P190	P191	P192	$\bar{x} \pm \sigma$
LI	0.55	0.60	0.68	0.75	0.47	0.66	0.48	0.60	0.60 ± 0.10
XY1	0.82	0.69	0.76	0.60	0.83	0.70	0.59	0.54	0.69 ± 0.11
XY2	1.11	1.12	0.49	2.20	0.57	0.86	0.86	1.32	1.07 ± 0.54

Table 4.13: Values of the polymerization index I_p calculated from spectra obtained with three different instruments on the colourless glazes of Capodimonte excavation fragments ($\bar{x}$: mean value; σ: standard deviation)

It is clear even from this very preliminary work that the choice of an appropriate instrument for the Raman analysis of glazes is of fundamental importance in terms of identification of glaze type, and in view of a significant comparison among data coming from different sources (different labs, instruments,

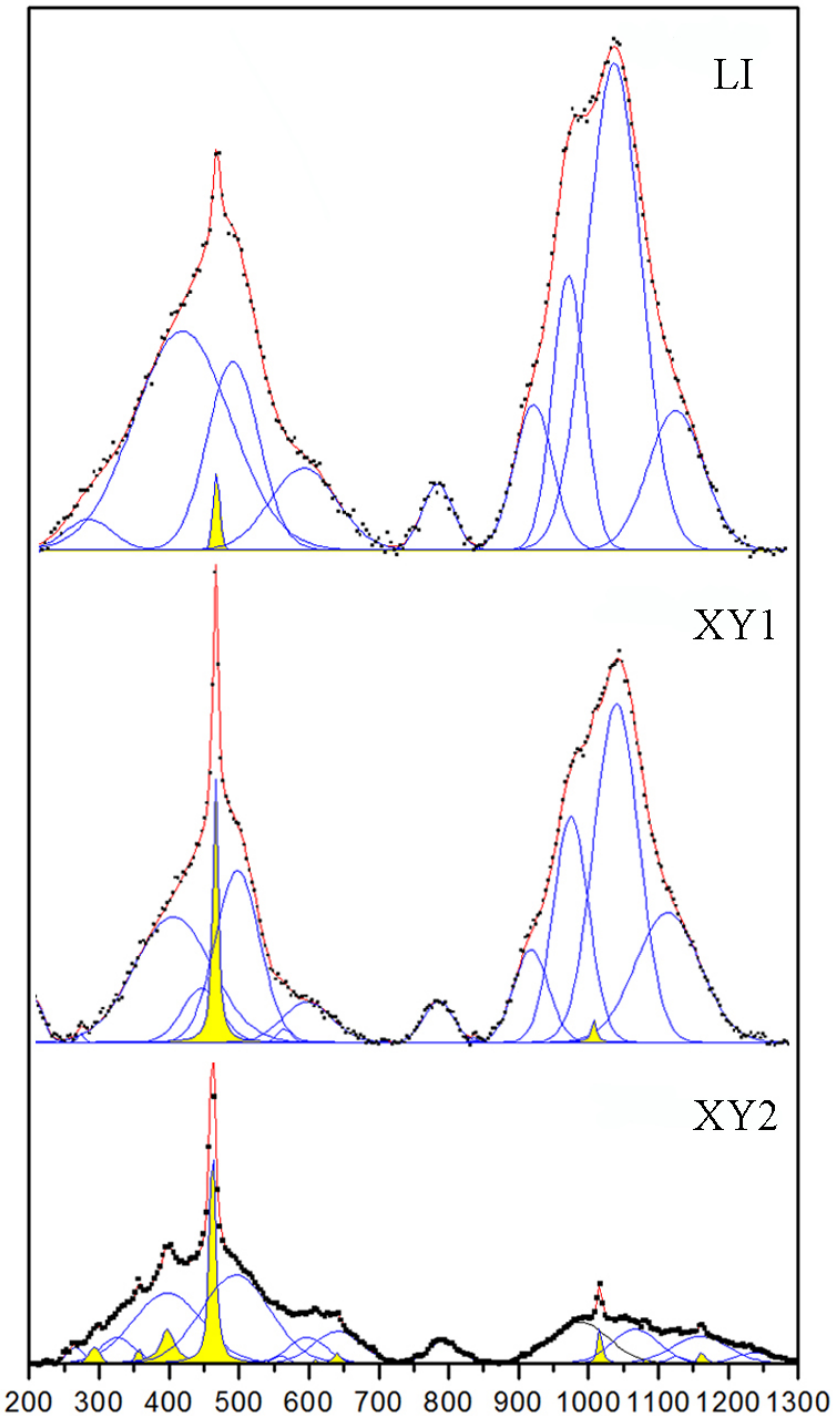

Figure 4.19: Raman spectra acquired with three different instrument on the colourless glaze of sample P182. LI and XY1: microanalysis; XY2: macroanalysis. Yellow peaks are attributed to crystalline phases

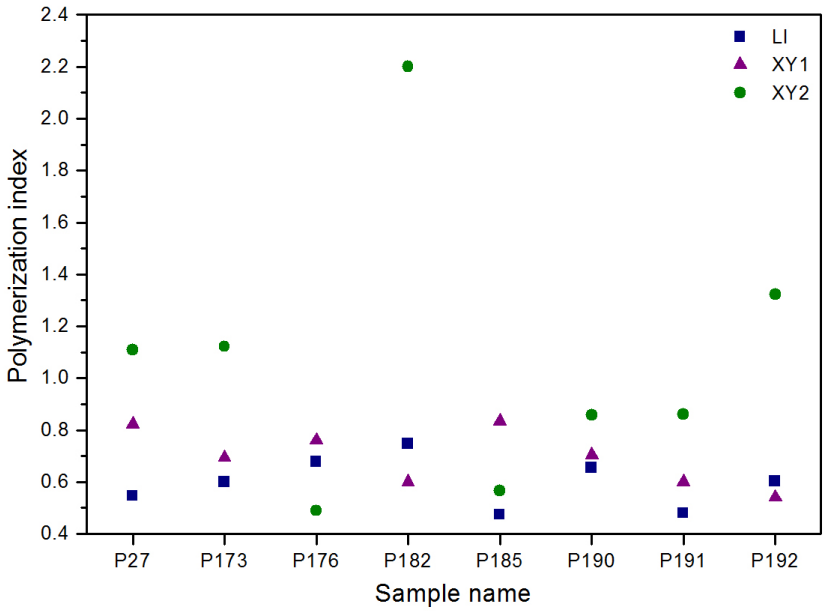

Figure 4.20: Plot of the values of the polymerization index I_p calculated from spectra obtained with three different instruments on the colourless glazes of Capodimonte excavation fragments

and experimental conditions). Future work on this subject should include a more detailed treatment of Raman parameters extracted from spectra obtained with different instruments, by means of statistical methods (such as PCA and cluster analysis).

The difference between the microscopic and macroscopic approach, and therefore the importance of the probed depth, could be better specified by appropriate sets of experiments. The evolution of the Raman spectrum could be followed for example while analyzing one fixed spot with different objectives (e.g. macro, 5x, 10x, ...). Such a procedure would also in some way provide an indirect measure of the glaze thickness. It also seems interesting to further investigate the reproducibility of the Raman analysis of glazes, by comparing a certain number of spectra obtained on different areas of one sample, with the same spectrometer and in unvaried experimental conditions.

4.4 Comparison with Raman analyses of other porcelain productions

The Characterization of the productions of Capodimonte and Buen Retiro has been completed by a comparison with the Raman analysis of objects issued by other manufactures, in order to both underline possible similarities and to check the possibility to unambiguously identify CdM and BR products on the sole basis of their Raman spectra. This comparison has first been carried out using some already published data relative to artefacts which bear some similarities (in composition and/or Raman signatures) with those of Capodimonte, such as the already mentioned "Medici porcelain", very rich in silica and probably obtained by milling the traditional glazemaker's marzacotta sinter with added fine sand and clay (Kingery and Vandiver 1984). Similarities with the spectra of CdM samples are found also in the Raman analysis of a type of "modified" soft paste experimentally produced at Sèvres around 1880 by C. Lauth and G. Vögt (D'Albis 2003, p. 30). Further analyses have also been undertaken on a series of objects, once again mostly belonging to the Sèvres Museum and Manufacture. A synthetic description of all the samples which have been the object of this comparison is given in table 4.14, and their pictures are shown in figure 4.21, or can be found in published works (Colomban 2005; Colomban and Treppoz 2001; Colomban *et al.* 2004b).

A confrontation has then been made between the results obtained on Capodimonte glazes during this work and the Raman spectra of all these materials, taking into account both pastes and glazes. Table 4.15 recalls the paste groups defined in table 4.7, and includes all the analyzed porcelain pastes.

It can be observed in figure 4.22 that the Medici paste differs from that of Capodimonte mostly because of the presence of undissolved feldspars (peak at 512 cm^{-1}), which are typical of a hard paste signature, and therefore constitutes a group of its own. Samples TV, SCV, SCD and PHC all show very few peaks, and only quartz can be identified as a characteristic phase; for this reason they have been added to group 1. The paste of sample SM contains quartz, cristobalite and some glassy phase, and can therefore be included in group 2. Finally, both the samples of Vögt paste (PTV and PV) contain β-wollastonite and have Raman signatures entirely similar to the samples of group 3.

Sample	Provenance	Mark	Manufacture and notes
Medici[1]:	Sèvres Museum		Medici
several objects			
PTV[2]: round plaque	Sèvres Manufacture		Manufacture of Sèvres
(glazing test)			"Vögt soft paste", 19^{th} century
SM: figurine	Sèvres Museum	blue RFR	Naples manufacture
(mother and child)	MNC 5165		acquired in 1897
			incised signature: "F."
SP: figurine	Sèvres Museum	blue crowned N	Naples manufacture
(Spring)	MNC 23140		basket of flowers unglazed
			acquired in 1961
TV and SCV:	Sèvres Museum	unmarked	Manufacture of Vicenza
biscuit cup and saucer	MNC 766-1		unglazed, acquired in 1820
TD and SCD:	MNC 5534-9	unmarked	Ginori (Doccia) manufacture
white cup and saucer			White flowery decoration in relief
			bought in 1860, dated 1763-1800
PHC: figurine	Private collection	blue crowned N	Naples manufacture?
(couple of lovers)			incised signature: "Roger"
			marked "Capodimonte" with a pencil
PV: round plaque	Sèvres Manufacture		Manufacture of Sèvres
			"Vögt soft paste"? (incised PV)
			flowery multicolour decoration

[1]Colomban *et al.* (2004b) and Colomban (2005), [2]Colomban and Treppoz (2001)

Table 4.14: Description of the analyzed artefacts from other porcelain manufactures

Figure 4.21: The analyzed objects from the other manufactures (images not to scale). Inventory numbers (when present) and object descriptions can be found in table 4.14

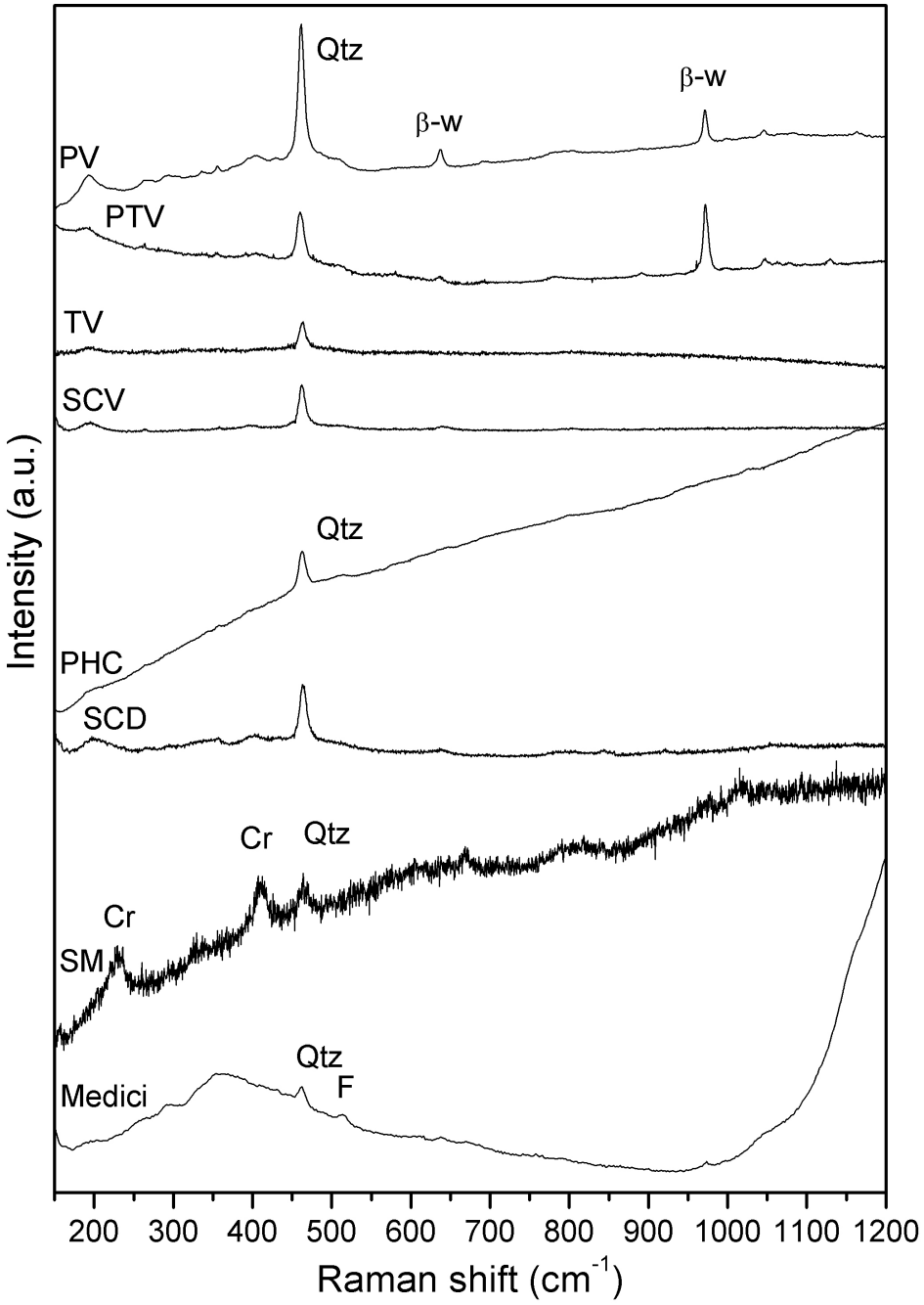

Figure 4.22: Representative Raman spectra of the pastes of objects from several porcelain manufactures (Qtz: quartz, β-w: β-wollastonite, Cr: cristobalite, F: feldspars). Spectra have been acquired with different instruments

Group	Samples	Characteristic Raman signatures
1	3 Cdm exc., TV, SCV, SCD, PHC	Quartz
1b	1 BR exc. (1^{st} period)	Quartz, (clino)enstatite
2	5 CdM exc., GUE, SH, CRU, TB, SCB, T_Or, SM, 2 BR exc. (1^{st} and 3^{rd}? period)	Quartz, cristobalite, tr. trydimite, glassy phase
3	8 CdM exc., COUV, TA, PTV, PV	Quartz, cristobalite, trydimite, β-wollastonite
4	3 BR exc. (3^{rd} period)	Quartz, cristobalite, tr. trydimite, (proto)enstatite
5	V1BR, V2BR	Quartz, tr. cristobalite, tr. trydimite, α-wollastonite, scapolite
6	Medici	Quartz, feldspars

Table 4.15: Schematic representation of the results of Raman analysis on the pastes of all the analyzed porcelain samples (exc.: excavation samples, tr: traces)

As far as glazes are concerned, figure 4.23 shows that the Medici glaze is characterized by the presence of an intense peak due to the presence of crystalline phosphates, which is never found in Capodimonte spectra. Undissolved feldspars can also be identified in this spectrum, as well as in the glazes of the cup and saucer produced by the Doccia manufacture (TD and SCD), in which the feldspar peaks are very intense and the overall spectral shape it typical of a true hard paste glaze (Colomban and Treppoz 2001). The glaze of sample PHC, possibly attributed to the Naples manufacture, shows a Raman signature which is completely different from all the other ones, and does not resemble even the glaze of the other artefact (SM) attributed to the Real Fabbrica, which is indeed very similar to all the Capodimonte "couvertes". Finally, the glazes of both samples of Vögt soft paste (PTV and PV) show high similarities with those of the analyzed CdM pieces, displaying the typical Raman signature of *Na-Pb* silicate glasses, along with the peaks of crystalline α-quartz and minor amounts of β-wollastonite. On the base of these results, it seems that it could be interesting to go further into the historical and analytical study of the Vögt soft paste; being about 100 years more recent than the Capodimonte production, one might hypotesize that the latter might have been used as a sort of model for the French material.

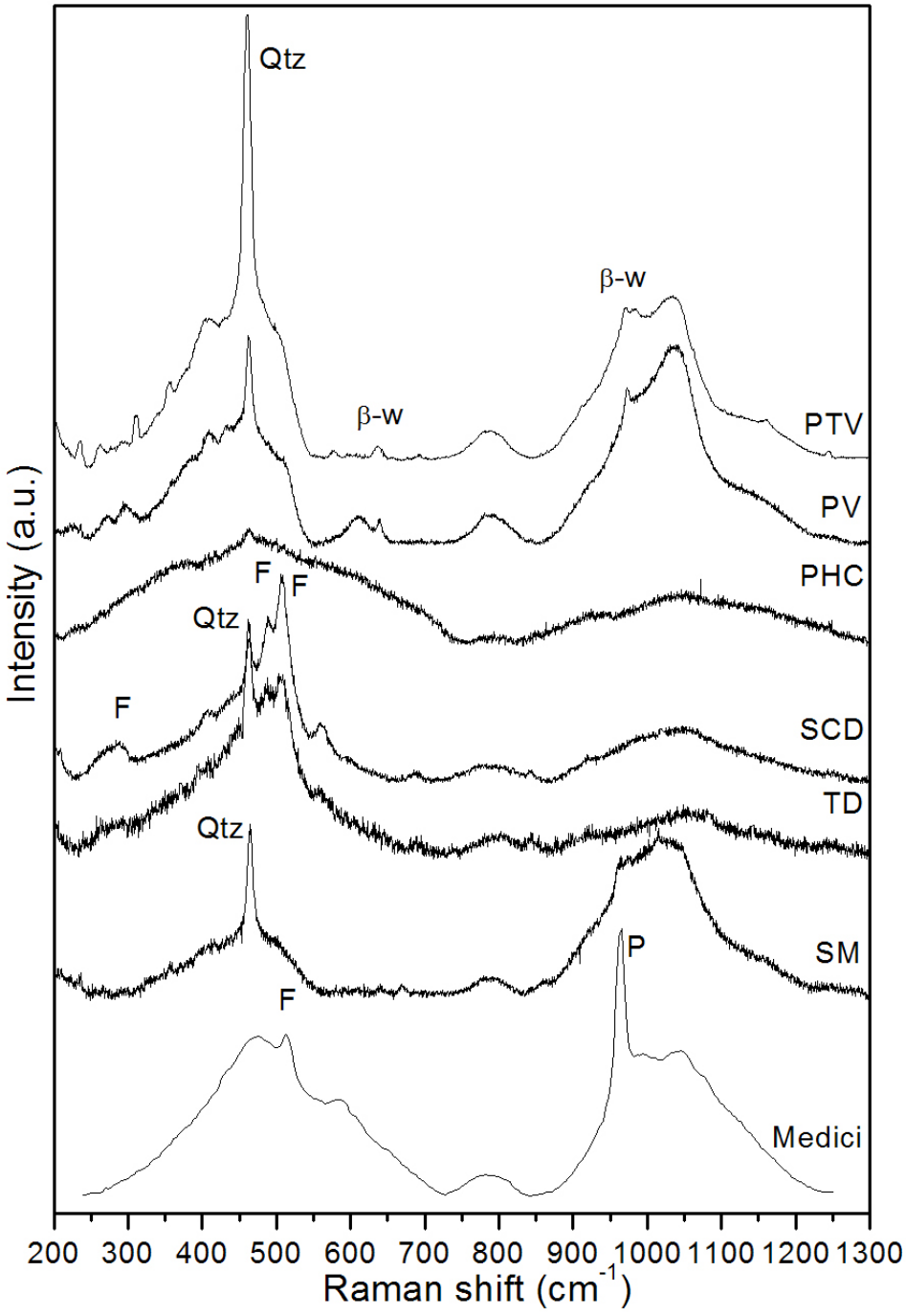

Figure 4.23: Representative spectra of the colourless glazes of objects from several porcelain manufactures (Qtz: quartz, β-w: β-wollastonite, F: feldspars, P: phosphates). Spectra have been acquired in microscopic configuration with different instruments

It seems useful to add some of our Raman data to those presented in a graph published by Colomban and co-workers, to validate in a way the reliability of our measures. Figure 4.24 is a modified version of figure 9a from Colomban *et al.* (2006), and shows the plot of I_p values vs. ν_{MAX} *Si-O* wavenumbers for all the colourless porcelain glazes analyzed in this thesis (closed symbols). Open symbols refer to published data and represent some *Na-Pb* silicate glazes of pottery samples, as well as some hard-paste porcelain glazes which were analyzed during this previous study.

A distribution of values can be observed, apparently without a precise separation between soft-paste and hard-paste glazes, which a larger number of data would perhaps help to specify. Our results seem however to contribute to enlarge and better define the variation range of the Raman parameters of *Na-Pb* silicate glasses. The two Sureda (coloured) glazes have been added to the graph, and appear well separated from all the other samples.

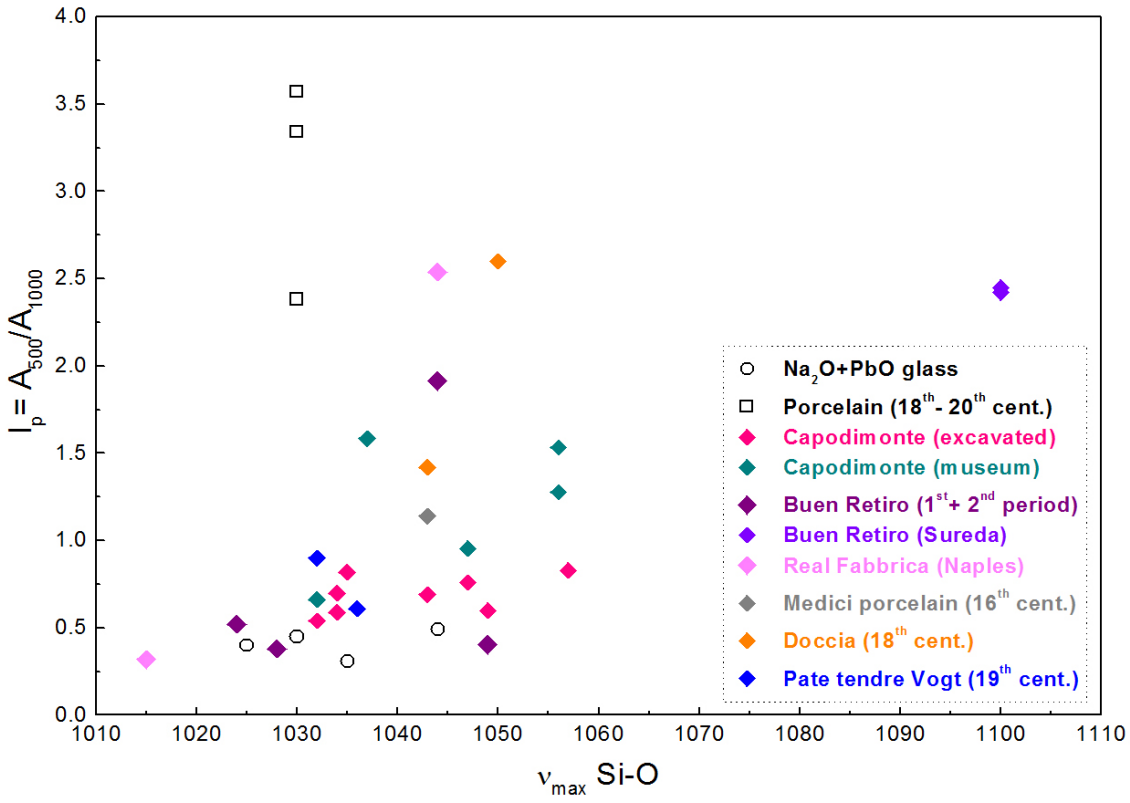

Figure 4.24: Plot of I_p values vs. ν_{MAX} *Si-O* wavenumbers for all the analyzed porcelain glazes (closed symbols). Open symbols refer to previously published data (Colomban *et al.* 2006, modified from figure 9a)

Finally, totally separate comments need to be made about the figurine representing Spring, attributed to the Real Fabbrica. It has not been possible to acquire any usable spectrum of the paste or glaze of this object with the Dilor XY1 spectrometer; in both cases a very intense signal, probably due to fluorescence, hindered the identification of any recognizable spectral features (fig. 4.25b). A partial characterization of this artefact's glaze was nonetheless achieved with the Dilor XY2 instrument; also in this case however, the fluorescence signal was very high. Even after baseline subtraction, the acquired spectrum does not have a very well defined shape, especially in the high wavenumber region (700-1300 cm^{-1}, fig. 4.25a). One can still distinguish the main peaks of crystalline α-quartz, and an overall shape similar to that of a typical hard paste glaze. These observation do not seem sufficient for a sure characterization of this object; an accurate investigation of its surface might help identify the causes of the difficulties encountered during its analysis by Raman spectroscopy.

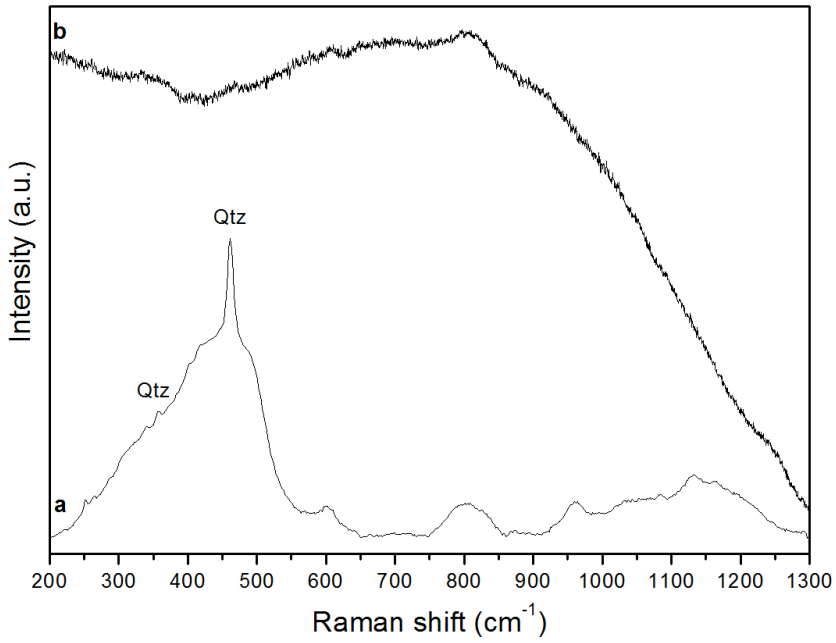

Figure 4.25: Raman spectra of the colourless glaze of sample SP, acquired with the XY1 (a, baseline subtracted) and the XY2 (b, raw spectrum) spectrometer (Qtz: quartz)

The combined Raman analysis of pastes and glazes of a few porcelain samples of different origin allowed pointing out the similarities and the differences existing with the Capodimonte production. Medici porcelain, for example, turned

out to be easily recognizable from its Raman spectra, even though the chemical composition of its paste is very similar to that of Capodimonte. Analysis of the figurine SM showed how the production of the Real Fabbrica did not bear much difference from that of the earlier Neapolitan factory. Further analysis would instead be needed to thoroughly characterize the figurine of the two lovers (PHC), due to the strange spectrum obtained on its glaze, and the figurine representing Spring (SP), whose Raman analysis was particularly difficult.

The paste signature of the biscuit samples from Vicenza (TV and SCV) cannot be distinguished from that of Capodimonte. This result underlines the importance of the combined characterization of both paste and glaze for a correct identification of the products; many pastes in fact yield signatures characterized only by the peaks of the polymorphs of crystalline silica (quartz, cristobalite, trydimite). This is for example the case of the objects from Doccia (TD, SCD), whose paste is totally similar to that of Capodimonte, but which show a peculiar glaze signature. Finally, the Vögt soft paste has Raman signatures completely comparable to those of Capodimonte in both paste and glaze.

4.5 On-site analyses at the Sèvres Museum

A Jobin Yvon Horiba HE532 (HE) portable spectrometer was recently acquired by the LADIR. It was used in the very last period of this thesis, in order to test its performances and to compare the obtained spectra with those acquired with the other, non-portable, instruments. The HE is equipped with a green Nd:YAG laser at 532 nm and of 500 mW maximum power at source, a grating with 1800 lines/mm and Notch filter, a CCD detector cooled to 200 K and optical fibers for conveying both the laser light and the Raman signal (fig. 4.26). It is also coupled to a 50x long focus objective, which yields a maximum power of about 84 mW at the sample.

The spectrometer was first tested at the lab on some of the same museum objects which had been previously characterized using the other instruments. Sample spectra are presented in figure 4.27; all were obtained with extremely short acquisition times, of the order of 1 to 3 seconds.

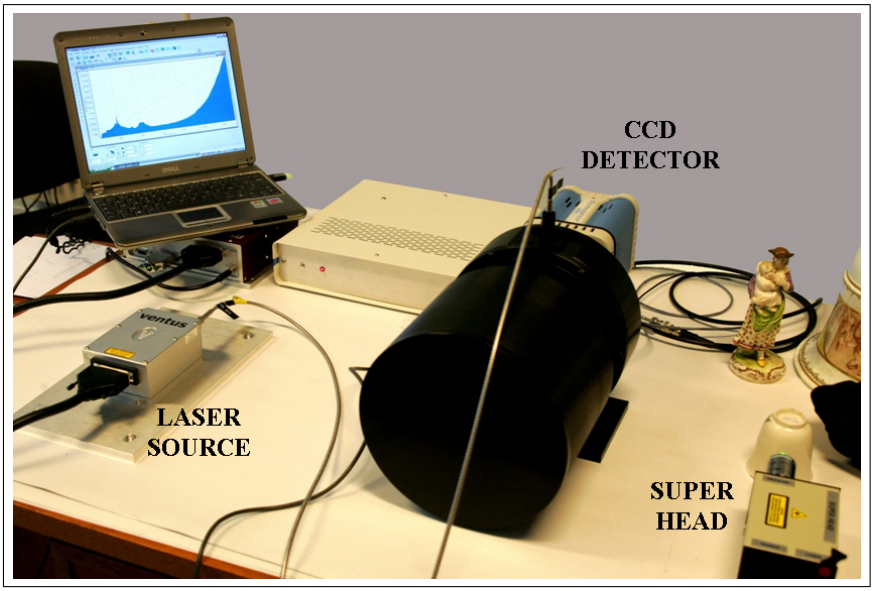

Figure 4.26: The Jobin Yvon Horiba HE532 (HE) portable spectrometer at the LADIR

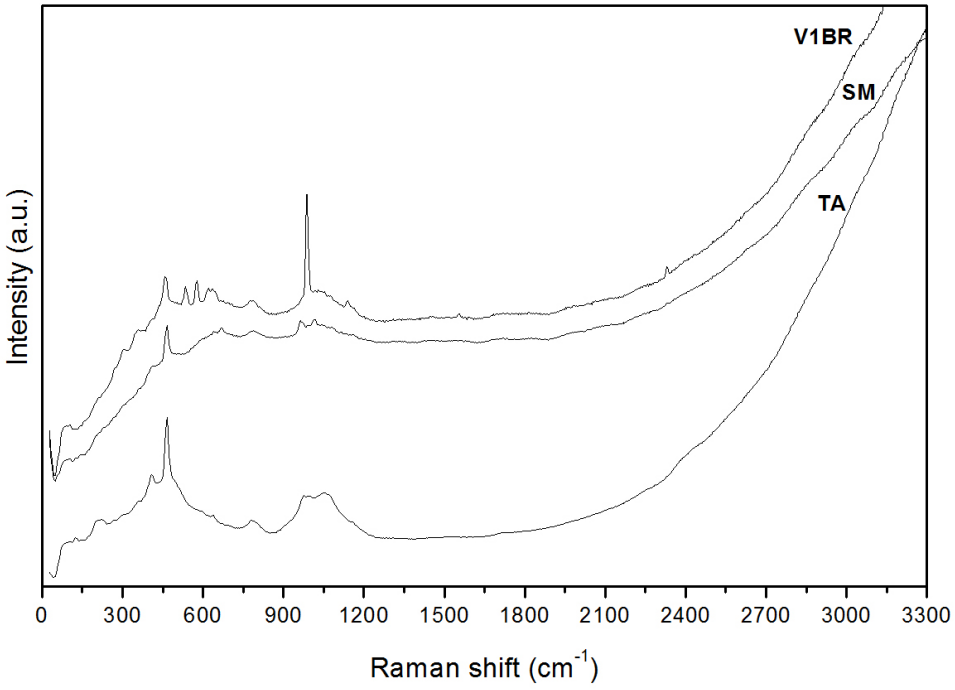

Figure 4.27: Sample Raman spectra (raw) acquired on the glazes of the Buen Retiro cup (TA), one of the figurines (SM), and one of the ornamental vases (V1BR), during lab tests of the HE spectrometer

Figure 4.28 shows the comparison between the Raman spectra of one of the ornamental vases (V1BR) acquired with three different instruments, after baseline subtraction. Experimental details of each measure are reported in table 4.16. It can be seen how the portable spectrometer benefits of a high luminosity, which yields very intense and sharp spectra even with a very short acquisition time. It is also clear how the focus on the surface of the glaze is not easily obtained with the HE; the model used in fact lacks a camera coupled to the objective. The camera would allow achieving a more precise focus and avoiding the influence of the paste signature on the acquired spectra. On the other hand, the focus position can be identified without much difficulty by acquiring several spectra, each keeping the measuring head in a different position, more or less near the surface. Figure 4.29 shows as an example the spectra acquired on-site at the Sèvres Museum on the glaze of a tall Capodimonte vase attributed to the decorator Giovanni Caselli, one of the most renowned workers of the manufacture. The sequence of the spectra from a to d corresponds to the "super head" being positioned closer and closer to the vase. This is clearly reflected in the spectra showing more and more pronounced peaks due to the crystalline phases present at the interface and within the paste.

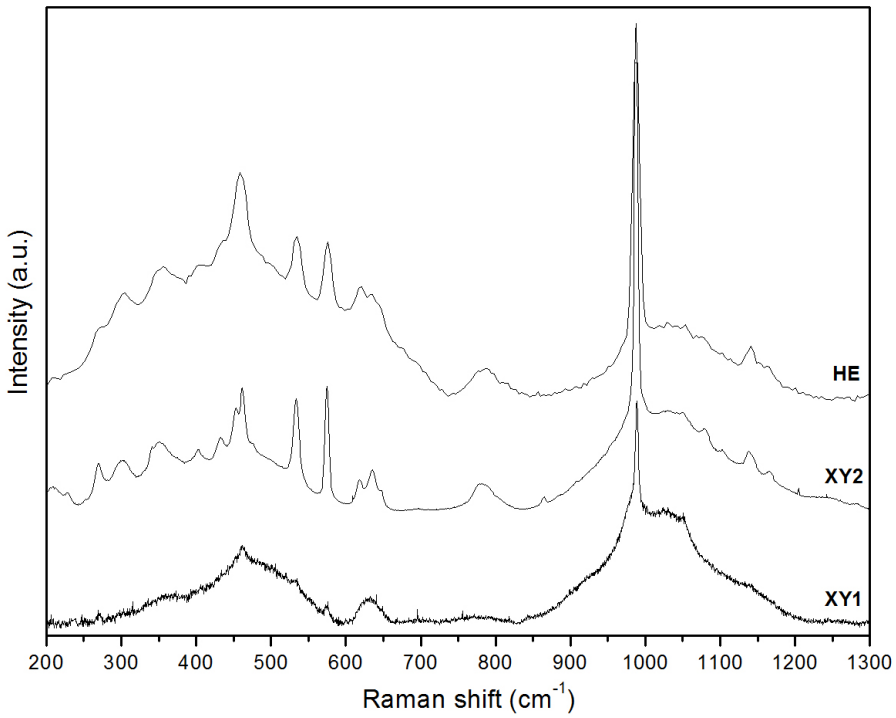

Figure 4.28: Comparison of Raman spectra acquired on the glaze of one of the ornamental vases with three different instruments: XY1, XY2 and HE (baseline subtracted)

Spectrometer	Acquisition time (sec) x Number of accumulations
XY1	800 x 2
XY2	60 x 4
HE	2.5 x 9

Table 4.16: Acquisition details of the Raman spectra shown in figure 4.28

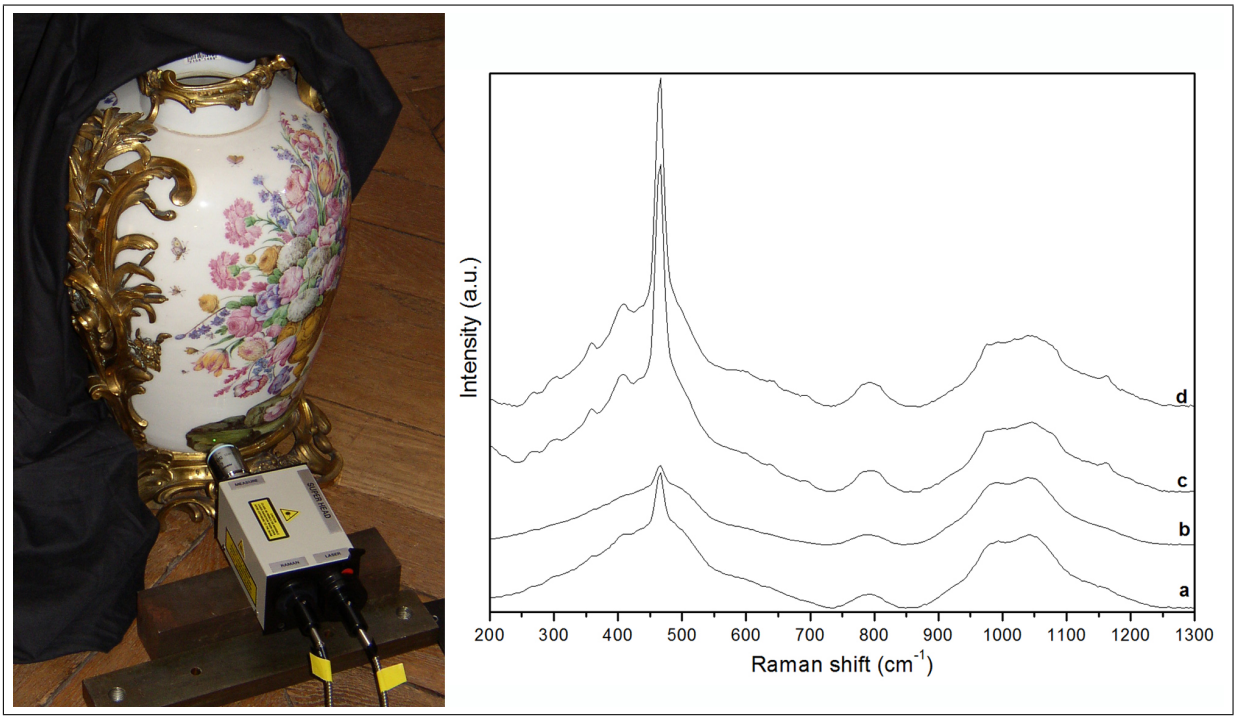

Figure 4.29: Sample Raman spectra (right, baseline subtracted) acquired on the glaze of a Capodimonte vase (left) during on-site analyses at the Sèvres Museum

4.6 References

Almagro M. (1966). Las ceramicas Españolas. In *Ceramica Española. De la prehistoria a nuestros dias*, pp. 23–43. Ministerio de Educacion Nacional - Direccion General de bellas artes.

Amato F., Clery D., Fabbri B., Giusti P., Gualtieri S., Napoli L., Pinto L., Ruffini A. (2007). Caratteristiche tecnologiche delle porcellane di Capodimonte. In *Le classi*

ceramiche: la situazione degli studi. Atti della X Giornata di Archeometria della Ceramica. In press.

Casanovas M. A. (1995). La porcellana di Buen Retiro. In *Giornate di studio sulla ceramica europea: con la presentazione della ricerca sulla composizione e tecnologia di produzione della porcellana d'epoca di Capodimonte*, pp. 115–146. De Costanzo, Naples, Italy.

Colomban P. (2003). Polymerization degree and Raman identification of ancient glasses used for jewelry, ceramic enamels and mosaics. *Journal of Non-Crystalline Solids*, **323**, 180–187.

Colomban P. (2005). Raman μ-spectrometry, a unique tool for on-site analysis and identification of ancient ceramics and glasses. In *Mater. Res. Soc. Symp. Proc.*, vol. 852. OO8.3.

Colomban P., Milande V. (2006). On-site Raman analysis of the earliest known Meissen porcelain and stoneware. *Journal of Raman Spectroscopy*, **37**, 606–613.

Colomban P., Paulsen O. (2005). Non-destructive determination of the structure and composition of glazes by Raman spectroscopy. *Journal of the American Ceramic Society*, **88**(2), 390–395.

Colomban P., Treppoz F. (2001). Identification and differentiation of ancient and modern European porcelains by Raman macro- and micro-spectroscopy. *Journal of Raman Spectroscopy*, **32**, 93–102.

Colomban P., Robert I., Roche C., Sagon G., Milande V. (2004a). Identification des porcelaines "tendres" du 18^{eme} siècle par spectroscopie Raman: Saint-Cloud, Chantilly, Mennecy et Vincennes/Sèvres. *Revue d'Archéométrie*, **28**, 153–167.

Colomban P., Milande V., Lucas H. (2004b). On-site Raman analysis of Medici porcelain. *Journal of Raman Spectroscopy*, **35**, 68–72.

Colomban P., Tournié A., Bellot-Gurlet L. (2006). Raman identification of glassy silicates used in ceramics, glass and jewellery: a tentative differentiation guide. *Journal of Raman Spectroscopy*, **37**, 841–852.

D'Albis A. (2003). *Traité de la porcelaine de Sèvres*. Editions Faton, Dijon.

De Aza A. H., De La Torre A. G., Aranda M. A. G., Valle F. J., De Aza S. (2004). Rietveld quantitative analysis of "Buen Retiro" porcelains. *Journal of the American Ceramic Society*, **87**, 449–454.

Edwards H. G. M., Colomban P., Bowden B. (2004). Raman spectroscopic analysis of an English soft-paste porcelain plaque-mounted table. *Journal of Raman Spectroscopy*, **35**, 656–661.

Elliott J. (2000). El Palacio del Buen Retiro. El contexto histórico. In *El Palacio del Buen Retiro y el Nuevo Museo del Prado*, pp. 29–41. Museo Nacional del Prado - Tf. Editores, Madrid.

Istituto G. Caselli (1995). Appendice: la ricerca condotta dall'istituto "Caselli" sulla "composizione e tecnologie di produzione della porcellana d'epoca di Capodimonte". Indagini svolte. In *Giornate di studio sulla ceramica europea: con la presentazione della ricerca sulla composizione e tecnologia di produzione della porcellana d'epoca di Capodimonte*, pp. 147–181. De Costanzo, Naples, Italy.

Kingery W. D. (1987). The development of European porcelain. In *High-technology ceramics - past, present and future.* Kingery W. D. (ed.) in Ceramics and civilization, number 3, pp. 153–180. The American Ceramic Society, Westerville, Ohio.

Kingery W. D., Vandiver P. B. (1984). Medici porcelain. *Faenza*, **LXX**(5-6), 441–452.

Lane A. (1954). *Italian porcelain.* Faber & Faber, London.

Le Breton G. (1879). *Céramique Espagnole. Le Salon en Porcelaine du Palaio Royal de Madrid et les porcelaines de Buen Retiro.* Librairie Raphael Simon, Paris.

Leslie K. A. (2003). Identification of porcelain type using Raman spectroscopy. In *Ceramic in the Society - Proceedings of the 6th EMAC, Fribourg, Switzerland, 3-6 October 2001.* Di Pierro S., Serneels V., Maggetti M. (eds.), pp. 189–196. Earth Science Dept., University of Fribourg, Switzerland.

Levin E. M., Robbins C. R., McMurdie H. F. (1974). *Phase diagrams for ceramists.* The American Ceramic Society, Columbus, Ohio, 3rd edition.

Mascolo G. (1995). Ricerche attuali sulle porcellane di Carlo di Borbone - La porcellana di Capodimonte: tra mito e realtà. In *Giornate di studio sulla ceramica europea: con la*

presentazione della ricerca sulla composizione e tecnologia di produzione della porcellana d'epoca di Capodimonte, pp. 79–98. De Costanzo, Naples, Italy.

McMillan P. (1984). Structural studies of silicate glasses and melts - applications and limitations of Raman spectroscopy. *American Mineralogist*, **69**, 622–644.

Memoria del proyecto de investigación. Estudio de los pavimentos para el embaldosado de la casa del Labrador del palacio de Aranjuez. Projecto financiado por la Dirección General de Investigación de la Consejería de Educación de la Comunidad de Madrid - n. 06/0112/02.

Minieri Riccio C. (1878a). Delle porcellane della Real Fabbrica di Napoli. Delle vendite fattene e delle loro tariffe. Memoria letta all'accademia nella tornata del 7 aprile 1878. In *Atti dell'accademia pontaniana*, pp. 347–404. Stamperia della Regia Università, Napoli. Cfr. the anastatic reprint (1980) edited by G. Novi, Forni ed., Sala Bolognese.

Minieri Riccio C. (1878b). Gli artefici ed i miniatori della Real Fabbrica dalla porcellana di Napoli. Memoria letta all'accademia nella tornata del 3 e 17 marzo 1878. In *Atti dell'accademia pontaniana*, pp. 267–346. Stamperia della Regia Università, Napoli. Cfr. the anastatic reprint (1980) edited by G. Novi, Forni ed., Sala Bolognese.

Minieri Riccio C. (1878c). La fabbrica della porcellana in Napoli e sue vicende. Memoria letta all'accademia nella tornata del 27 gennaio 1878. In *Atti dell'accademia pontaniana*, pp. 231–251. Stamperia della Regia Università, Napoli. Cfr. the anastatic reprint (1980) edited by G. Novi, Forni ed., Sala Bolognese.

Minieri Riccio C. (1878d). Notizie intorno alle ricerche fatte dalla R. Fabbrica della porcellana di Napoli per rinvenire materiali a migliorare e perfezionare sempre più la manifattura della pasta della porcellana, le sue dorature e le miniature. Memoria letta all'accademia nella tornata del 10 febbraio 1878. In *Atti dell'accademia pontaniana*, pp. 252–266. Stamperia della Regia Università, Napoli. Cfr. the anastatic reprint (1980) edited by G. Novi, Forni ed., Sala Bolognese.

Musella Guida S. (1993). La manifattura di Capodimonte. Storie, produzione e fonti documentarie. In *Porcellane di Capodimonte. La Real Fabbrica di Carlo di Borbone 1743-1759*, pp. 9–22. Electa, Napoli.

Pascual C., Recio P., Valle F. J., Criado E., De Aza A. H., Martínez R., De Aza S. (2006). The last period of "Buen Retiro" porcelain factory. In *Heritage, weathering and conservation International Conference. Book of Abstracts*, p. 137.

Pepe I. (1995). Rassegna critica delle notizie storiche concernenti le materie prime e le tecniche usate per la produzione della porcellana di Capodimonte. In *Giornate di studio sulla ceramica europea: con la presentazione della ricerca sulla composizione e tecnologia di produzione della porcellana d'epoca di Capodimonte*, pp. 107–114. De Costanzo, Naples, Italy.

Rebuffat O. (1905). Studi chimici sulla porcellana di Napoli. In *Atti del Regio Istituto d'Incoraggiamento*, pp. 1–9. Società Cooperativa Tipografica, Naples, Italy.

Trinity Fine Art. Catalogue n. 28 - European Porcelain. London 2007.

Chapter 5

Raman characterization of mosaic glasses

Mosaic glass *tesserae* are a range of materials of very varied and complex nature, within which crystalline mineral phases may be dispersed, serving as opacifying and/or colouring agents. Ancient glasses were generally obtained by a mixture of naturally occurring materials containing silica, alkali and lime. Beach sand and a crude source of alkali were typical ingredients, with both the sand and the alkali containing enough lime or magnesia to give adequate chemical stability. Early eastern Mediterranean glasses used natron (hydrated Na_2CO_3) available from Northern Egypt as favoured source of alkali; this practice continued all across the Mediterranean region through late antiquity. Glass was usually coloured by adding small amounts of certain salts (mostly of copper, iron, and manganese); this addition of colorants was probably the first example of the use of minor ingredients to change glass properties to produce a desired effect. Opaque glasses were obtained by suspension of relatively large crystals, quite insoluble within the glass matrix, such as calcium- and lead-antimoniate, and tin oxide.

As shown in chapter 2, Raman spectroscopy is a powerful tool for the analysis of glasses, both for a study of surface weathering and for the characterization of bulk structure, but in the field of cultural heritage it has not yet been extensively used to study ancient mosaic glasses. This section of my thesis aims at further exploring the analytical possibilities of Raman spectroscopy applied to quite an homogeneous corpus of ancient alkali-silicate glasses, mostly in the form of mosaic tesserae.

5.1 Materials

A total of 20 samples have been analyzed, all coming from excavations in different regions of the Italian peninsula (fig. 5.1), and dating to the first five centuries AD. Different typologies and colours are represented, together with some basic colourless glass fragments; all coloured glasses are opaque. Additionally, a blue restoration *tessera* from Pompeii, and a modern turquoise transparent *tessera* with golden foil and *cartellina* were also analyzed. A synthetic description of the provenance, typology, age, and colour of the samples is given in table 5.1, along with the codes used to identify them throughout this work; images of all the samples are presented in figure 5.2. Almost all of them have already been the object of archaeometric studies dealing with specific historical and/or technological questions, most of which have been published (Abu Aysheh 2006; Boschetti *et al.* 2007;

Figure 5.1: Location of the archaeological sites of provenance of the analyzed mosaic glasses

Corradi *et al.* 2005; Macchiarola *et al.* 2006, 2007; Santoro *et al.* 2006). Table 5.2 contains the 20 chemical compositions which have been determined during previous analytical work on these samples (some of which unpublished). These compositions have been converted from weight % of oxides and are now reported as mole % of single elements, differently from what done in the preceding chapters. The need for such conversion is the particular kind of data treatment which was done for these glass samples, reported in section 5.4.

5.2 Identification of crystalline phases

Besides the typical features of a glassy phase, most spectra acquired in macroscopic configuration show also the characteristic peaks of one or more crystalline phases, detailed in table 5.3, not all of which have been identified yet. Some other crystalline phases can be identified when analyzing the samples with higher magnifications (Labram Infinity spectrometer, 50x or 100x objective):

- the macroscopic analysis of sample MAC2 shows a peak at 518 cm^{-1}, superimposed to the glassy spectrum and also found, together with weaker peaks/bands at 305, 466, 570, and 832 cm^{-1}, in the analysis of white crystals within the glass. Colomban and co-workers (2003) found the very same series of peaks in a blue glass bead (n. 62) and a green mosaic *tessera* (n. 13) and attributed it to undissolved feldspars;

- samples MAC2, MAC11, MAC13 and MAC19 show a sharp peak at 995-996 cm^{-1}, whose attribution is still unclear. A peak in the same position was also found in the blue glazes and pigments of Capodimonte porcelain samples (cfr. section 4.3.3), and thought to be related to their cobalt content. Not all of these four mosaic glass samples, however, contain a relevant amount of Co, so that the origin of this peak is still much of a question;

- samples MAC3, MAC11, MAC12 and MAC17 show a couple of peaks of equal intensity at about 480-485 and 633 cm^{-1}, which can possibly be attributed to cassiterite, as it has been done e.g. by Galli *et al.* (2004). Cassiterite was used as an opacifier only for a short period during the late Roman and Byzantine Age (Verità 2000), and it can be observed that with the exception of MAC3, the other three are the most recent among the ancient samples analyzed, and all date to the V to VI century A.D. Still, this attribution seems unlikely, as these samples contain very little Sn,

Code	Original name	Provenance	Description	Period	Colour
MAC1	VetrobasePom	Pompeii (NA)	basic glass	I AD	colourless
MAC2	7/05 CL	Collesalvetti (LI)	*tessera*	III AD	blue
MAC3	8/05 CL	Collesalvetti (LI)	*tessera*	III AD	turquoise
MAC4	1A/05 D.V. BC	Suasa (AN)	*tessera*	II AD	red
MAC5	1C/05 D.V. BC	Suasa (AN)	*tessera*	II AD	red/striped
MAC6	1A/05 sectile	Suasa (AN)	*tessera*	II AD	green
MAC7	1/05 D.V. P	Suasa (AN)	*tessera*	II AD	green
MAC8	13 P.T. 06	Pietratonda (GR)	transparent fragment	II-III AD	colourless
MAC9	14 P.T. 06	Pietratonda (GR)	transparent fragment	II-III AD	colourless
MAC10	16 P.T. 06	Pietratonda (GR)	transparent fragment	II-III AD	colourless
MAC11	S.M.O. 4	S.Maria di Olivola (FG)	*tessera*	V-VI AD	green
MAC12	Far blu'05	Faragola (FG)	*tessera*	V AD ?	blue
MAC13	FR1	Faragola (FG)	small *tessera*, opus sectile	IV AD	turquoise
MAC14	FR4	Faragola (FG)	small *tessera*, opus sectile	IV AD	green
MAC15	FR3	Faragola (FG)	small *tessera*, opus sectile	IV AD	red
MAC16	FR2	Faragola (FG)	small *tessera*, opus sectile	IV AD	dark/black
MAC17	S.M.O. 10	S.Maria di Olivola (FG)	*tessera*	V-VI AD	light blue
MAC18	VCM 5	Pompeii (NA)	*tessera*	I AD	red/striped
MAC19	VCM 10	Pompeii (NA)	*tessera*	I AD	blue
MAC20	CGT 5	Pompeii (NA)	*tessera*	I AD	red altered to green
MAC21	CDS 7	Pompeii (NA)	*tessera*	restoration	blue
MAC22			*tessera*	modern	turquoise (transparent) with golden leaf and *cartellina*

Table 5.1: Synthetic description of the analyzed mosaic glasses

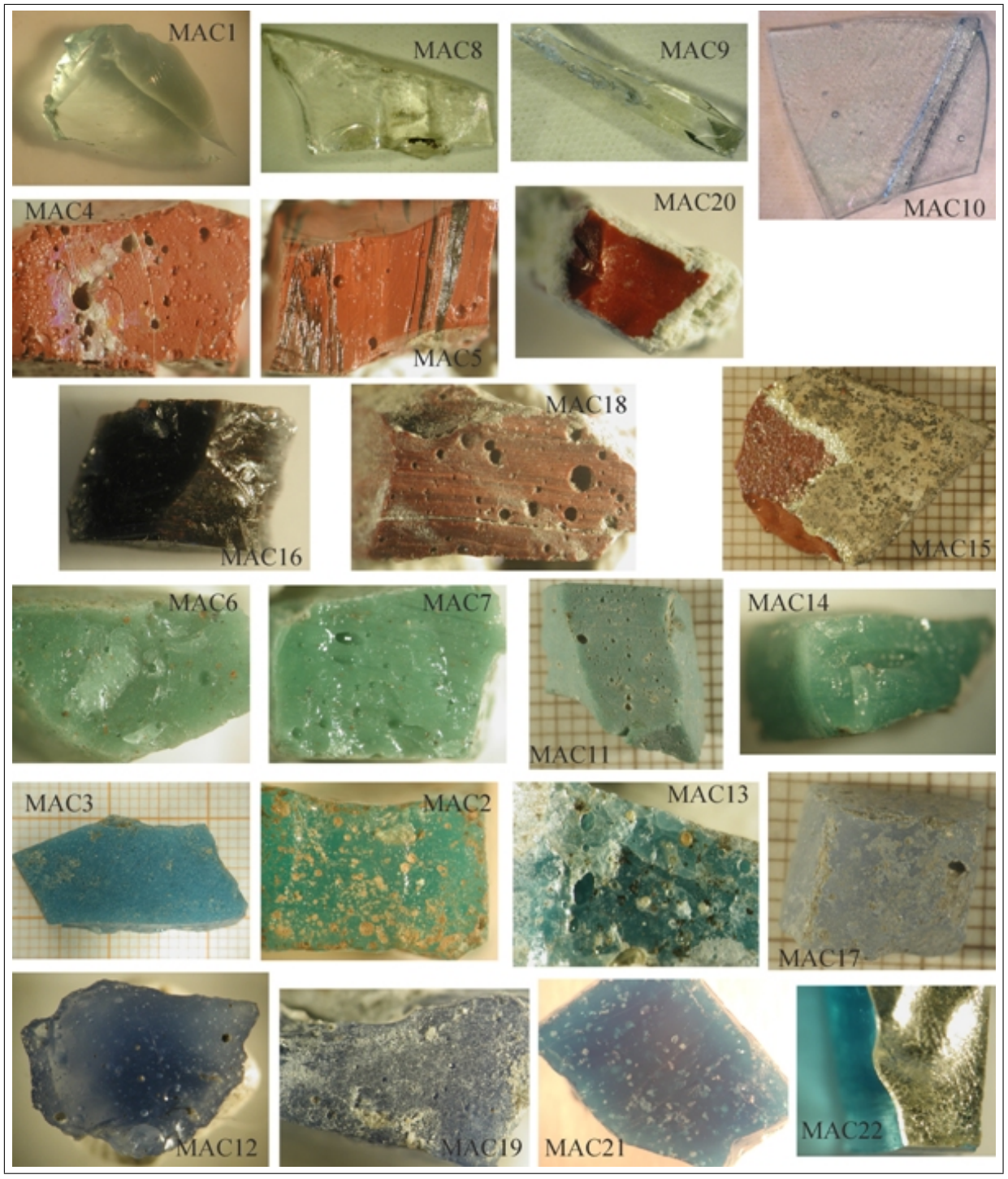

Figure 5.2: The analyzed glass samples, grouped by colour (images not to scale)

	Si	Al	Fe	Mg	Ca	Mn	Na	K	Pb	Sn	Cu	Sb	P	S	O
MAC1	23.23	1.08	0.10	0.35	3.27	0.15	12.33	0.40	0.01	0.00	0.01	0.01	0.05	0.11	58.88
MAC2	23.47	0.82	0.17	0.29	2.34	0.02	13.32	0.21	0.00	0.00	0.48	0.18	0.01	0.00	58.66
MAC3	23.65	0.85	0.15	0.34	2.03	0.04	13.48	0.26	0.02	0.01	0.34	0.10	0.01	0.00	58.69
MAC4	22.47	0.92	0.54	1.05	2.74	0.09	10.96	0.73	0.81	0.03	0.49	0.07	0.19	0.00	58.87
MAC5	23.43	0.94	0.58	0.37	2.21	0.04	11.91	0.38	0.56	0.00	0.31	0.12	0.02	0.00	59.09
MAC6	23.61	1.04	0.20	0.31	2.22	0.10	12.53	0.35	0.27	0.00	0.31	0.07	0.01	0.00	58.93
MAC7	24.15	0.92	0.22	0.32	2.12	0.13	11.58	0.35	0.22	0.03	0.40	0.06	0.02	0.00	59.44
MAC8	24.03	0.87	0.16	0.33	2.65	0.01	12.26	0.30	0.01	0.00	0.00	0.11	0.04	0.00	59.21
MAC9	24.03	0.90	0.17	0.32	2.67	0.01	12.19	0.32	0.00	0.00	0.00	0.11	0.04	0.00	59.22
MAC10	24.57	0.86	0.09	0.20	2.09	0.12	12.39	0.25	0.00	0.00	0.01	0.00	0.02	0.00	59.39
MAC11	22.61	1.30	0.15	0.26	2.28	0.09	11.86	0.41	0.01	0.05	0.90	0.80	0.04	0.18	59.04
MAC13	25.19	1.22	0.13	0.20	2.15	0.05	9.74	0.25	0.01	0.00	0.34	0.12	0.02	0.03	60.53
MAC14	23.59	1.14	0.15	0.28	2.29	0.12	12.50	0.30	0.15	0.01	0.27	0.11	0.02	0.04	59.01
MAC15	22.25	1.05	0.27	1.20	3.85	0.08	10.89	1.01	0.02	0.03	0.38	0.05	0.18	0.02	58.69
MAC16	23.51	1.08	0.44	0.28	2.18	0.07	12.87	0.30	0.04	0.01	0.13	0.09	0.02	0.03	58.92
MAC17	24.07	1.18	0.11	0.24	2.86	0.12	11.15	0.25	0.00	0.00	0.01	0.27	0.03	0.05	59.65
MAC18	22.77	1.07	0.48	0.88	2.63	0.17	11.55	0.52	0.32	0.00	0.53	0.00	0.15	0.00	58.89
MAC19	24.12	0.88	0.29	0.32	2.41	0.21	11.92	0.23	0.00	0.00	0.07	0.06	0.06	0.00	59.38
MAC20	20.45	0.86	0.24	0.29	1.88	0.04	10.16	0.28	3.95	0.03	3.25	0.36	0.10	0.00	58.08
MAC21	24.08	1.83	0.03	0.05	4.72	0.00	8.20	0.19	0.00	0.00	0.29	0.00	0.11	0.00	60.49

Table 5.2: Chemical composition of the analyzed glass samples, as results from previous analyses (mole % elements normalized to 100; n.d. = not determined). Trace amounts of Ti, Co and Zn are included in the normalization but not reported in the table. Samples MAC19 and MAC21 contain 0.03 and 0.02 mole % of Co, respectively

	Position of peaks (cm^{-1})	Phase assignment
MAC2	457	quartz
	518	feldspars
	995	?
MAC3	465	quartz
	671	Ca-antimoniate
	480, 633	cassiterite?
MAC6	141vs, 340, 456, 508	$Pb_2Sb_2O_7$ bindheimite
MAC7	141vs, 337, 453, 510	$Pb_2Sb_2O_7$ bindheimite
MAC8	156vw, 283, 714, 1088	calcite
MAC9	1088	calcite
MAC10	462	quartz
MAC11	485, 633	cassiterite?
	238, 325, 338, 521, 671vs	Ca-antimoniate
	995	?
MAC12	482, 633	cassiterite?
MAC13	238, 324, 338, 671	Ca-antimoniate
	996	?
MAC14	141vs, 339, 455, 510	$Pb_2Sb_2O_7$ bindheimite
	585, 965vs, 1011, 1023, 1044	?
MAC15	460	quartz
MAC17	481, 635	cassiterite?
MAC19	671	Ca-antimoniate
	996	?
MAC20	218	cuprite
	589w	?
MAC21	320	fluorite
	496w	?

Table 5.3: Raman peaks of crystalline phases identified in the macroscopic spectra of glass samples (vs: very strong; w: weak; vw: very weak)

and the chemical analysis of sample MAC17 found no tin at all. It seems that it could be useful to repeat the chemical characterization of these four samples, and at the same time to further investigate the possible nature of the Raman signature identified in their spectra;

- samples MAC11 and MAC13 show a series of peaks, the most intense of which is found at 671 cm^{-1} and can also be identified in samples MAC3 and MAC19. Exactly the same series of peaks (at 250, 325, 335 and 665 cm^{-1}) had been identified in two blue mosaic *tesserae* (n. 5 and n. 6, only the main peak in the latter) in the above mentioned work by Colomban *et al.* (2003), and there assigned to cassiterite. Galli *et al.* (2004) observed a narrow peak at 670 cm^{-1} in a blue mosaic *tessera* from a Roman villa and proposed an attribution to an iron and/or manganese oxide. It seems more likely that these peaks should be assigned to calcium antimoniate ($Ca_2Sb_2O_7$ or $CaSb_2O_6$), whose use as an opacifier in blue and turquoise glasses in the Roman Age is well documented (Galli *et al.* 2003; Verità 2000), but whose Raman signature does not seem to have been recognized anywhere in the scientific literature on mosaic glasses. A reference spectrum of $CaSb_2O_6$, found in a work on a completely different subject (Husson *et al.* 1984), can however be easily compared to that of our unidentified compound, as shown in figure 5.3. A further support for this attribution came from a later SEM-EDS inspection of samples MAC3 and MAC13, aimed precisely at trying to identify the nature of the whitish crystals of irregular shape that could be observed throughout the glass matrix. In both samples, a number of such crystals yield fluorescence spectra such as the one shown in figure 5.4, which can quite clearly be identified as calcium antimoniate, given its chemical composition containing $\sim$ 12% atomic Ca and $\sim$ 23% atomic Sb (the exact quantification of calcium content is hindered by the superposition of one of its fluorescence peaks with the peak of carbon);

- cuprite crystals have been observed during the SEM analysis throughout sample MAC20; all its spectra do in fact contain the characteristic signature of this compound. This sample contains also white acicular crystals which yield peaks at 218, 278vs, 326 and 615 cm^{-1}. The first and fourth of these peaks are assigned once again to cuprite; as for the others, they can tentatively be attributed to a copper salt, such as chalcopyrite $CuFeS_2$, which might be residual of the raw material;

- SEM-EDS analysis detected a high concentration of fluorine throughout sample MAC21, and in fact all its spectra show the main peak of fluorite CaF_2, which must have been used as a flux. This is an evident difference between this restoration sample and all the ancient ones; the use of fluorite is here a proof of a more recent production of this glass with respect to the others.

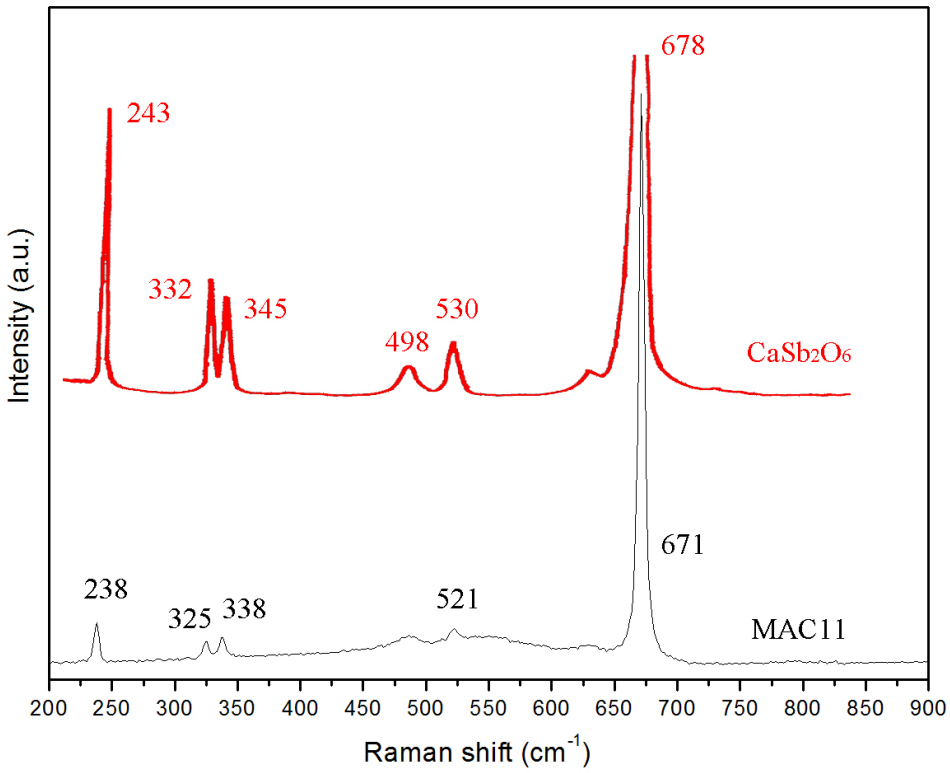

Figure 5.3: Raman spectrum of sample MAC11 (XY2 macroscopic analysis) and reference spectrum of $CaSb_2O_6$, modified from Husson *et al.* (1984, fig.3)

5.3 Relationship between the Raman spectra and glass colour

Colour differences among the glasses are not reflected in marked differences between the spectra; some interesting comments can nonetheless be made, because some features of the Raman spectra do depend on the chemical composition of the samples, and this is

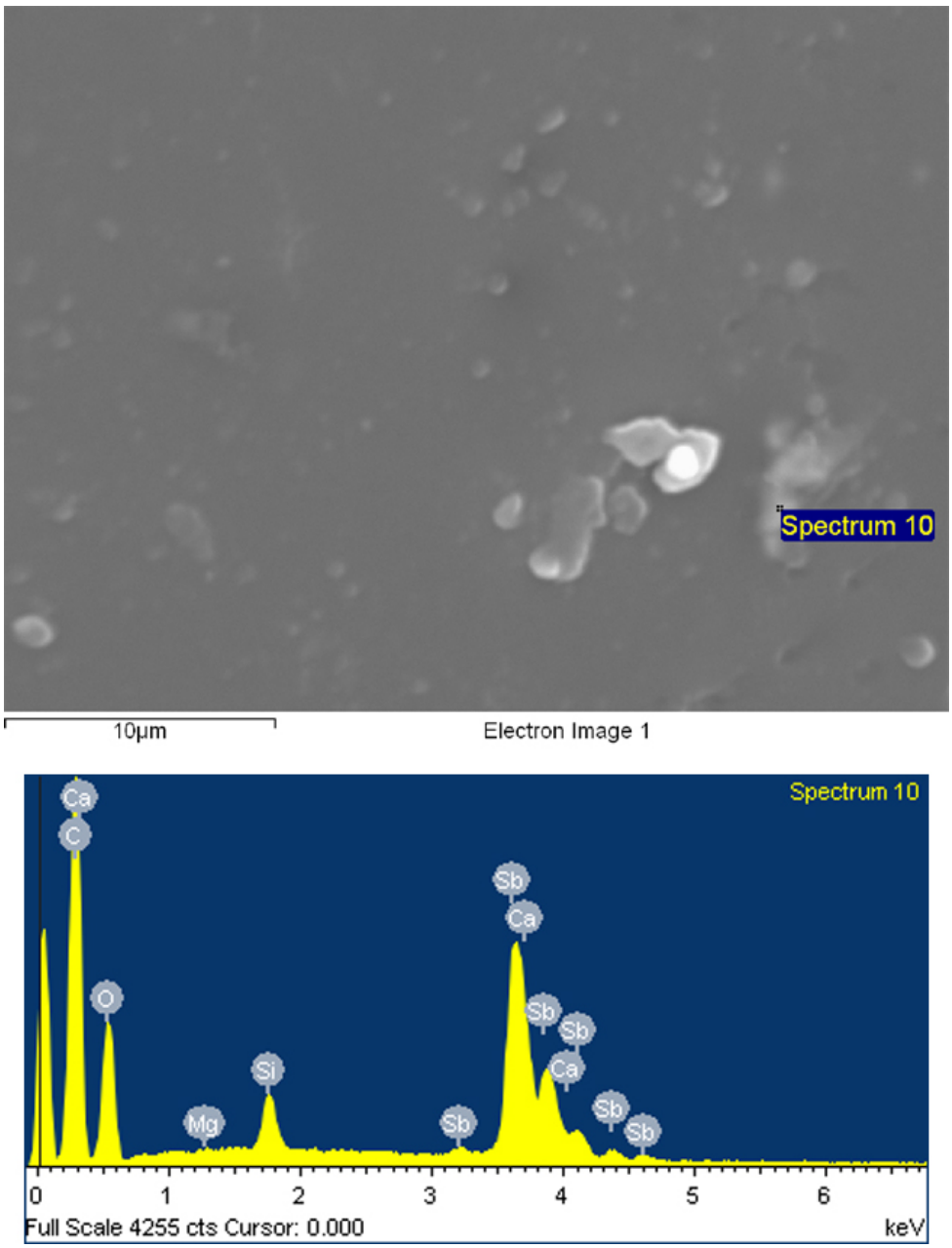

Figure 5.4: Representative SEM image and EDS point spectrum of a whitish crystal in sample MAC13

often related to their colour.

Red and dark/black glasses (MAC4, MAC5, MAC15, MAC16, MAC18 and MAC20) do not show any peaks which can be related to crystalline phases giving origin to their colour, which is in most cases quite clearly due to the elevated iron content of the samples. Fragment MAC20 stands as an exception; it belongs to a rare typology of red mosaic glasses found at Pompeii, which are strongly altered and have developed a greenish appearance and degradation products in the form of *Pb*-carbonates and *Cu*-oxides/hydroxides (Corradi *et al.* 2005) . All Raman analyses on this sample have been made on the red (unaltered) part; the analysis of the green (altered) parts yielded only a very intense background signal. All the spectra of MAC4, MAC5 and MAC18 do have a shape which is slightly different from that of the other samples' spectra, in that both glassy massifs show a shoulder on their left side (at about 500, and between 900 and 1000 cm^{-1}). The first of these is compatible with the description of the spectra of *Pb*-silicate glasses (Colomban *et al.* 2006), and with the fact that these samples show the highest amounts of lead content, respectively 7.94, 5.71 and 3.27 % *PbO* as opposed to an average of 0.54 % *PbO* for the rest of the samples. All these samples also have a medium to high potassium and magnesium content, and the second shoulder is probably linked to this characteristic.

As for green glasses, the spectra of three of them (MAC6, MAC7 and MAC14) consistently show three wide peaks (at about 338, 455 and 510 cm^{-1}, plus a very strong peak at 141 cm^{-1}. Numerous pale crystals can be observed through the microscope to be dispersed within the glassy matrix. By acquiring the spectra of such crystals, it is evident that they are responsible for the three bands which are superimposed to the first massif in the macroscopic spectra. Such peaks are associated with the presence of bindheimite $Pb_2Sb_2O_7$ (Bouchard and Smith 2003; Colomban *et al.* 2001), in agreement with the fact that the *Pb* content of these samples is comprised between 1.54 and 2.84 % *PbO*, which are the second-highest values after those of the above mentioned red samples. All other samples have a lead content smaller than 0.5 % *PbO*. Bindheimite acts as both a colouring and an opaquening agent in these glasses. They contain as much *Cu* as the blue and turquoise ones, but more lead; copper would therefore yield a blue colour, but these samples appear green because of the contemporary presence of the yellowish crystals of bindheimite, which also accounts for the opacification of the glass. Sample MAC11

is the only green *tessera* which is visually different and shows different spectral features from the other green samples; all its spectra show the above mentioned series of very well pronounced crystalline peaks (the strongest of which lies at 671 cm^{-1}) which can be attributed to calcium antimoniate, which accounts for the opacification of this material. It has probably been coloured with copper salts (such as tetrahedrite $(Cu, Fe)_{12}Sb_4S_{13}$), of which no trace is evident in the spectra. This possibility is supported by the fact that this sample contains the highest amounts of Sb, Cu, and S among all 20 samples of which the chemical composition is known.

All the remaining (ancient) samples (transparent and colourless, turquoise and blue) do not seem to show spectral features which distinguish them on the base of their colour. Finally, the two modern samples yield spectra whose shapes are evidently different from those of all the other ones, but this is related to the different nature of these glasses, rather than to colour differences (cfr. section 5.4).

5.4 Characterization of the glass structure

Before proceeding to the analytical deconvolution of representative spectra of the glasses, a few comments can already be made on a simple visual basis, looking at the representative spectra shown in figures 5.5 and 5.6, in which the colour of each spectrum corresponds to the colour of the glass, and the plots of colourless glasses are drawn in black. All comparisons in this section are made with respect to the seven "glass families" (GF) which are described in the work of Colomban *et al.* (2006), and all numerical values cited also refer to that article. The shape of all the spectra is typical of alkali-silicate glasses, here used to indicate soda-lime silicate glasses (corresponding to GF n. 3), which is what the chemical composition indicates our samples to be. The only exceptions are samples MAC20-22, which are indeed different from the other ones. Sample MAC20 is in fact a *Pb-Na* silicate glass (GF n. 4), while the two modern *tesserae* must differ at least technologically from all the ancient ones. Comments hereafter will therefore refer only to samples MAC1-19, and mostly to spectra acquired in macroscopic configuration with the Dilor XY2 spectrometer. These have in fact shown to be the most representative of all spectra of these ancient glasses, allowing the best reproducibility, with the exception of sample MAC18, of which for no evident reason no usable spectra have been obtained

with XY2.

When compared with a "typical" spectrum of an alkali-silicate glass, our spectra show a compatible position of ν_{MAX} *Si-O* (1095 vs. 1090 cm^{-1}), while δ_{MAX} *Si-O* is shifted towards lower wavenumbers (557 vs. 580 cm^{-1}) , and halfway towards a typical value for *Na*-silicate glasses (540 cm^{-1}, GF n. 4). It should be observed that the average *CaO* content of our samples (6.6 ± 1.2 % *CaO*) is lower than the calcium content of two representative samples of GF n. 3 (which contain 8.3 and 9.2 % *CaO*, respectively), so that the sodic component of the glass gives evidently a greater contribution to the Raman spectrum.

Values of the polymerization index I_p vary in the range 0.45-1.03 , with an average of 0.68 ± 0.12, which is quite low when compared to the average value of GF n. 3 (I_p = 1.02); still, it must be observed that the spectra shown in the work of Colomban *et al.* (2006) were acquired with all three spectrometers described in section 2.3. It has already been pointed out how the choice of one or the other instrument can lead to slight differences in the values of calculated Raman parameters (cfr. section 4.3.5), and interestingly the spectra acquired with the Labram Infinity on our glass samples yield values of I_p comprised between 0.76 and 1.76, with an average of 1.24 ± 0.25, which is totally comparable to that evaluated for GF n. 3. Most probably, in this case it is the shape of the background, and the consequent calculation of the baseline, which play a non-negligible role in the definition of the final shape of the spectra, and therefore on the values of the polymerization index.

> *All the spectra of the analyzed tesserae show one of the salient features of alkali-silicate glasses, a small band centered at 990 cm^{-1}, which is not usually included in the general deconvolution model describing the vibration modes of the silicate tetrahedral network.*
> *The very small variances of all parameters calculated from the representative spectra (I_p, ν_{MAX}, δ_{MAX}, cfr. table 5.4) show the extreme homogeneity of our corpus from the compositional and technological point of view, also justifying the difficulty in finding "trends" based on glass colour and/or provenance.*

Robinet *et al.* (2006a,b) have already pointed out the relative utility of I_p as a classification tool within homogeneous groups of samples. They propose alternative methods

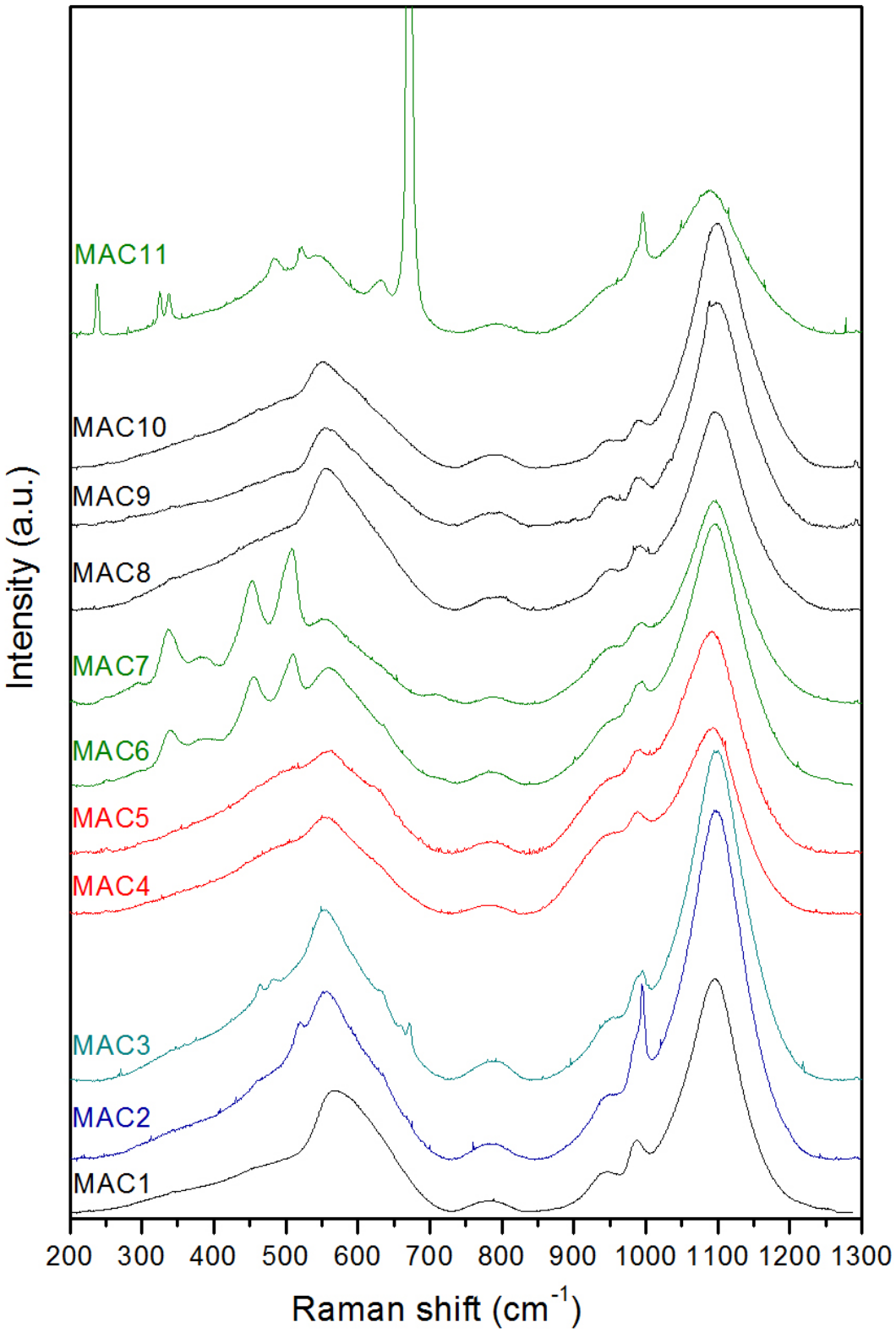

Figure 5.5: Representative Raman spectra of samples MAC1-11 (XY2 macroscopic analysis)

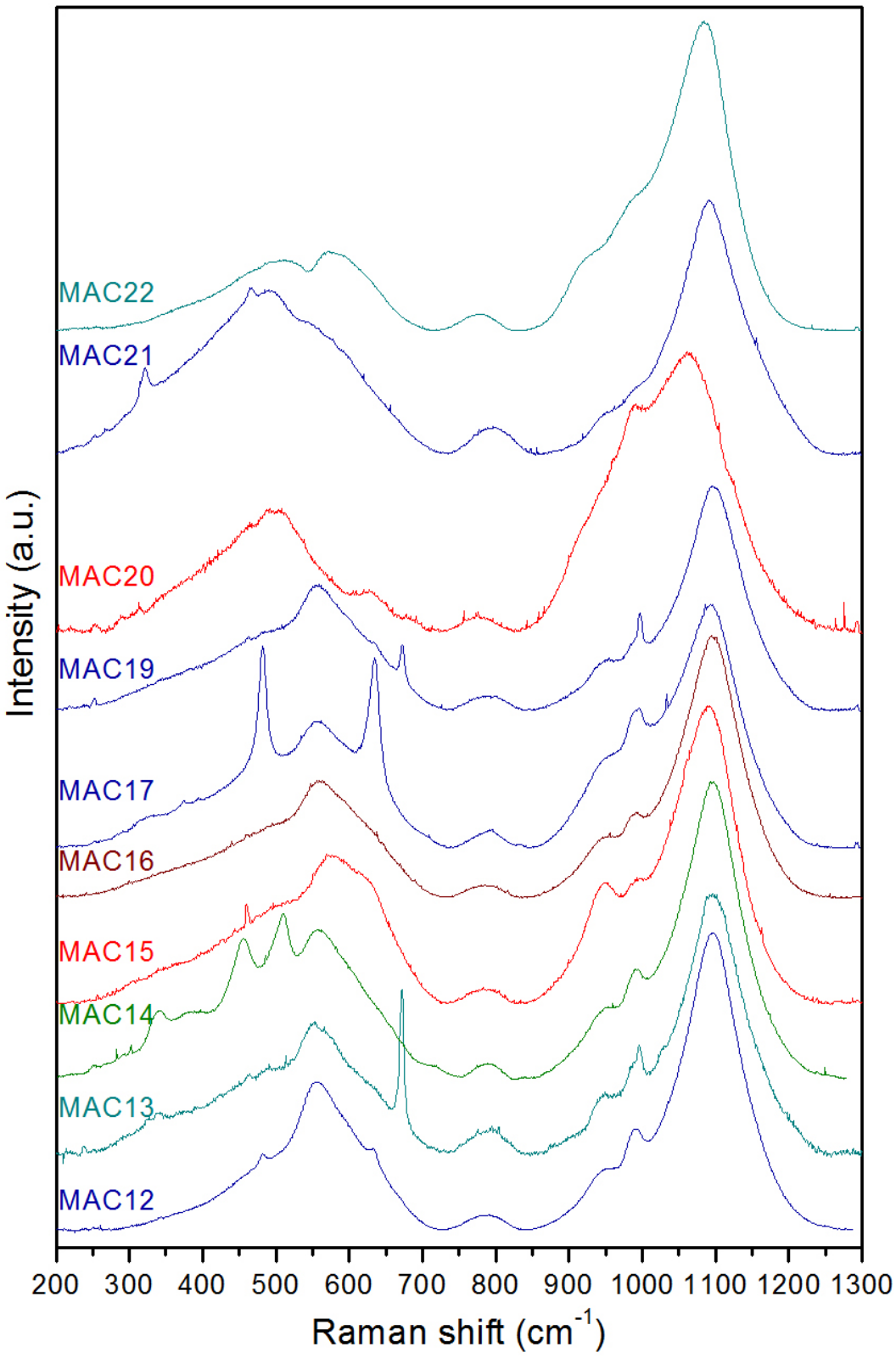

Figure 5.6: Representative Raman spectra of samples MAC12-22 (XY2 macroscopic analysis; no exploitable spectrum of sample MAC18 has been obtained with this instrument)

Sample	XY2 spectra				LI spectra			X_2
	I_p	δ_{MAX} *Si-O*	ν_{MAX} *Si-O*	B_{550}	I_p	δ_{MAX} *Si-O*	ν_{MAX} *Si-O*	
MAC1	0.76	567	1096	556.87	1.76	570	1096	0.79
MAC2	0.68	555	1097	556.55	1.31	556	1098	0.80
MAC3	0.73	553	1098	555.17	1.07	556	1101	0.81
MAC4	0.63	555	1094	554.87	0.84	559	1092	0.76
MAC5	0.64	560	1091	570.64	0.87	565	1098	0.79
MAC6	0.53	560	1097	555.25	1.23	559	1095	0.80
MAC7	0.46	552	1095	548.91	1.38	557	1100	0.81
MAC8	1.03	556	1097	553.23	1.31	555	1100	0.81
MAC9	0.68	555	1100	550.7	1.39	556	1097	0.81
MAC10	0.73	552	1099	548.32	1.92	543	1096	0.83
MAC11	0.58	541	1088	556.12	1.11	548	1092	0.77
MAC12	0.58	557	1096	555.91	1.49	554	1098	n.d.
MAC13	0.72	552	1095	545.84	1.29	550	1093	0.83
MAC14	0.64	558	1095	551.34	1.20	559	1097	0.80
MAC15	0.72	575	1092	568.83	1.53	582	1101	0.76
MAC16	0.67	559	1094	554.85	1.18	563	1101	0.80
MAC17	0.66	556	1094	563.07	1.40	559	1098	0.81
MAC18	n.d.	n.d.	n.d.	n.d.	0.76	571	1095	0.77
MAC19	0.85	556	1095	556.44	1.23	556	1096	0.81
MAC20	0.45	490	1063	n.d.	0.43	484	1060	0.70
MAC21	1.16	492	1090	n.d.	1.46	491	1089	0.80
MAC22	0.39	571	1083	n.d.	0.54	570	1083	n.d.

Table 5.4: Raman parameters extracted from the XY2 and LI spectra of glass samples (wavenumber positions in cm^{-1}). Cfr. text for the exact definition of B_{550} (calculated on the base of the decomposition model presented in table 5.5) and X_2 (calculated on the base of the chemical composition of each sample)

to determine and compare the degree of polymerization within a group of alkali-silicate glasses, together with a slightly different, and somewhat more refined, decomposition model for the Raman spectra of this kind of glasses. Such model, presented in table 5.5, has been tentatively applied to representative XY2 spectra of samples MAC1-19, and relative data are hereunder reported.

Frequency (cm^{-1})	Bandwidth (cm^{-1})	Assignment suggested
330-380	-	δ *Si-O-Si* Q_4
460-500	-	δ *Si-O-Si* Q_4
540-590 (B_{550})	-	δ *Si-O-Si* Q_3
580-640	-	δ *Si-O-Si* Q_2
(640-690)	-	-
770-800	-	*Si* motion in tetrahedral
(800-830)	-	oxygen cage
(895-910)	-	ν *Si-O* Q_2
950	50	ν *Si-O* Q_2
990	33	ν *Si-O* Q_2
1040	70	-
1100	65	ν *Si-O* Q_3
1150	-	ν *Si-O* Q_4 + ν *Si-O* Q_3

Table 5.5: Decomposition model for alkali silicate glasses, from Robinet *et al.* (2006b, table 2) (underlined: values fixed; in brackets: components which sometimes disappeared due to band superposition)

In the high wavenumber region, this model is similar to that used in previous works for alkali-silicate glasses, with the difference of two additional components at 895-910 and 990 cm^{-1}, both assigned to the Si-O stretching of the Q_2 species. Also, none of the bands is attributed to Q_1 species. Regardless the chemico-physical bases on which the model was built, it certainly provides very good fits for the spectra of alkali-silicate glasses. Additionally, it allows establishing some interesting correlations between Raman data and chemical composition of the materials. In particular, the position of the band at 550 cm^{-1}, named B_{550}, can be directly correlated to the silica content or the total cation charge, and hence to the degree of polymerization of the glass. The SiO_2 content is calculated as X_2=$2x_{Si}/x_O$, where x_{Si} and x_O are expressed in mole % of each element.

Figure 5.7 shows data relative to our samples, together with the regression line $y = -387x + 868$ ($R^2 = 0.978$) calculated by Robinet *et al.* (2006b). It is easy to see that the fit works quite well, though not perfectly, with most of our data. All the samples whose data lay far from the line do not seem to have any specific common features.

On the other hand, other correlations established in the cited work between Raman data and chemistry and/or stability of alkali-silicate glasses do not seem to work quite as well with the data relative to our mosaic *tesserae*. It seems that further verifications of the validity of these correlations could be interesting, and should include the enlargement of the corpus of the analyzed samples, in order to achieve results as general as possible.

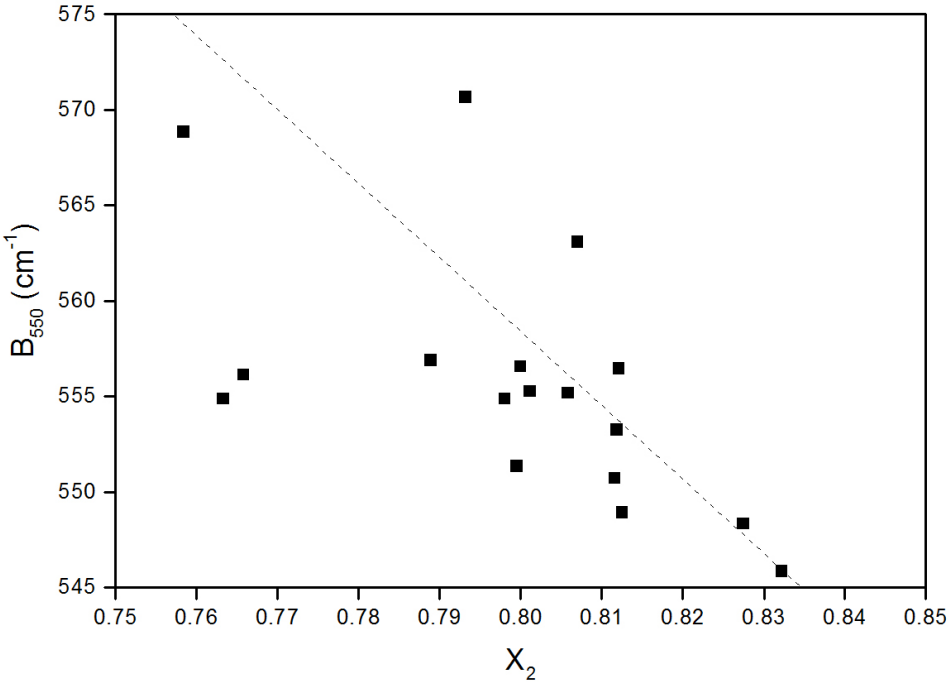

Figure 5.7: Plot of the wavenumber position of B_{550} vs. X_2=$2x_{Si}/x_O$ of samples MAC1-17 and MAC19. The dashed line is the regression equation calculated by Robinet *et al.* (2006b)

The extreme homogeneity of the Raman spectra of all the ancient tesserae reflects the limited variability of their chemical composition, and gives yet another proof of the high level of standardization of glass production in the Roman Age, through a completely non-destructive analytical approach. The ancient

degraded sample from Pompeii (MAC20) has a composition much richer in Pb, and as such more easily subject to weathering. Its greater lead content and its advanced degradation state are both mirrored in the peculiar shape of its Raman spectrum. Finally, the restoration and modern tesserae (MAC21 and MAC22) can easily be distinguished from the ancient samples, as their spectra show clear differences with respect to the others, which have instead all the features of "typical" alkali-silicate glasses.

This homogeneous corpus also allowed testing the validity of some proposed correlations between chemical composition and Raman data.

5.5 References

Abu Aysheh M. S. (2006). Studio archeometrico-tecnologico delle tessere in vetro dei mosaici della *domus* dei *Coiedii* di Suasa: uno strumento per la risoluzione di problematiche archeologiche e di conservazione. *OCNUS - Quaderni della scuola di specializzazione di archeologia. Alma Mater Studiorum - Università di Bologna*, **14**, 245–248.

Boschetti C., Corradi A., Fabbri B., Leonelli C., Macchiarola M., Ruffini A., Santoro S., Speranza M., Veronesi P. (2007). Caratterizzazione archeometrica dei mosaici del ninfeo della *domus* del centenario. In *Indagini diagnostiche e geofisiche e analisi archeometriche su muri, malte, pigmenti, colori, mosaici*. Santoro S. (ed.), pp. 259–308. Bologna.

Bouchard M., Smith D. C. (2003). Catalogue of 45 reference Raman spectra of minerals concerning research in art history or archaeology, especially on corroded metals and coloured glass. *Spectrochimica Acta Part A*, **59**, 2247–2266.

Colomban P., Sagon G., Faurel X. (2001). Differentiation of antique ceramics from the Raman spectra of their coloured glazes and paintings. *Journal of Raman Spectroscopy*, **32**, 351–360.

Colomban P., March G., Mazerolles L., Karmous T., Ayed N., Ennabli A., Slim H. (2003). Raman identification of materials used for jewellery and mosaics in Ifriqiya. *Journal of Raman Spectroscopy*, **34**, 205–213.

Colomban P., Tournié A., Bellot-Gurlet L. (2006). Raman identification of glassy silicates used in ceramics, glass and jewellery: a tentative differentiation guide. *Journal of Raman Spectroscopy*, **37**, 841–852.

Corradi A., Leonelli C., Veronesi P., Fabbri B., Macchiarola M., Ruffini A., Boschetti C., Santoro S. (2005). Ancient glass deterioration in mosaics of Pompeii. *Surface Engineering*, **21**(5-6), 402–405.

Galli A., Martini M., Montanari C., Sibilia E. (2003). The use of antimony and its implication for the luminescence properties of ancient mosaic *tesserae*. *Journal of Non-Crystalline Solids*, **323**, 72–77.

Galli S., Mastelloni M., Ponterio R., Sabatino G., Triscari M. (2004). Raman and scanning electron microscopy and energy-dispersive x-ray techniques for the characterization of colouring and opaquening agents in Roman mosaic glass tesserae. *Journal of Raman Spectroscopy*, **35**, 622–627.

Husson E., Repelin Y., Vandenborre M. T. (1984). Spectres de vibration et champ de force de l'antimoniate et de l'arseniate de calcium $CaSb_2O_6$ et $CaAs_2O_6$. *Spectrochimica Acta*, **40A**(11/12), 1017–1020.

Macchiarola M., Zeolla L., Ercolani G. (2006). La *cenatio* della villa tardoantica di Faragola (Ascoli Satriano, FG): studio archeometrico delle lastrine vitree dei pannelli in *opus sectile*. In *Proceedings of the XI Colloquio dell'AISCOM*, pp. 441–452. Ed. Scripta Manent, Tivoli.

Macchiarola M., Abu Aysheh M. S., Ruffini A., Starinieri V. (2007). Studio archeometrico di tessere in vetro dai mosaici pavimentali della *domus* dei *Coiedii*, Suasa (AN). In *Proceedings of the XII Colloquio dell'AISCOM*, pp. 555–564. Ed. Scripta Manent, Tivoli.

Robinet L., Coupry C., Eremin K., Hall C. (2006a). Raman investigation of the structural changes during alteration of historic glasses by organic pollutants. *Journal of Raman Spectroscopy*, **37**, 1278–1286.

Robinet L., Coupry C., Eremin K., Hall C. (2006b). The use of Raman spectrometry to predict the stability of historic glasses. *Journal of Raman Spectroscopy*, **37**, 789–797.

Santoro S., Boschetti C., Speranza M., Corradi A., Leonelli C., Veronesi P., Fabbri B., Macchiarola M., Ruffini A., De Giorgio V. (2006). Nuovi sviluppi nelle indagini archeometriche sui mosaici dei ninfei a scala pompeiani. In *Proceedings of the XI Colloquio dell'AISCOM*, pp. 537–546. Ed. Scripta Manent, Tivoli.

Verità M. (2000). Tecniche di fabbricazione dei materiali musivi vitrei. Indagini chimiche o mineralogiche. In *Medieval mosaics: light, color, materials*. Borsook E., Gioffredi Superbi F., Pagliarulo G. (eds.), pp. 47–64. Florence.

General conclusions

This thesis was conceived to be an "exploration" in three domains of application of Raman spectroscopy as a diagnostic tool for the non-destructive study of cultural heritage materials, namely ancient pottery, porcelains and mosaic glasses. While the use of this technique is well established for the analysis of historic pigments and precious stones, its application to these three types of materials is more recent and still an expanding field.

Raman spectroscopy proved a unique tool to investigate the anatase to rutile transition within ceramics. This study also allowed reasserting how careful the researcher should be when attempting to use this transition as a temperature marker for pottery firing.

The study of slips and decorations of ancient pottery showed how Raman spectroscopy in this case cannot completely replace other techniques, but it can be useful for preliminary screening, e.g. to identify which seem to be the most significant samples on which a more comprehensive analytical study should be carried out.

As for the engobes of "sgraffito" pottery, interesting results came from the combination of the Raman and chemical characterization. A larger set of data might allow putting on more sound ground some of the hypotheses which have been made regarding the raw materials used and the possibility to differentiate among production sites. Glaze analysis rapidly confirmed the use of well established recipes.

Raman analyses confirmed the uniqueness of the Capodimonte production, to some extent similar to traditional hard paste, but with a glaze closer to that of soft paste. The Raman analysis of the glazes yielded parameters that were related to the chemical composition, and allowed making hypoteses about the nature of the chromophore species found in the coloured glazes. The acquired data could be further treated, also by means of statistical methods (such as PCA and cluster analysis), in order also to investigate more deeply the correlations existing between the results of Raman analysis and those obtained

from other (destructive) techniques.

Some specific Raman signatures were identified for both pastes and glazes of Capodimonte samples, which might serve as a "reference" group for the identification of products issued from this manufacture. High similarities were found within the Raman signatures of some Buen Retiro samples, which would assign them to the early stage of the Spanish production. On the other hand, the two Buen Retiro vases seem to belong to a later period of the same factory, and display peculiar signatures both in the paste and in the glaze. The same can be said of some samples attributed to the Sureda years, whose spectra are easily recognizable, mainly due to the presence of enstatite in the paste.

Besides those presented in this work, a number of other early European productions of porcelain have so far been characterized by Raman spectroscopy, and numerous data have appeared, spread in articles published in several specialized journals (cfr. the review present in section 1.3). There seems now to be a great need for the systematization of such a large corpus of spectroscopic data, in order to identify "reference" Raman signatures for each manufacture and possibly to standardize the experimental procedure for Raman analyses on ancient porcelains. Up to now a similar need has been fulfilled for the Raman spectra of pigments, which have been the object not only of many publications, but also of some systematization and implementation over the internet. Hopefully the establishment of such a database and experimental protocol will be the object of more research in the near future.

The Raman analysis of mosaic *tesserae* allowed a good characterization of both the glass matrix and the crystalline inclusions. It also led to the identification in some blue, turquoise and green *tesserae* of calcium antimoniate, whose Raman signature does not seem to have been recognized so far in the scientific literature on mosaic glasses. Moreover, the extreme homogeneity of the Raman spectra of all the ancient samples well reflected the limited variability of their chemical composition, and gave yet another proof of the high level of standardization of glass production in the Roman Age, through a completely non-destructive analytical approach.

Studying such different types of materials allowed making some comments on the importance of choosing the "best" kind of spectrometer for the analysis of each of them. Different laser colours, instrumental optics and filters yield differences in the Raman spectra

which can have a non negligible effect on their interpretation. For example, macroscopic analyses seem most indicated for highly homogeneous samples of considerable thickness, while the use of a microscopic approach is of fundamental importance when analyzing e.g. a porcelain glaze of limited depth, in order to avoid interferences from the underlying paste. Finally, a last generation portable Raman spectrometer was used for the on-site analysis of some porcelain museum objects, and its high-standard performances could be underlined, which are fully comparable with those of lab instruments.

This work follows the path designed by many researchers in the past few years, towards the classification of Raman signatures of cultural heritage materials. More specifically, much of it rests upon the work of Colomban and co-workers, who were the first to sort the Raman spectra of historic glasses into well-defined categories, and to provide some practical numerical tools for such grouping. That is why it seems interesting to add all the Raman data on glasses and glazes acquired during this work to some of the published graphs, to support the proposed classifications and thus to validate in a way the reliability of both the analytical technique and the methods used for data treatment. The figure on page 154 is an expansion of figure 4.24 and shows the plot of I_p values vs. ν_{MAX} *Si-O* wavenumbers for all the glazes and glasses analyzed in this thesis (closed symbols). Open symbols refer to published data and represent all seven glass "families" identified among all the glassy samples of different nature which were analyzed during previous studies (Colomban *et al.* 2006, modified from figure 9a). It is clear how the data relative to the mosaic glasses and the glazes of the "sgraffito" pottery fall exactly within the categories of alkali-silicate and lead-silicate glasses, respectively. Data relative to porcelain glazes contribute instead to enlarge and better define the variation range of the Raman parameters of *Na-Pb* silicate glasses.

Generally speaking, this work showed once again the usefulness of Raman spectroscopy for the non-destructive analysis of cultural heritage materials. More particularly, its capability to characterize glassy structures should be underlined. Further results could be obtained by enlarging the set of samples of which both the chemical composition and the Raman spectra be known. This may in fact improve the correlations established in previous works and in the present thesis. This would in turn enhance the reliability of Raman spectroscopy and support its role as a routine technique, both fast and non-

invasive, useful for preliminary screenings of large numbers of artefacts. At the same time, it seems important to proceed to a standardization of experimental procedures and data processing methods, in order to facilitate comparisons among results obtained in different labs.

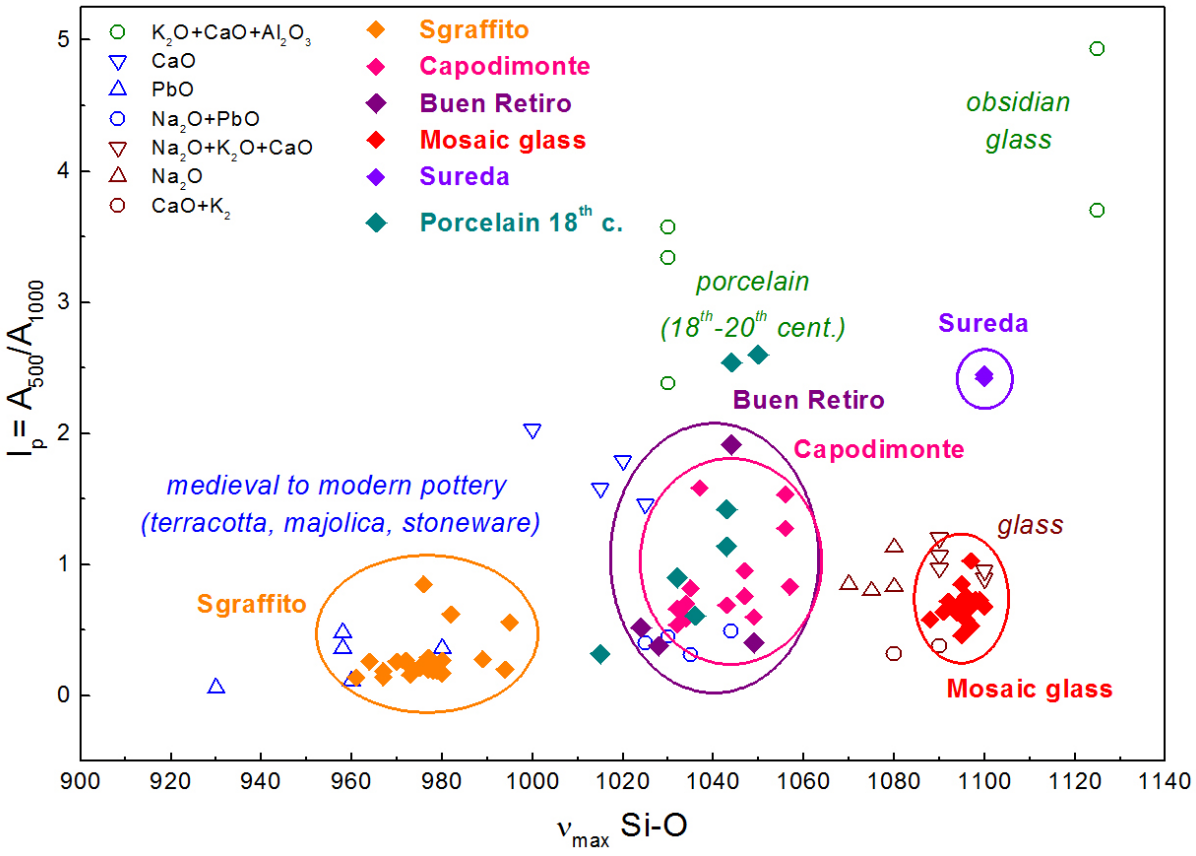

Appendix A
Glossary of mineral phases

Name	**Chemical formula**	**Abbreviation**
α-wollastonite	$CaSiO_3$	α-w
β-wollastonite	$CaSiO_3$	β-w
γ-alumina	Al_2O_3	γ-Al
Anatase	TiO_2	An
Bindheimite	$Pb_2Sb_2O_7$	
Calcite	$CaCO_3$	Ca
Calcium antimoniate	$Ca_2Sb_2O_7$	
Carbon (amorphous)	C	C
Cassiterite	SnO_2	Cs
Chalcopyrite	$CuFeS_2$	
Chlorite	$(Fe, Mg, Al)_6(Si, Al)_4O_{10}(OH)_8$	Ch
Cristobalite	SiO_2	Cr
Cuprite	Cu_2O	
Diopside	$CaMgSi_2O_6$	Di
Dolomite	$CaMg(CO_3)_2$	
Enstatite	$MgSiO_3$	En
Feldspars (Ca)	$CaAl_2Si_2O_8$	F
Feldspars (K)	$KAlSi_3O_8$	F
Feldspars (Na)	$NaAlSi_3O_8$	F
Fluorite	CaF_2	
Forsterite	Mg_2SiO_4	Fo
Hematite	Fe_2O_3	Hem

Name	**Chemical formula**	**Abbreviation**
Hercynite	$FeAl_2O_4$	
Illite	$(K, H_3O)(Al, Mg, Fe)_2(Si, Al)_4O_{10}[(OH)_2, (H_2O)]$	Ill
Magnetite	Fe_3O_4	
Minium	Pb_3O_4	
Mullite	$Al_6Si_2O_{13}$	Mu
Quartz	SiO_2	Qtz
Rutile	TiO_2	R
Scapolites (Na)	$Na_4(Al, Si)_{12}O_{24}Cl$	Sc
Scapolites (Ca)	$Ca_4(Si, Al)_{12}O_{24}(CO_3, SO_4)$	Sc
Spinel (Mg,Fe)	$(Mg, Fe)Al_2O_4$	Sp
Talc	$Mg_3Si_4O_{10}(OH)_2$	
Tetrahedrite	$(Cu, Fe)_{12}Sb_4S_{13}$	
Trydimite	SiO_2	Tr

Appendix B
Publications and scientific production

Refereed papers

- Gigante G. E., Ricciardi P., Ridolfi S., Areas and limits of employment of portable EDXRF equipment for in situ investigations. ArcheoSciences − Revue d'Archéométrie 29(2005), p. 51−60

- Ricciardi P., Nodari L., Fabbri B., Gualtieri S., Russo U., Contribution for a mineralogical thermometer to be applied to low−fired and/or non carbonate ceramics. Proceedings of EMAC'05 (2007), p. 13-18

- Ricciardi P., Nodari L., Gualtieri S., De Simone D., Fabbri B., Russo U., Firing techniques of black slipped pottery from Nepal (12^{th}-3^{rd} century B.C.): the role of Mössbauer spectroscopy. Journal of Cultural Heritage, accepted for publication on December 4^{th}, 2007

- Ricciardi P., Colomban Ph., Milande V., Non−destructive characterization of Capodimonte and Buen Retiro porcelain. Journal of Raman Spectroscopy, accepted for publication on December 10^{th}, 2007

Other publications

- Roma S., Fabbri B., Gualtieri S., Ricciardi P., Dall'argilla al vaso: tecnologia della ceramica nel sito neolitico di Sammardenchia (UD). Risultati preliminari delle analisi archeometriche e prospettive della ricerca. Proceedings of the conference "Preistoria dell'Italia Settentrionale. Studi in ricordo di Bernardino Bagolini" (2006), p. 357−362

- Amato F., Gualtieri S., Ricciardi P., Archeometria. In A. M. Lega (ed.), Ceramica: materia e tecnica, notes of the course held at the International Ceramic Museum (MIC) of Faenza in April 2006, MIC Faenza and Phase s.r.l. Firenze (2006), p. 55−82

- Gligor M., Ricciardi P., Gualtieri S., Varvara S., Fabbri B., Consideratii preliminare cu privire la tehnologia de confectionare a ceramicii pictate de tip "Lumea Noua", descoperita în asezarea neolitica de la Alba Iulia−Lumea Noua. Acta Musei Porolissensis XXVIII, Muzeul Judetean de istorie si arta, Zalau, Romania (2006), in press

- Ricciardi P., Varvara S., Fabbri B., Gualtieri S., Gligor M., Analisi archeometriche su ceramica neolitica ingobbiata e dipinta (cultura di Lumea Noua, IV millennio a.C.) da siti in Transilvania (Romania). Proceedings of the X Giornata di archeometria della Ceramica, in press

Conferences - oral presentations

- Varvara S., Gligor M., Fabbri B., Gualtieri S., Ricciardi P., Archaeometric investigations on Lumea Noua painted pottery. 37^{th} Pontica Session. Constanta (Romania), 5−8 October 2005

- Ricciardi P., Nodari L., Fabbri B., Gualtieri S., Russo U., Contribution for a mineralogical thermometer to be applied to low−fired and/or non carbonatic clays. EMAC'05. Lyon (France), 26−29 October 2005

- Ricciardi P., Varvara S., Fabbri B., Gualtieri S., Gligor M., Analisi archeometriche su ceramica neolitica ingobbiata e dipinta (cultura di Lumea Noua, IV millennio a.C.) da siti in Transilvania (Romania). X Giornata di archeometria della Ceramica. Roma, 2−6 April 2006

- Fabbri B., Gualtieri S., Nodari L., Ricciardi P., Russo U., Determinazione dei parametri di cottura di ceramiche a vernice nera nepalesi (VI-I sec. a.C.): l'importanza della spettroscopia Mössbauer. XCII Congress of the Italian Society of Physics (SIF). Torino, 18-23 September 2006

- Ricciardi P., Colomban Ph., Caratterizzazione tecnologica delle porcellane di Capodimonte mediante spettroscopia Raman. XI Giornata di Archeometria della Ceramica. Pesaro, 16−17 April 2007

- Ricciardi P., Colomban Ph., Milande V., Non−destructive characterization of Capodimonte and Buen Retiro porcelain. Raman in Art and Archaeology 2007. Modena, 5−8 September 2007

- Ricciardi P., Colomban Ph., Non−destructive characterization of Capodimonte and Buen Retiro porcelain glazes by means of Raman spectroscopy. EMAC'07 − Vessels: inside and outside. Budapest (Hungary), 24−27 October 2007

Conferences - posters

- Varvara S., Gligor M., Fabbri B., Gualtieri S., Ricciardi P., Rinaldi M., Archaeometric investigations on technological aspects and provenance of Neolithic pottery (5^{th}−4^{th} millennium B.C.) from Transylvania (Romania). 11^{th} EAA Annual Conference. Cork (Ireland), 5−11 September 2005

- Roma S., Fabbri B., Gualtieri S., Ricciardi P., Dall'argilla al vaso: tecnologia della ceramica nel sito neolitico di Sammardenchia (UD). Risultati preliminari delle analisi archeometriche e prospettive della ricerca. Preistoria dell'Italia Settentrionale. Studi in ricordo di Bernardino Bagolini. Udine, 23−25 September 2005

- Varvara S., Fabbri B., Gualtieri S., Ricciardi P., Gligor M., Neolithic pottery from Alba Iulia-Lumea Noua and Limba archaeological sites in Transylvania (Romania): composition and technological aspects. EMAC'07 − Vessels: inside and outside. Budapest (Hungary), 24−27 October 2007

- Ricciardi P., Amato F. M., Colomban Ph., Raman spectroscopy as a tool for the non−destructive characterization of slips and glazes of a "sgraffito" Renaissance production. EMAC'07 − Vessels: inside and outside. Budapest (Hungary), 24−27 October 2007

List of Figures

List of Tables